

Investigation of the M6.6 Niigata-Chuetsu Oki, Japan, Earthquake of July 16, 2007

Robert Kayen, Brian Collins, Norm Abrahamson, Scott Ashford, Scott J. Brandenberg, Lloyd Cluff, Stephen Dickenson, Laurie Johnson, Yasuo Tanaka, Kohji Tokimatsu, Toshimi Kabeyasawa, Yohsuke Kawamata, Hidetaka Koumoto, Nanako Marubashi, Santiago Pujol, Clint Steele, Joseph I. Sun, Ben Tsai, Peter Yanev, Mark Yashinsky, Kim Yousok



Open File Report 2007–1365

2007

U.S. Department of the Interior
U.S. Geological Survey

U.S. Department of the Interior
Dirk Kempthorne, Secretary

U.S. Geological Survey
Mark D. Myers, Director

U.S. Geological Survey, Reston, Virginia 2007

For product and ordering information:

World Wide Web: <http://www.usgs.gov/pubprod>

Telephone: 1-888-ASK-USGS

For more information on the USGS—the Federal source for science about the Earth, its natural and living resources, natural hazards, and the environment:

World Wide Web: <http://www.usgs.gov>

Telephone: 1-888-ASK-USGS

Suggested citation:

Kayen, R., Collins, B.D., Abrahamson, N., Ashford, S., Brandenberg, S.J., Cluff, L., Dickenson, S., Johnson, L., Kabeyasawa, T., Kawamata, Y., Koumoto, H., Marubashi, N., Pujol, S., Steele, C., Sun, J., Tanaka, Y., Tokimatsu, K., Tsai, B., Yanev, P., Yashinsky, M., and Yousok, K., 2007. Investigation of the M6.6 Niigata-Chuetsu Oki, Japan, Earthquake of July 16, 2007:

U.S. Geological Survey, Open File Report 2007-1365, 230pg;

[available on the World Wide Web at URL

<http://pubs.usgs.gov/of/2007/1365/>].

Any use of trade, product, or firm names is for descriptive purposes only and does not imply endorsement by the U.S. Government.

Although this report is in the public domain, permission must be secured from the individual copyright owners to reproduce any copyrighted material contained within this report

Contents

Section 1 - Introduction.....	4
Section 2 - Seismological Aspects.....	10
Section 3 - Landslides.....	33
Section 4 - Liquefaction.....	45
Section 5 - Building and Industrial Structures.....	80
Section 7 -Tanks.....	151
Section 8 - Ports and Harbors.....	160
Section 9 - Transportation Systems.....	190
Section 10 - Lifeline Systems.....	205
Section 11 - Response and Recovery Issues.....	217

Investigation of the M6.6 Niigata-Chuetsu Oki, Japan, Earthquake of

July 16, 2007

Robert Kayen¹ (EERI-GEER Leader), Brian Collins¹, Norm Abrahamson², Scott Ashford³, Scott J. Brandenberg⁴, Stephen Dickenson⁴, Laurie Johnson⁵, Toshimi Kabeyasawa⁶, Yohsuke Kawamata⁴, Hidetaka Koumoto⁷, Nanako Marubashi⁷, Santiago Pujol⁸ (EERI Co-Leader), Clint Steele¹, Yasuo Tanaka⁹, Kohji Tokimatsu¹⁰, Ben Tsai³, Peter Yanev¹², Mark Yashinsky¹¹, Kim Yousok⁸

Section 1 - Introduction

1.1 Introduction

The M6.6 mainshock of the Niigata Chuetsu Oki (offshore) earthquake occurred at 10:13 a.m. local time on July 16, 2007, and was followed by a sequence of aftershocks that were felt during the entire time of the reconnaissance effort (USGS, <http://earthquake.usgs.gov/eqcenter/eqinthenews/2007/us2007ewac/#details>). The mainshock had an estimated focal depth of 10 km (USGS, 2007) and struck in the Japan Sea offshore Kariwa. Analysis of waveforms from source inversion studies indicates that the event occurred along a thrust fault with a NE trend. The fault plane is either a strike of 34 degrees with a dip of 51 degrees or a strike of 238 degrees with a dip of 41 degrees (<http://www.eri.u-tokyo.ac.jp/topics/20070716/>). Which of these two planes is associated with the mainshock rupture is unresolved, although attenuation relationship analysis indicates that the northwest-dipping fault is favored. The quake affected an approximately 100-km-wide area along the coastal areas of southwestern Niigata prefecture. The event triggered ground failures as far as the Unouma Hills, located in central Niigata approximately 50 km from the shore and the source area of the 2004 Niigata Chuetsu earthquake. The primary event produced tsunami run-ups that reached maximum runup heights of about 20 centimeters along the shoreline of southern Niigata Prefecture.

¹ U.S. Geological Survey

² Pacific Gas and Electric Company

³ Oregon State University

⁴ University of California at Los Angeles

⁵ Kyoto University

⁶ University of Tokyo

⁷ Nagoya Institute of Technology

⁸ Purdue University

⁹ Kobe University

¹⁰ Tokyo Institute of Technology

¹¹ California Dept. of Transportation

¹² Independent Consultant

The JMA (Japan Meteorological Agency) seismic intensity was 6+ (IX in MMI) in Kariwa-cho, Kashiwazaki city, and Nagaoka city in Niigata prefecture, and Ohzunamachi in Nagano prefecture. An instrument maintained by K-NET (Kyoshin Network, National Research Institute for Earth Science and Disaster Prevention of Japan) recorded a value of peak ground acceleration of 0.67g near Kashiwazaki's city municipal building. The earthquake resulted in eleven fatalities and nearly two thousand injuries (<http://www.pref.niigata.jp/seisaku/kokusai/english/>). Close to 1,100 collapses of residential structures took place. These collapses occurred almost exclusively in old houses with wood and clay walls and heavy kawara, clay-tile roofs. In many cases, reconnaissance team members observed that collapses occurred in the store houses of the residences, rather than the residences themselves, although hundreds of homes also collapsed.

Damage occurred in lifeline utilities of gas, water, and electricity. Electric power generation recovered in areas without downed power lines within a day in most of the epicentral area. The water supply system and gas network were also damaged in areas of soft ground. Water service had not been restored in Kashiwazaki one week following the event. The team saw a strong presence of the Japan Self-Defense Forces distributing water at community centers throughout the city during the entire duration of the reconnaissance.

Kariwa village is home to the world's largest nuclear power plant with seven reactors and a total output of 8200 Megawatts. This facility is instrumented with 97 strong motion recorders that were triggered by the July 16, 2007 event. Records obtained by a number of these instruments were lost because of overwrites that occurred during aftershocks. Several members of our team visited Kashiwazaki-Kariwa nuclear power plant facility and preliminary observations are presented in Chapter 5. The power plant is located above the inferred fault planes in a region of high iso-seismal intensity, as inferred from the observed damage patterns in the area. Critical structures appeared to have performed well given the intensity of the ground shaking, large ground settlement, and evidence of liquefaction near the waterfront.

The reconnaissance was a combined effort of the Earthquake Engineering Research Institute (EERI) - Learning From Earthquakes, and the Geo-Engineering Earthquake Reconnaissance (GEER) activity of the National Science Foundation (NSF). EERI and GEER dispatched the first reconnaissance team to Niigata, Japan within three days of the earthquake. The EERI-GEER team was led by Robert Kayen of the United States Geological Survey (USGS) and composed of Scott Ashford, Steve Dickenson, and Yohsuke Kawamata from the School of Civil and Construction Engineering at Oregon State University; Brian Collins of the USGS; and Scott Brandenburg of the University of California at Los Angeles. EERI and PEER (Pacific Earthquake Engineering Research Center) supported the reconnaissance efforts of Santiago Pujol (co-leader) of Purdue University in collaboration with Toshimi Kabeyasawa, Nanako Marubashi, and Yousok Kim from the Japan Association of Earthquake Engineering (JAEE) to specifically examine the performance of buildings during the earthquake. The EERI-GEER team was joined by international GEER members Yasuo Tanaka and Hidetaka Koumoto of Kobe University, and Kohji Tokimatsu of Tokyo Institute of Technology. Norm Abrahamson

and Ben Tsai, of Pacific Gas and Electric Company synthesized the seismological information about the event. A third group of EERI participants - Laurie Johnson, Mark Yashinsky and Peter Yanev, visited the region in early August to document the emergency response and performance of bridges.

This earthquake reconnaissance effort was made possible by funding from the U.S. National Science Foundation, cost sharing by the U.S. Geological Survey, and volunteer work by the team participants. Cooperation with the following Japanese researchers and organizations was invaluable: Kazuo Konagai, University of Tokyo, Toshikatsu Ichinose of Nagoya Institute of Technology, Toshikazu Kabeyasawa and Toshinori Kabeyasawa of the University of Tokyo, Kobe University and the staff of the Research Center for Urban Safety and Security (RCUSS). This material is based upon work supported by the National Science Foundation under Grant No. CMS-032914 & National Science Foundation Grants supporting EERI. Any opinions, findings, conclusions or recommendations expressed in this material are those of the authors and do not necessarily reflect the views of the sponsoring organizations.

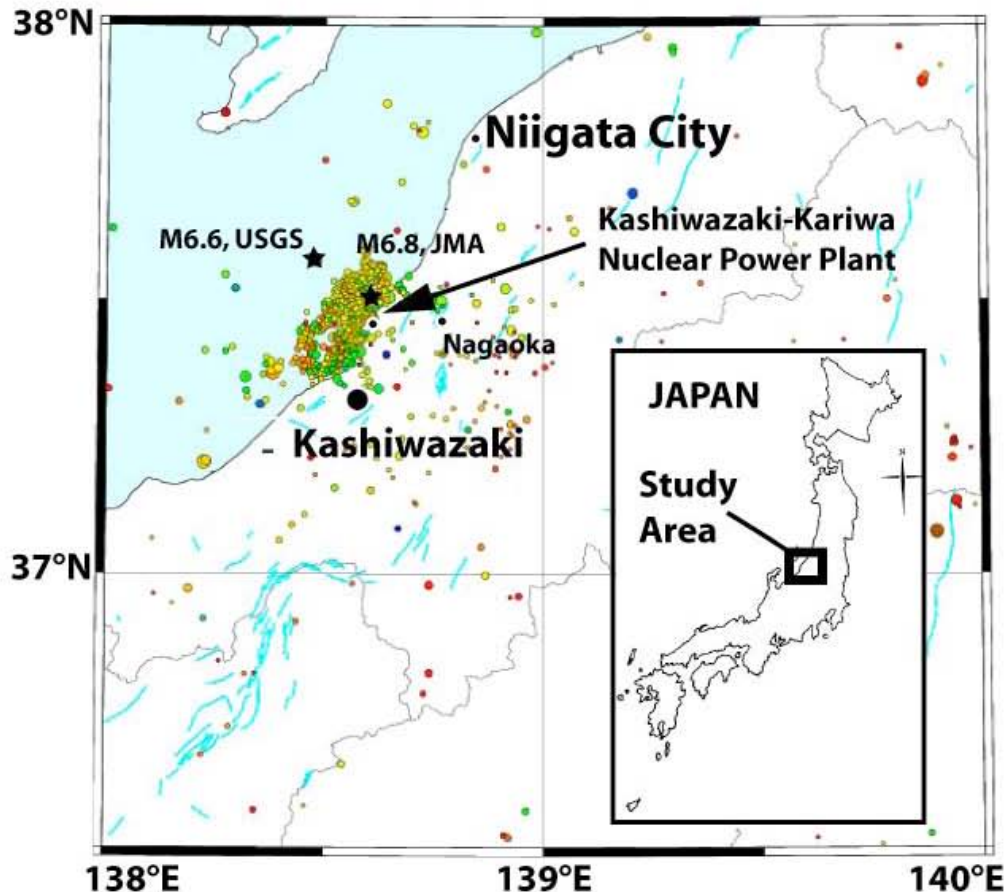


Figure 1.1: The reconnaissance effort covered the coastal region of southwest Niigata Prefecture, Japan. The epicenter and most of the aftershocks were immediately offshore City of Kashiwazaki and the Kashiwazaki-Kariwa Nuclear Power Plant.

1.2 Reconnaissance Method

A reconnaissance team sponsored by the National Science Foundation (NSF) was organized and sent to the epicentral region within the first 48 hours following the earthquake to assess the geo-engineering and soil-related structural damage aspects of this event. The team's main goal was to quantify the spatial extent and amplitude of ground failures, soil liquefaction, landslides, and damage to bridges, piers, ports and harbors, lifeline systems and critical structures.

During the five-day reconnaissance, from July 20 through July 24, three vehicles were used to cover most of the roads of the epicentral region. On the ground, we sought to quantify the severity and abundance of damage associated with ground and ground-structure interaction. Each of the three vehicles had teams equipped with hand-held two-way radios, digital cameras, maps, computers for recording site logs, and GPS units for recording track logs and site locations. In the evening, the reconnaissance team held meetings where the GPS data, site logs and digital pictures were merged into a common database. In the field, we generated Google Earth KML mark-up language files to display all of the written observations on dynamic digital maps (Figure 1.2), and damage-specific maps (e.g., Google Earth map of liquefaction damage). By observing damage in the Google Earth program, we identified unexplored areas for the next days reconnaissance, spatial trends in the observations, and any errors in the GPS logs and typed observations. The .kml files were also sent by email to the United States so that EERI and GEER members working on the reconnaissance effort could take virtual tours of the damage zone and plan for following reconnaissance efforts. Using the city of Kashiwazaki's Google Earth community display of 3D buildings and residences, we were also able to identify the locations of critical facilities such as the waster water plant, municipal waste incinerator, schools, and other municipal buildings.

Readers of this report should download and open the .kmz Google Earth map file to navigate through the report observation sites as they are described in the text. Clicking on the individual site name in the waypoints folder will direct the program to fly to that site. <http://walrus.wr.usgs.gov/infobank/n/nii07jp/html/n-ii-07-jp.sites.kmz> The file n-ii-07-jp.sites.kmz will be updated regularly on the USGS server. Each time readers visit the data set, we recommend that you visit the url, above, and download the latest file. Then, remove any older versions of that file from Google Earth before uploading the newest .kmz file.

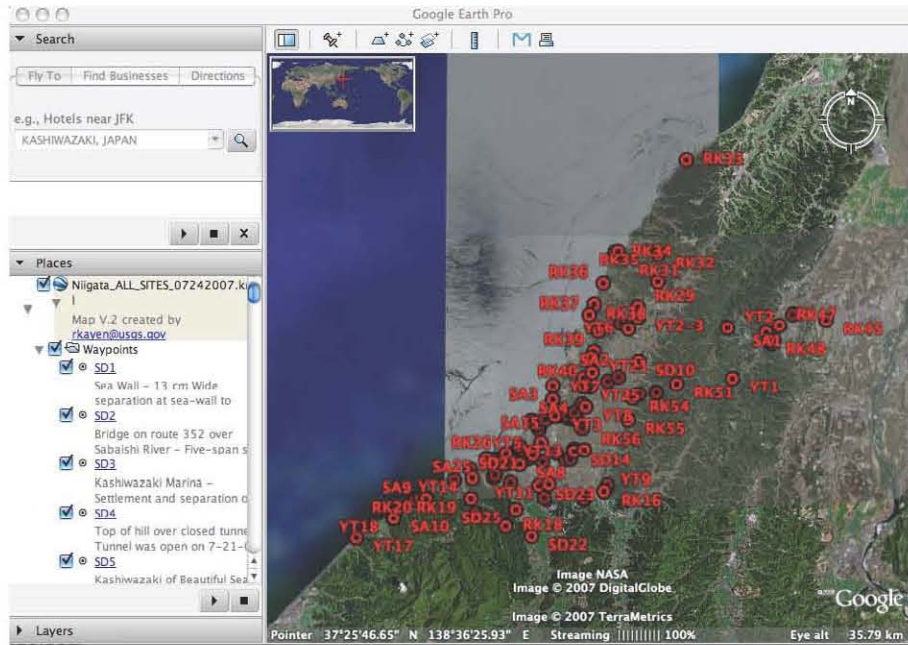


Figure 1.2: An interactive observation map of the Kashiwazaki, City area of Niigata Prefecture, Japan affected by the July 16, 2007 earthquake can be viewed at <http://walrus.wr.usgs.gov/infobank/n/nii07jp/html/n-ii-07-jp.sites.kmz>

Four teams of delegates from EERI and JAEE followed the team supported by NSF to document details of damage to structures, industrial facilities, bridges, and emergency response. These teams used the .kml file created with Google Earth to guide and map their observations.

High-resolution topographic data sets of the most significant damage features were collected for preservation of the event using the USGS terrestrial LiDAR (Light Detection and Ranging) system. Terrestrial LiDAR data were collected for the Omigawa landslide (Site RK20, Shin-etsu Train Station Landslide N37.34480°, E138.48888°); the Ozumi-Mishimayamachi Landslide (Site RK2, N37.44057°, E138.70467°); the Kashiwazaki incinerator lateral spread (Site RK6, N37.39343°, E138.58555°); and the Kashiwazaki South Harbor liquefaction induced lateral spread (Site RK25, N37.36713°, E138.53210°). The terrestrial LiDAR data collection technique consists of sending and receiving laser pulses to build a point file of three-dimensional coordinates of virtually any reflective surface. The time of travel for a single pulse reflection is measured along a known trajectory such that the distance from the laser and consequently the location of a point of interest is computed. The USGS system consisted of a Riegl Z210 instrument mounted on a tripod platform and linked with a set of Topcon DGPS RTK receivers. The instrument captured data at approximately 8000 points per second with a typical range of several hundred meters and at an accuracy of 15 mm for each point. Data from these sites will be made available in digital format once processed.

This reconnaissance report has been organized into sections that describe geotechnical and structural aspects of the damage caused by the earthquake. The report begins with a description of the seismological aspects of the earthquake in Section 2.

Section 3 describes landslides, Section 4 describes liquefaction, Section 5 describes damage and performance of buildings, Section 6 describes damage to bridges, and Section 7 describes damage to tanks. Section 8 describes damage to ports and harbors, Section 9 describes damage to transportation systems, Section 10 describes damage to lifeline systems, and Section 11 describes response and recovery issues.

Section 2 - Seismological Aspects

2.1 Tectonic Setting

The Niigata Chuetsu Oki, Japan earthquake occurred on July 16, 2007 at 10:13:22 local time (01:13:22 URC) along the west coast of Honshu (Fig. 2.1) in an area of relative high seismic activity.

Tectonically, Niigata is in a region of compressional deformation that is associated with the boundary between the Amur plate and the Okhotsk plate (two relatively small plates that lie between the larger Eurasia and Pacific plates). Figure 2.1 shows the seismicity in central Japan from 1990 to present. Overall, the pattern of seismicity shows a general deepening of hypocenters from east to west associated with the subducting slab (yellow, green, blue and purple symbols). The shallow crustal earthquakes in the Niigata region are shown by the orange symbols in the center of the figure. The seismic hazard in the Niigata region at long return periods is related to crustal earthquakes since they can be closer but less frequent.

2.2 Mainshock

The mainshock moment magnitude of this event was estimated to be 6.6 using teleseismic data (USGS) and estimated to be 6.7 using regional Japanese data. The JMA magnitude is 6.8. For comparisons with earthquakes around the world, the moment magnitude is used: for this event, we use a moment magnitude of 6.6.

The Niigata earthquake was a buried reverse-slip earthquake. The estimated hypocenter was at a depth of 8 km (NRI ESDP, 2007) which is slightly shallower than the USGS depth of 10 km from teleseismic data. The focal mechanism leads to two potential fault planes: the first at strike = 215° , dip = 49° , rake = 80° ; and the second at strike = 49° , dip = 42° , rake = 80° . Which of these two planes is associated with the mainshock rupture is unresolved. Aftershock locations fell along both planes, although the majority of the aftershocks were located along the SE dipping plane ($49^\circ/42^\circ/80^\circ$). However, aftershocks from reverse earthquakes often occur along backthrusts on the conjugate plane.

A finite source inversion based on the nearby strong motion data (NRI ESDP, 2007) could not resolve the mainshock rupture plane (Fig. 2.2). The fit of the velocity waveforms is similar for the two planes. The rupture length is 30 km and the down-dip fault width is 22 km for both planes. The hypocenter is at the northeast end of either plane and the rupture was toward the southwest. The slip models for both rupture planes show a single strong asperity in the western-end of the rupture. The top of rupture for the two models is 1 km for the northwest dipping model and 3 km for the southwest dipping model. The maximum computed slip was 3.5 m. For both models, there is an asperity in the southwest-end of the rupture.

2.3 Strong Motion Recordings

The Japanese nationwide strong motion network, K-net, recorded the earthquake at 390 stations, with 20 stations within 50 km. A subset of the regional K-net stations that recorded the event are shown in Figure 2.3 and the nearby stations to the epicentral area are shown in Figure 2.4. Estimates of the V_{S30} values were provided by Strasser (2007). The KiK-Net station locations are shown in these figures as open circles. We had not completed compiling the KiK-net data at the time this report was prepared. Most of the stations within 30 km of the rupture are the K-Net stations.

Acceleration time series are shown in Figure 2.5 for the four closest stations. The accelerograms at station NIG018 (close to the fault plane and within the observed damaged area) show strong low-frequency content, suggesting features associated with liquefaction in foundation soils below the instrument. A soil profile reported by K-Net for the site is shown in Figure 2.6. The spiky acceleration behavior of NIG018 in Figure 2.5 is consistent with the known behavior of sandy soils undergoing cyclic mobility in undrained loading, although no surficial observation of liquefaction was observed at the site. The accelerograms at the other stations are more consistent with one other and show durations of 10-15 seconds. The 5% damped response spectra for 20 of the nearby stations are shown in Figures 2.7a-e. Observe the unusual frequency content for NIG018.

The attenuation of peak ground acceleration (PGA) and spectral ordinates (at $T=0.2$ sec and $T=1.0$ sec) is shown in Figures 2.8a,b,c for the rupture plane dipping to the southeast (red plane in Fig. 2.4) and in Figures 2.9a,b,c for the rupture plane dipping to the northwest (blue plane in Fig. 2.4). The attenuation is compared to the Abrahamson and Silva (2007) model developed as part of the NGA project (Power et al, 2006). At PGA and SA($T=0.2$ sec), the ground motions from the Niigata earthquake are higher than estimated when using the southeast dipping source model (Fig. 2.8a,b). Using the northwest dipping source model, the PGA and $T=0.2$ sec data are in better agreement with the Abrahamson & Silva model. The $T=1$ sec data are equally well modeled by both source models. This is consistent with the inability of the source inversion, based on velocity time series, to distinguish between the two source models. Assuming that the Abrahamson and Silva (2007) model is applicable to crustal earthquakes in Japan at short distances, then the short period data suggest that the northwest dipping is favored.

2.4 Ground Motions at the Kashiwazaki-Kariwa Nuclear Power Plant

The seven-unit Kashiwazaki-Kariwa nuclear power plant, owned by Tokyo Electric Power Company (TEPCO) is located about 16 km from the epicenter determined by JMA (Japan Meteorological Agency) for this event. Figure 2.10 shows an aerial photograph from the Japanese Geographical Survey Institute (GSI) taken after the main shock. The plant has seven generators (Units 1 through 7) with a total output capacity of 8.2 GW located within a 4.2 km² area. There are two seismic instrument systems at the plant: an older system and a new system. The motions at 33 locations from the new system were recorded, but unfortunately, the recordings obtained at the other 66 locations from the older system, including two free-field down-hole arrays and most structural arrays were lost with the exception of the peak values. The recovered 33 recordings

included 27 from a majority of the reactor and turbine buildings and one 4-depth free-field array at the Service Hall. The ground motion data from the old system could not be automatically transmitted due to communication congestion and system overwrite settings - the aftershocks caused additional triggers of the recorders, which overwrote the mainshock recordings in the buffer as new data came in. Thus, the mainshock recordings were lost.

The peak acceleration on the foundations for the seven units, as well as down hole array and Units 1 and 5 arrays, are listed in Table 2.1 and Figure 2.11. The NS and EW directions of the seismometers were set in the two principal axes of the plant buildings as opposed to being aligned with true NS and EW directions. The data indicate a large range in the foundation motions for the EW components with PGA values ranging over a factor of two. On the other hand, the NS components show values more similar to one another. The large range in the EW component values is likely due to different SSI effects at the different units and spatial variation of the ground motion over short distances probably due to the near-fault rupture mechanism. The large range of PGA values on the EW component shows the need for multiple recordings at NPP sites to reliably determine the input ground motions for the structures.

At the Service Hall, the horizontal peak ground accelerations recorded at the surface were smaller than the accelerations measured 250 m below grade. In contrast, the up-down (UD) ground accelerations were larger near the surface (Fig. 2.11). Horizontal ground acceleration measured in the downhole arrays at Units 1 and 5 are shown in Figs. 2.12 and 2.13. Here, the accelerations were amplified more in the turbine building than in the reactor building. However, there is no consistent trend in the variations of measured peak horizontal acceleration with depth.

Table 2.1. Peak accelerations from the foundations of the seven units at the Kashiwazaki Kariwa nuclear power plant (from TEPCO, 2007)

Unit	PGA (gal)		
	NS	EW	Vertical
K-1	311	680	408
K-2	304	606	282
K-3	308	384	311
K-4	310	492	337
K-5	277	442	205
K-6	271	322	488
K-7	267	356	355

2.5 References

Abrahamson, N.A., and Silva, W.J., (2007). Abrahamson & Silva NGA Ground Motion Relations for the Geometric Mean Horizontal Component of Peak and Spectral Ground Motion Parameters: PEER Report 200x/xx, Pacific Earthquake Engineering Research Center, College of Engineering, University of California, Berkeley, July 9, 2007, Draft Version 2, 378p. http://peer.berkeley.edu/pdf/AbraSil_2007_v2.pdf.

NRI ESDP (2007) Source Process of the 2007 Niigata-ken Chuetsu-oki Earthquake Derived from Near-fault Strong Motion Data, <http://www.k-net.bosai.go.jp/k-net/topics/chuetsuoki20070716/inversion/>

Power, M., B. Chiou, N. Abrahamson, and C. Roblee (2006). The next generation of ground motion attenuation models (NGA) project: An overview. Proc. Eighth National Conf., Earthquake Engineering, Paper No. 22.

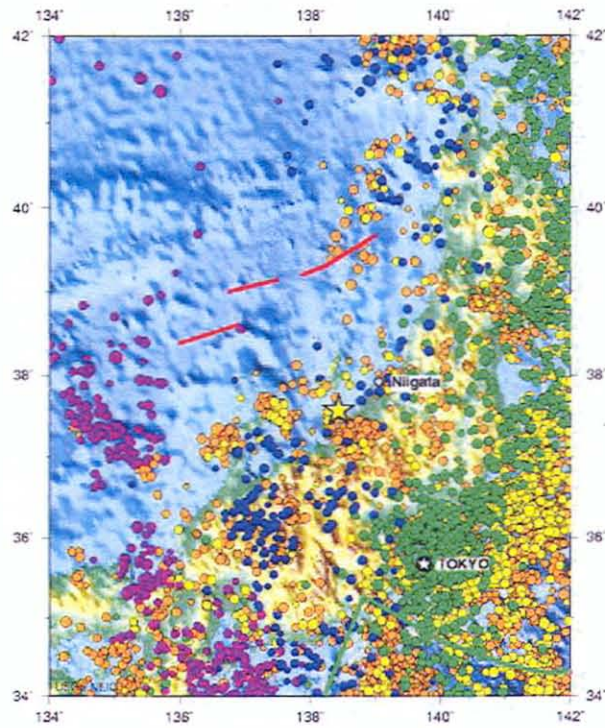
Strasser, F. (2007). Estimates of VS30 values for the K-Net stations based on extrapolation of the velocity profile, personal communication.

TEPCO (2007). Report on analysis of observed records at Kashiwazaki-Kariwa Nuclear Power Plant during the Niigata-Chuetsu-Oki earthquake 2007.

USGS, (2007). U.S. Geological Survey, Earthquake Hazards Program, http://neic.usgs.gov/neis/eq_depot/2007/eq_070716_ewac/neic_ewac_h.html.

Monday, July 16, 2007 at 01:13:22 UTC

Historic Seismicity



NEAR WEST COAST OF HONSHU, JAPAN

2007 07 16 01:13:28 UTC 37.57N 138.44E Depth: 55.4 km, Magnitude: 6.7

Seismicity 1990 to Present

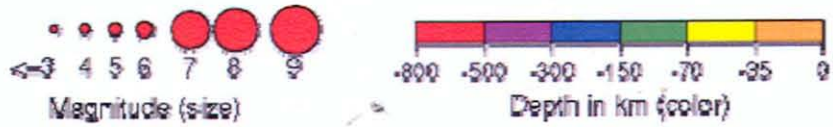


Figure 2.1: Seismicity in the Niigata region (Source: USGS, 2007).

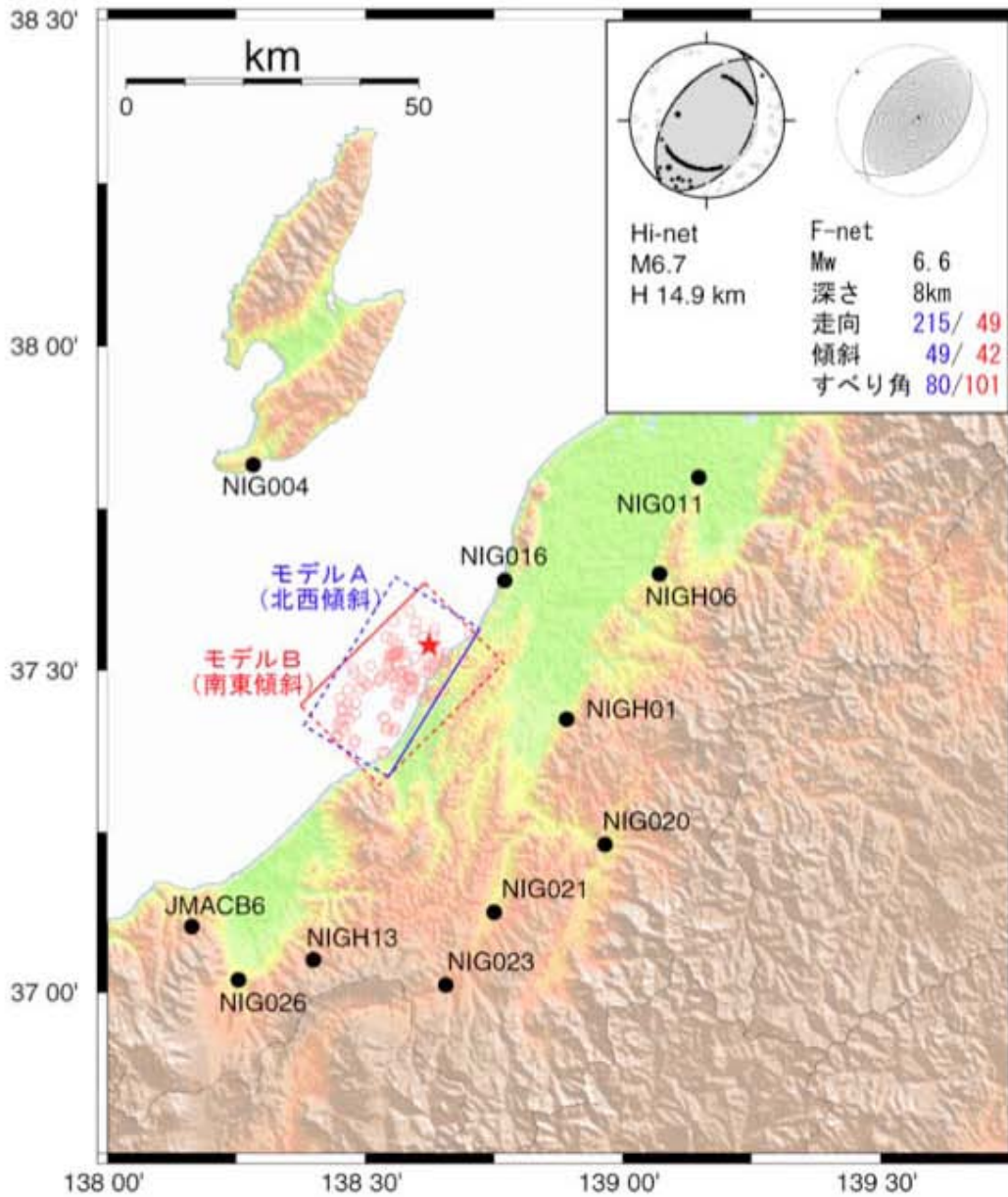


Figure 2.2: Strong motion stations used in the source inversion. The red and blue rectangles show the two alternative plausible fault planes with the solid line indicating the top of the rupture. (From NRI ESDP, 2007)

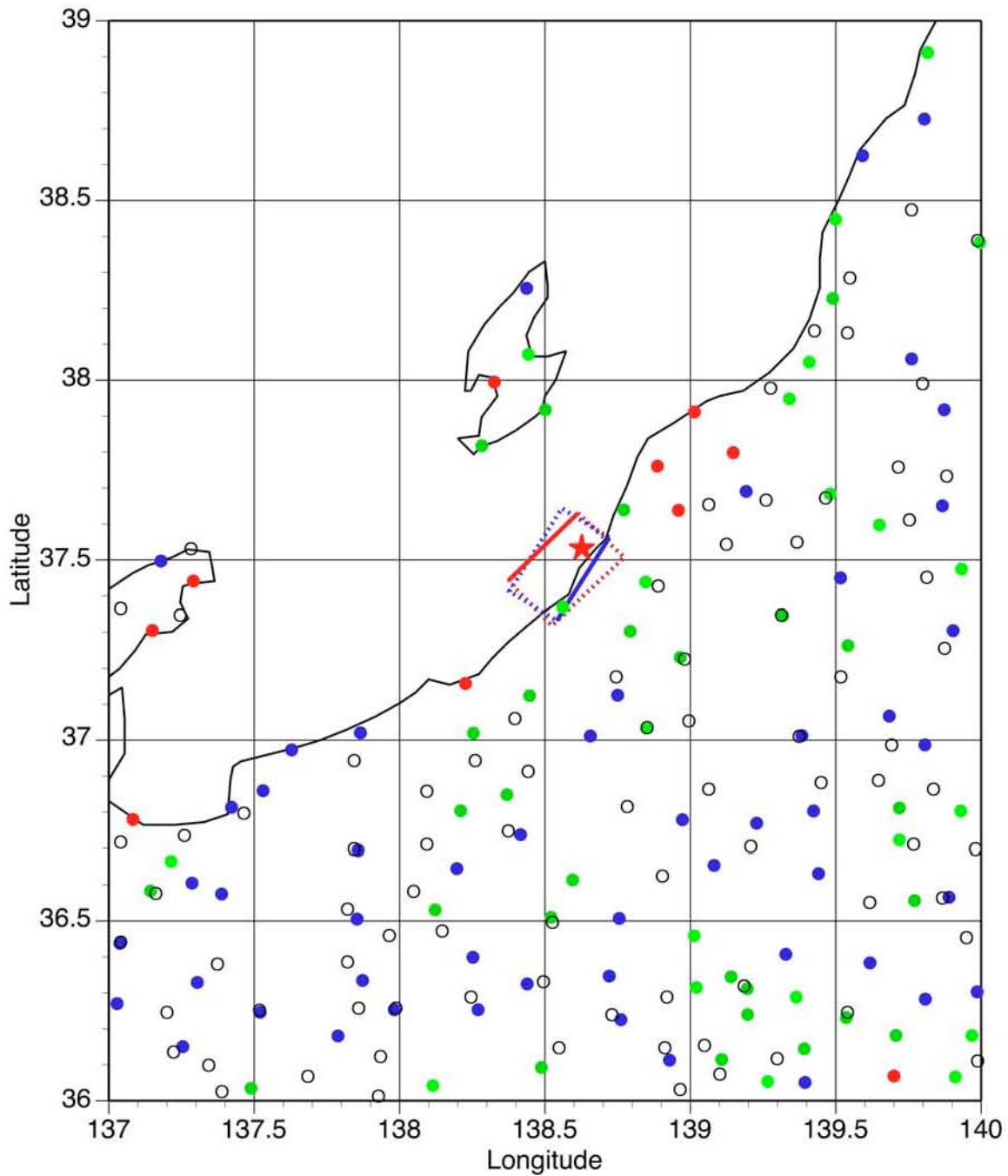


Figure 2.3: Regional subset of the K-net stations that recorded the Niigata earthquake. (Red: $V_{S30} < 180$ m/s; Green: $180 \leq V_{S30} < 360$; Blue: $360 \leq V_{S30} < 760$). The open black circles are the Kik-Net stations. The two alternative mainshock rupture planes are shown by the blue and red rectangles.

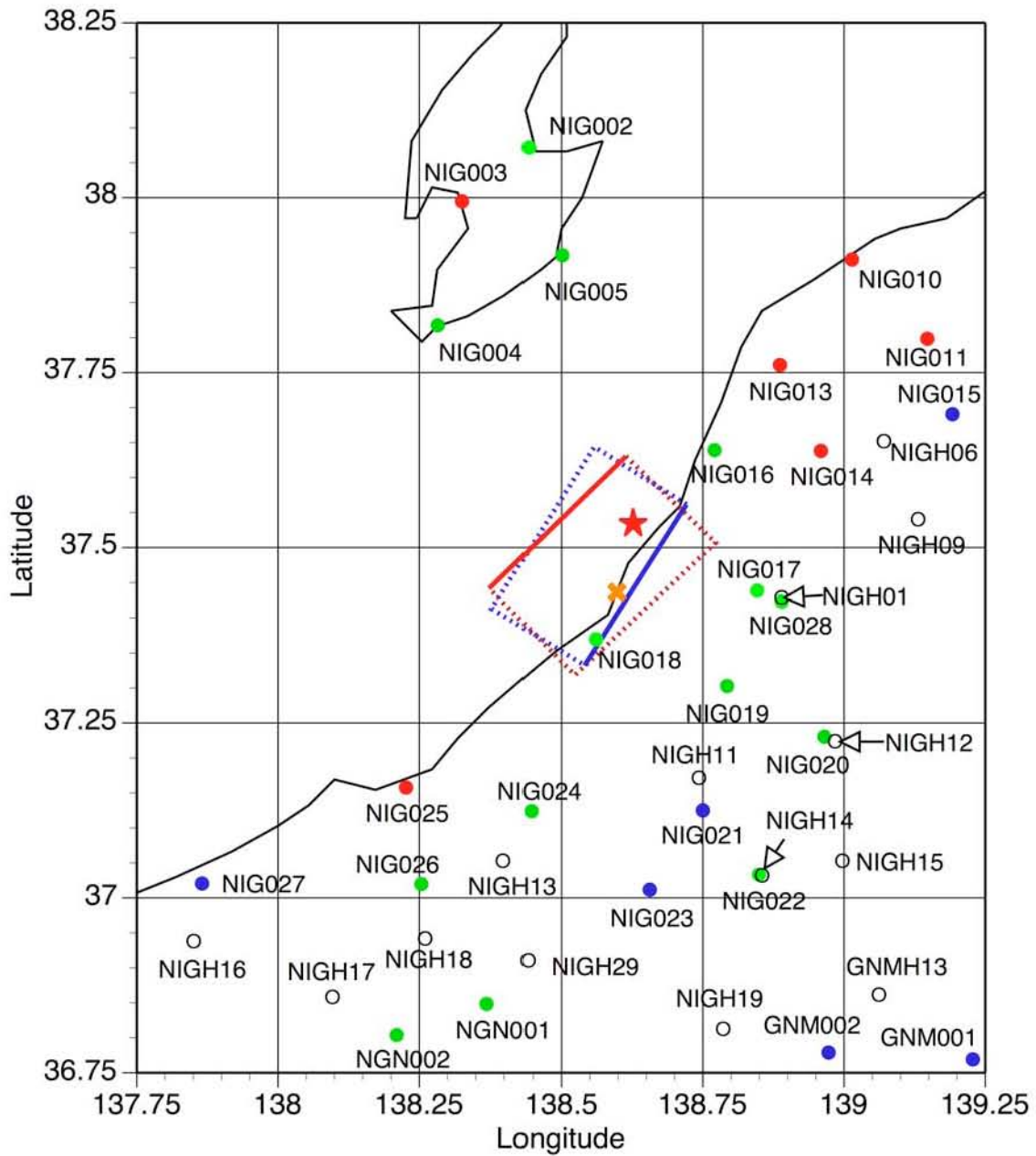


Figure 2.4: Nearby K-net stations that recorded the Niigata earthquake. (Red: $V_{s30} < 180$ m/s; Green: $180 \leq V_{s30} < 360$; Blue: $360 \leq V_{s30} < 760$). The open black circles are the Kik-Net stations. The two alternative mainshock rupture planes are shown by the blue and red rectangles.

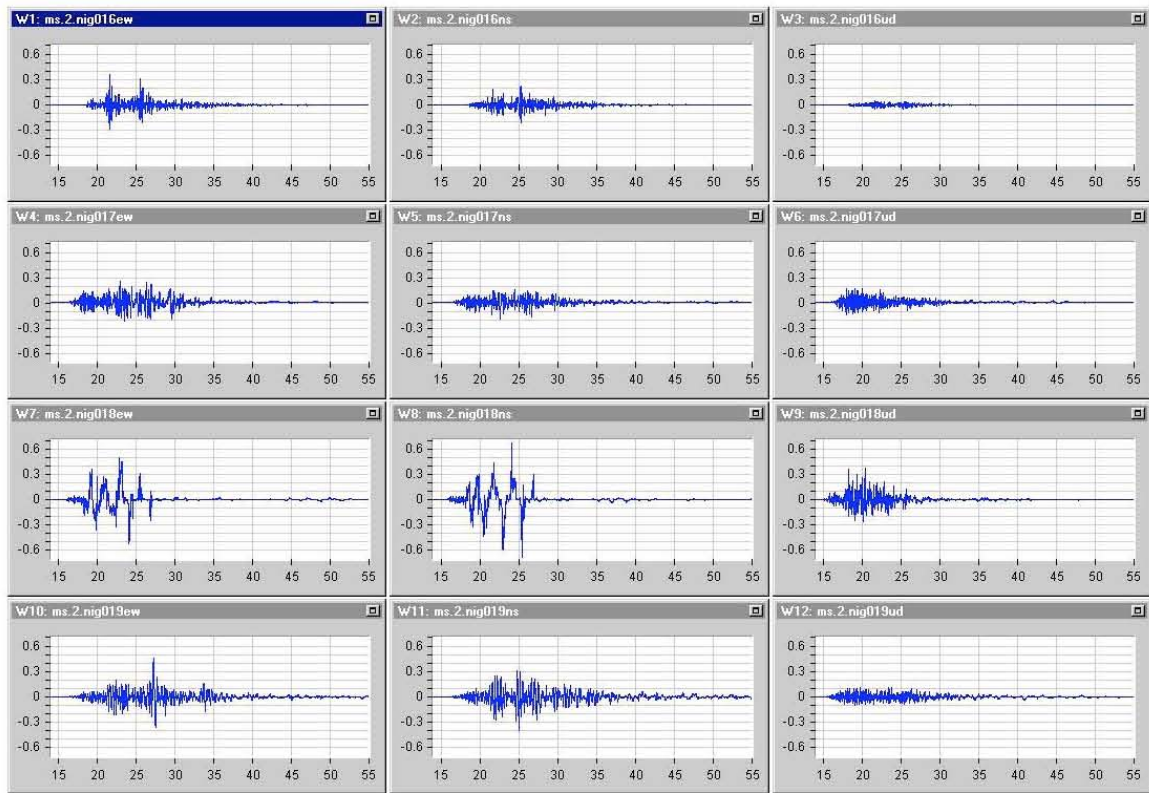


Figure 2.5: Example acceleration time histories of the near-source stations. From top to bottom: NIG016, NIG017, NIG018, NIG019. The horizontal axes represent time, in seconds, and the vertical axes represent ground acceleration as a fraction of the acceleration of gravity. The left panel is the EW component, middle panel is the NS component, right panel is the Z component.

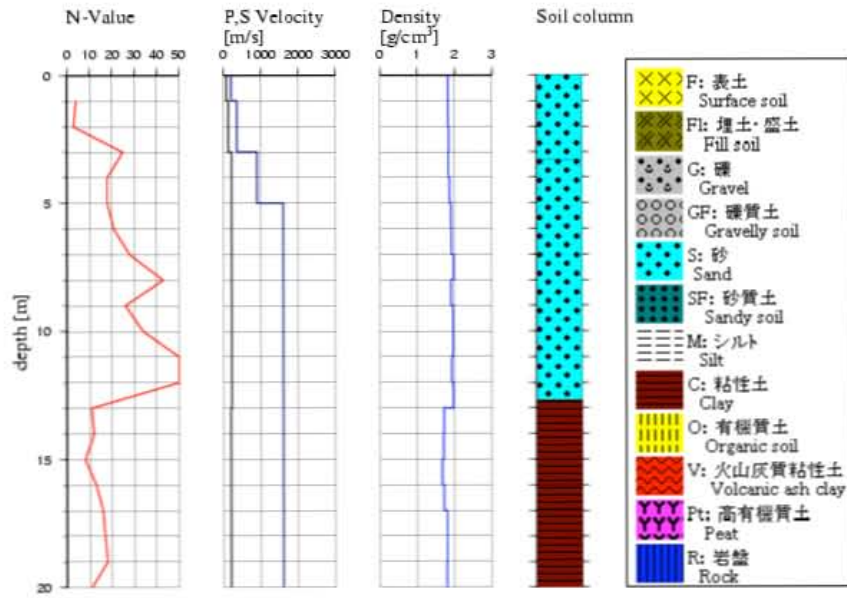


Figure 2.6. Soil profile at the K-NET Kashiwazaki Station (Source: K-NET)

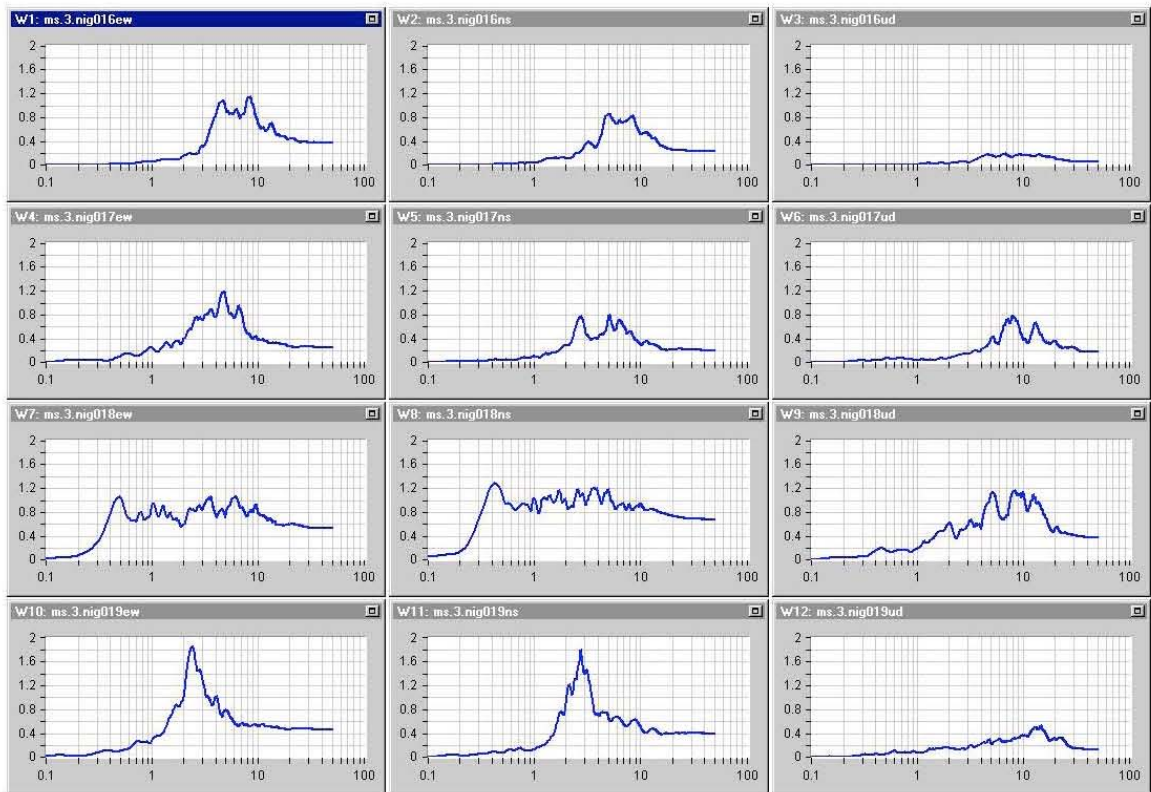


Figure 2.7a: 5% damped acceleration response spectra. From top to bottom: NIG016, NIG017, NIG018, NIG019. The horizontal axes represent frequency, in Hz, and the vertical axes represent absolute acceleration as a fraction of the acceleration of gravity. The left panel is the EW component, middle panel is the NS component, right panel is the Z component.

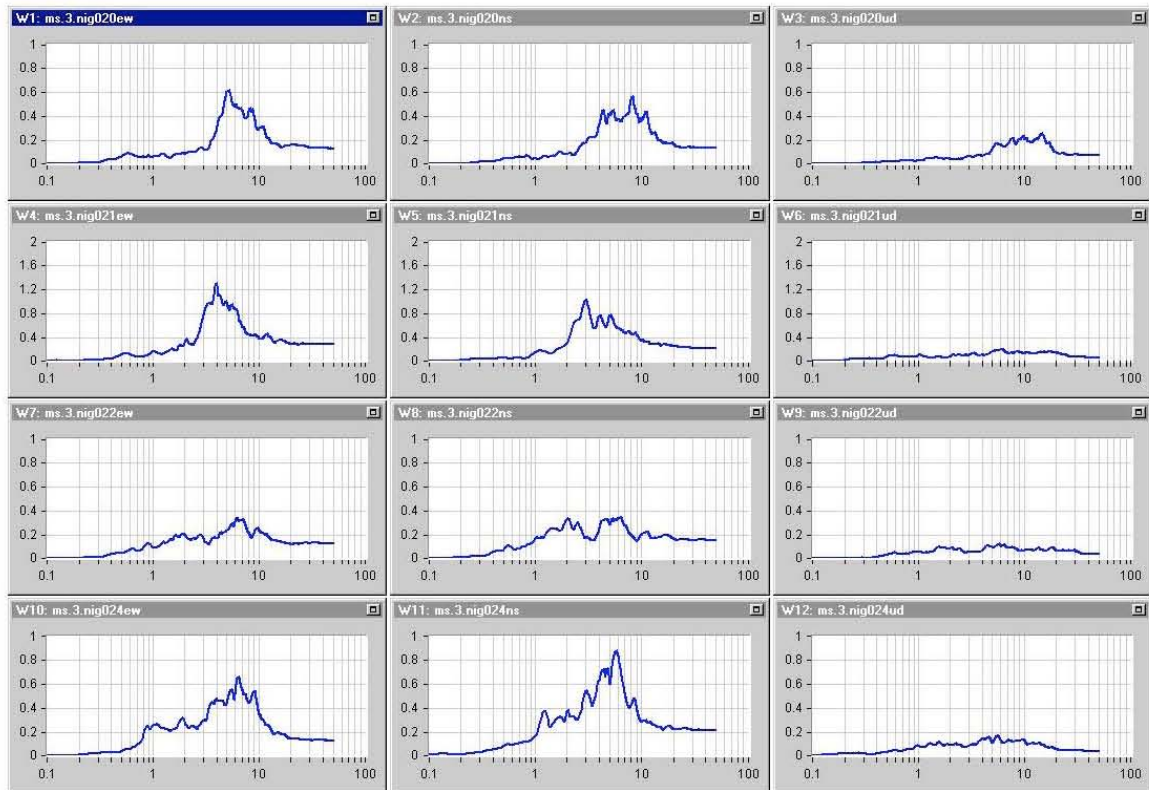


Figure 2.7b: 5% damped acceleration response spectra. From top to bottom: NIG020, NIG021, NIG022, NIG024. The horizontal axes represent frequency, in Hz, and the vertical axes represent absolute acceleration as a fraction of the acceleration of gravity. The left panel is the EW component, middle panel is the NS component, right panel is the Z component.

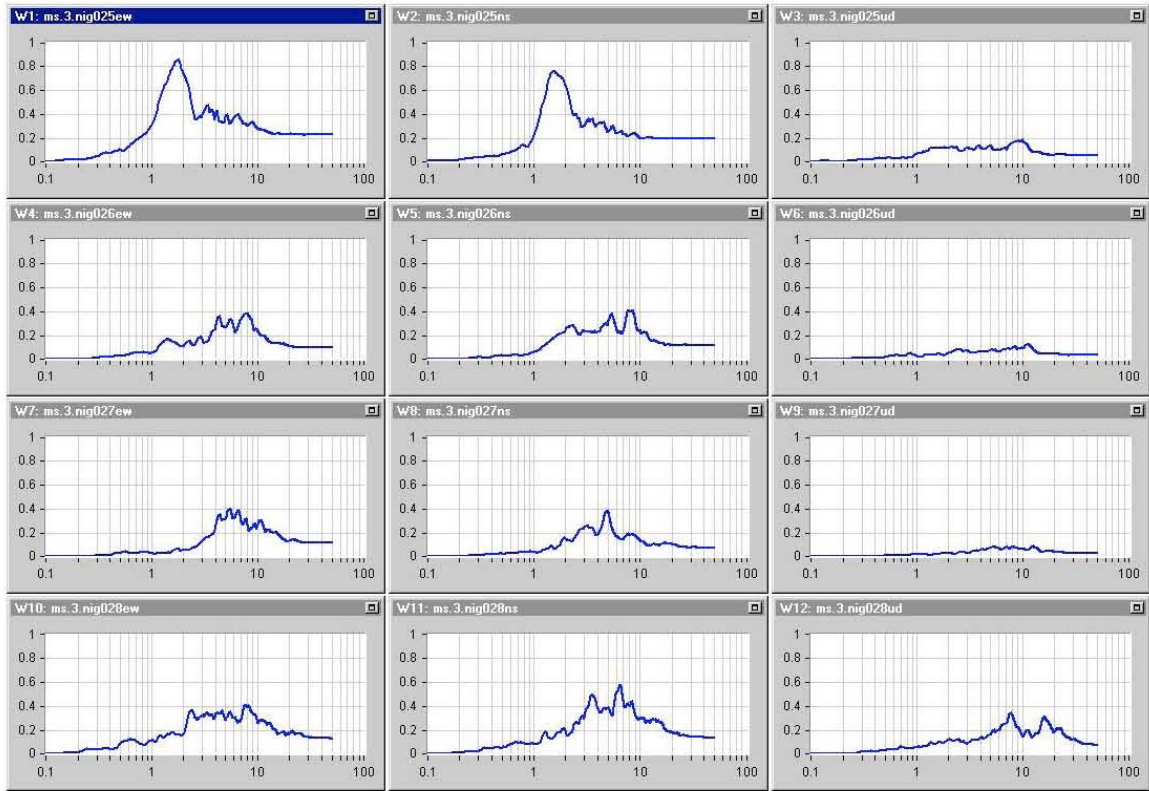


Figure 2.7c: 5% damped acceleration response spectra. From top to bottom: NIG025, NIG026, NIG027, NIG028. The horizontal axes represent frequency, in Hz, and the vertical axes represent absolute acceleration as a fraction of the acceleration of gravity. The left panel is the EW component, middle panel is the NS component, right panel is the Z component.

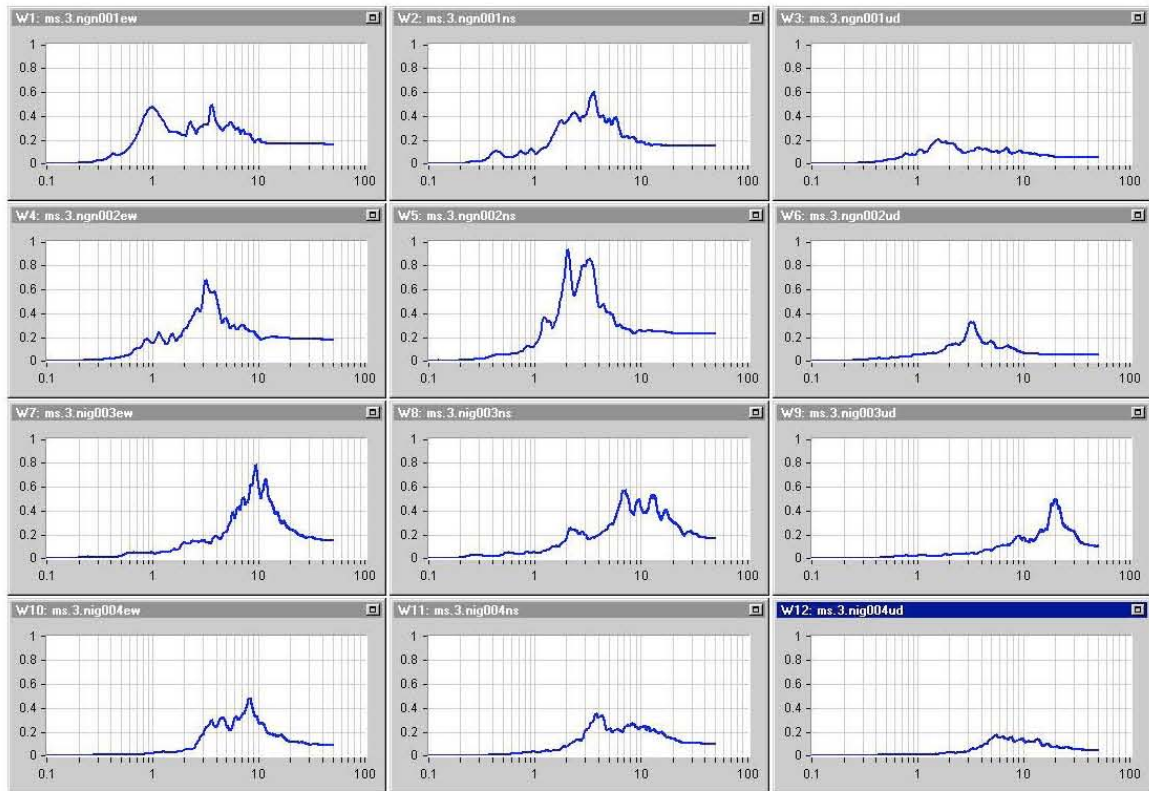


Figure 2.7d: 5% damped acceleration response spectra. From top to bottom: NGN001, NGN002, NIG003, NIG004. The horizontal axes represent frequency, in Hz, and the vertical axes represent absolute acceleration as a fraction of the acceleration of gravity. The left panel is the EW component, middle panel is the NS component, right panel is the Z component.

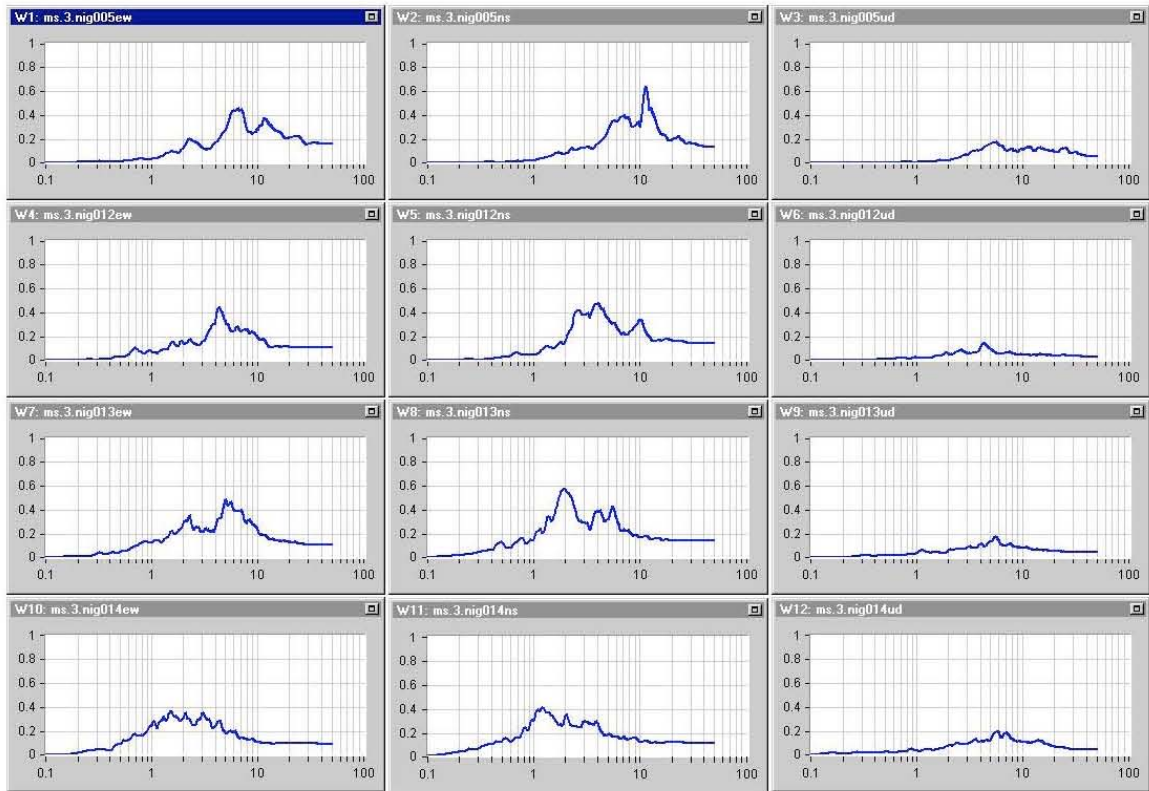


Figure 2.7e: 5% damped acceleration response spectra. From top to bottom: NIG005, NIG012, NIG013, NIG014. The horizontal axes represent frequency, in Hz, and the vertical axes represent absolute acceleration as a fraction of the acceleration of gravity. The left panel is the EW component, middle panel is the NS component, right panel is the Z component.

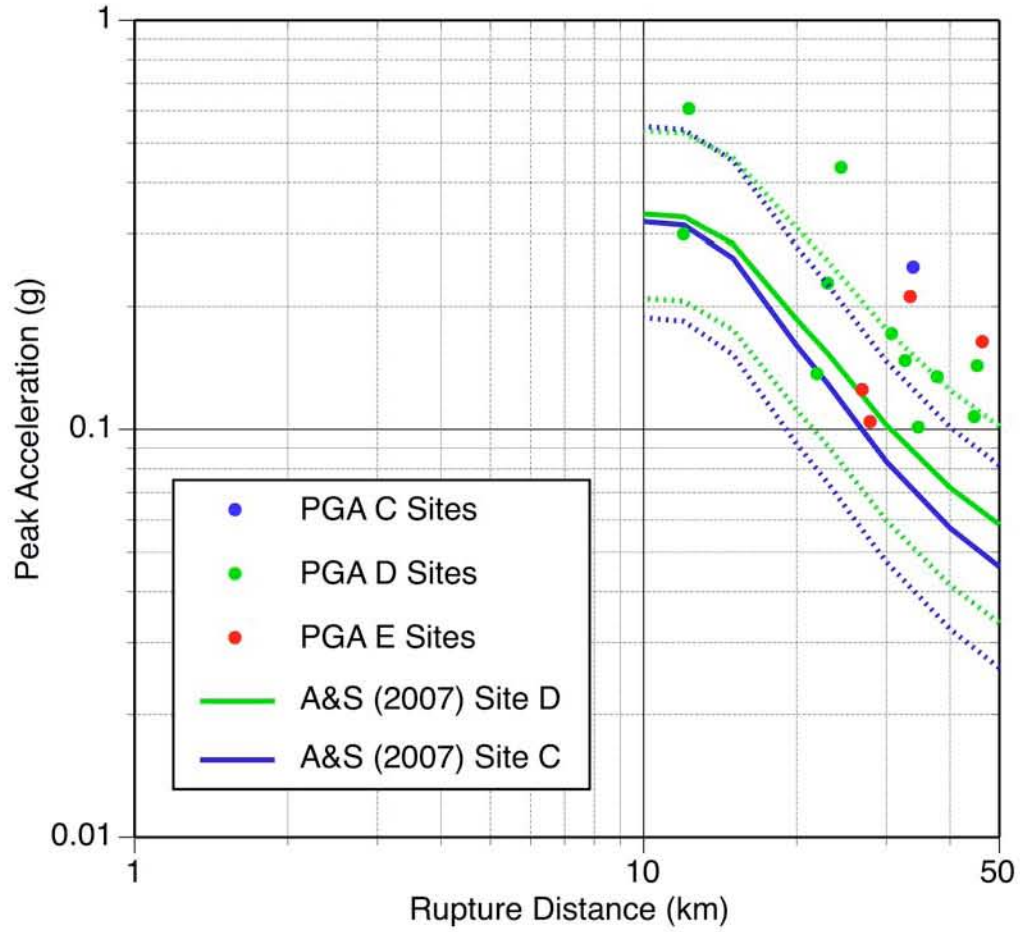


Figure 2.8a: PGA attenuation based on the southeast dipping source model. The Abrahamson and Silva model is for the hanging wall (HW) since most recording are on the HW side.

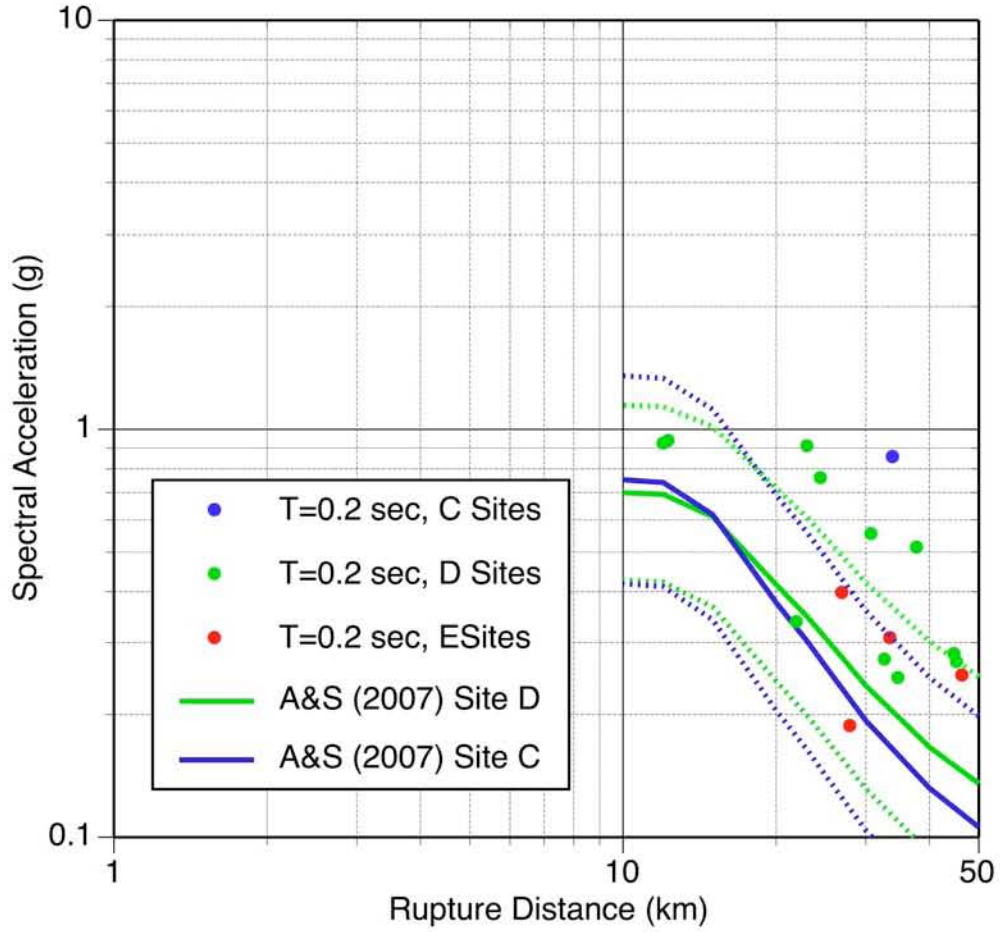


Figure 2.8b: T=0.2 attenuation based on the southeast dipping source model. The Abrahamson and Silva model is for the HW since most recording are on the HW side.

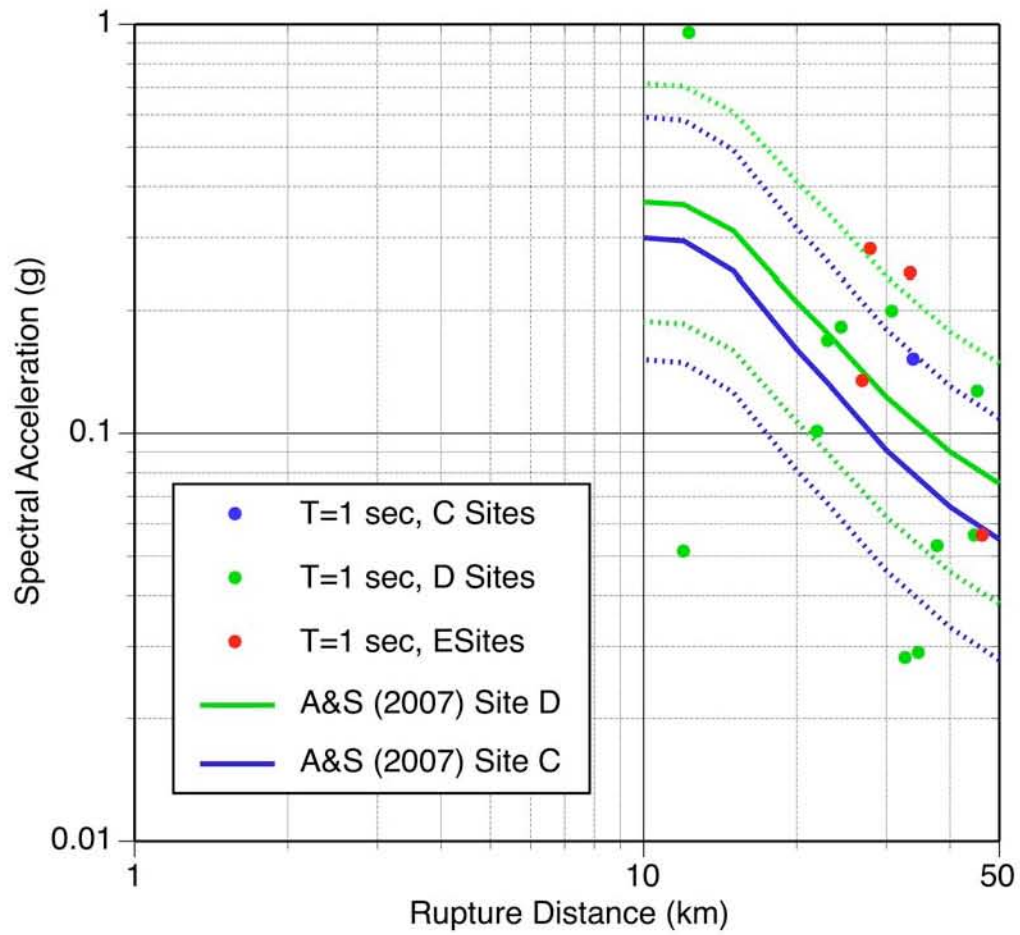


Figure 2.8c: T=1 sec attenuation based on the southeast dipping source model. The Abrahamson and Silva model is for the HW since most recording are on the HW side.

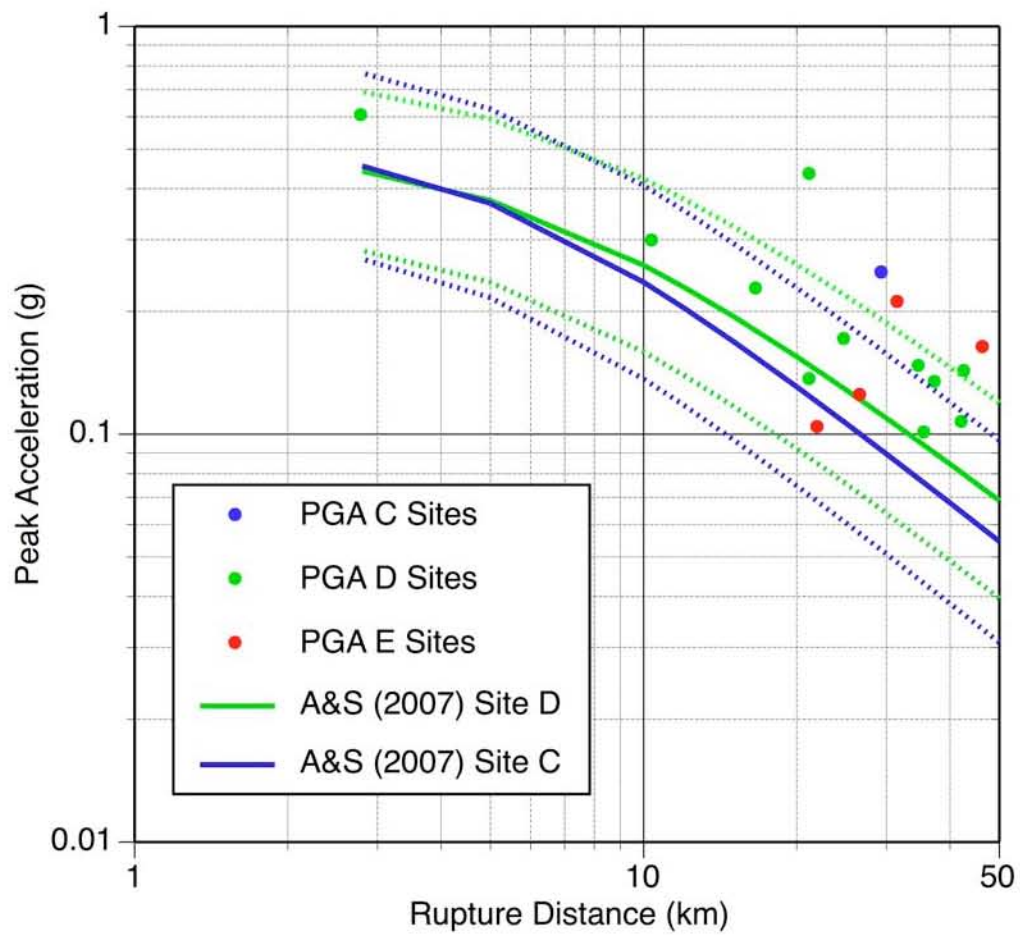


Figure 2.9a: PGA attenuation based on the northwest dipping source model. The Abrahamson and Silva model is for the FW since most recording are on the FW side.

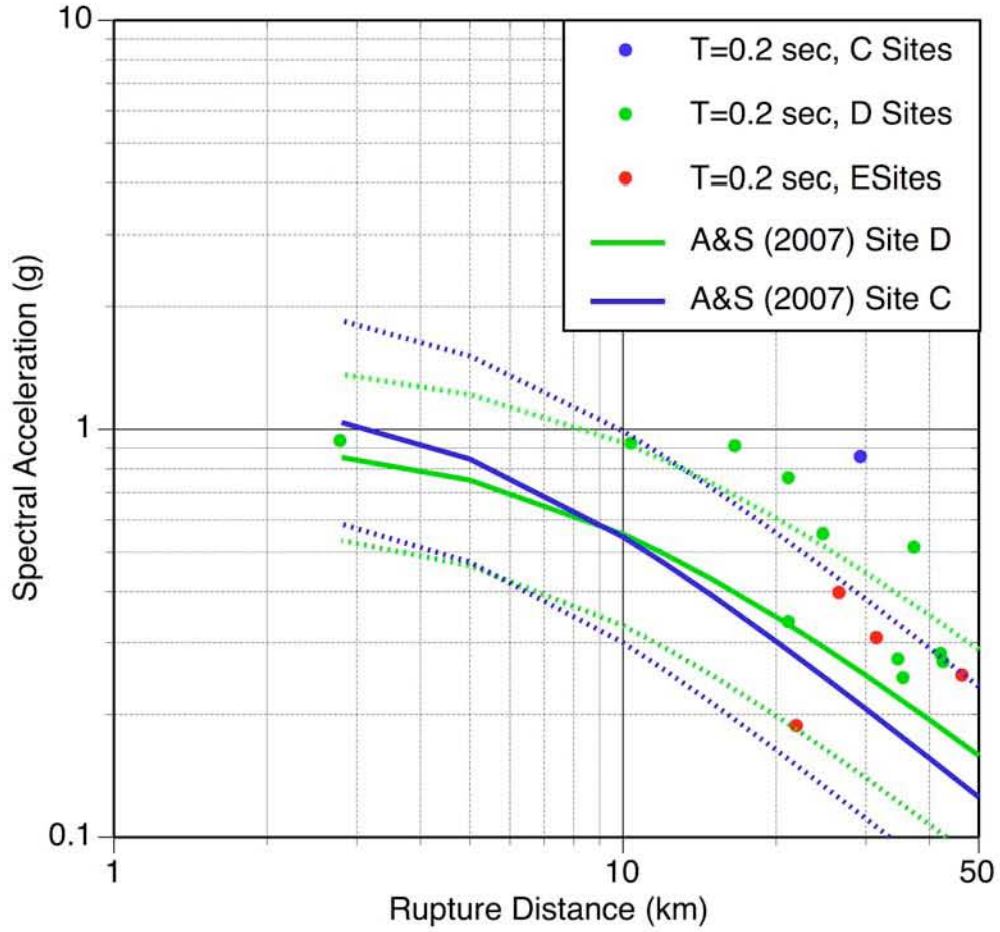


Figure 2.9b: T=0.2 sec attenuation based on the northwest dipping source model. The Abrahamson and Silva model is for the FW since most recording are on the FW side.

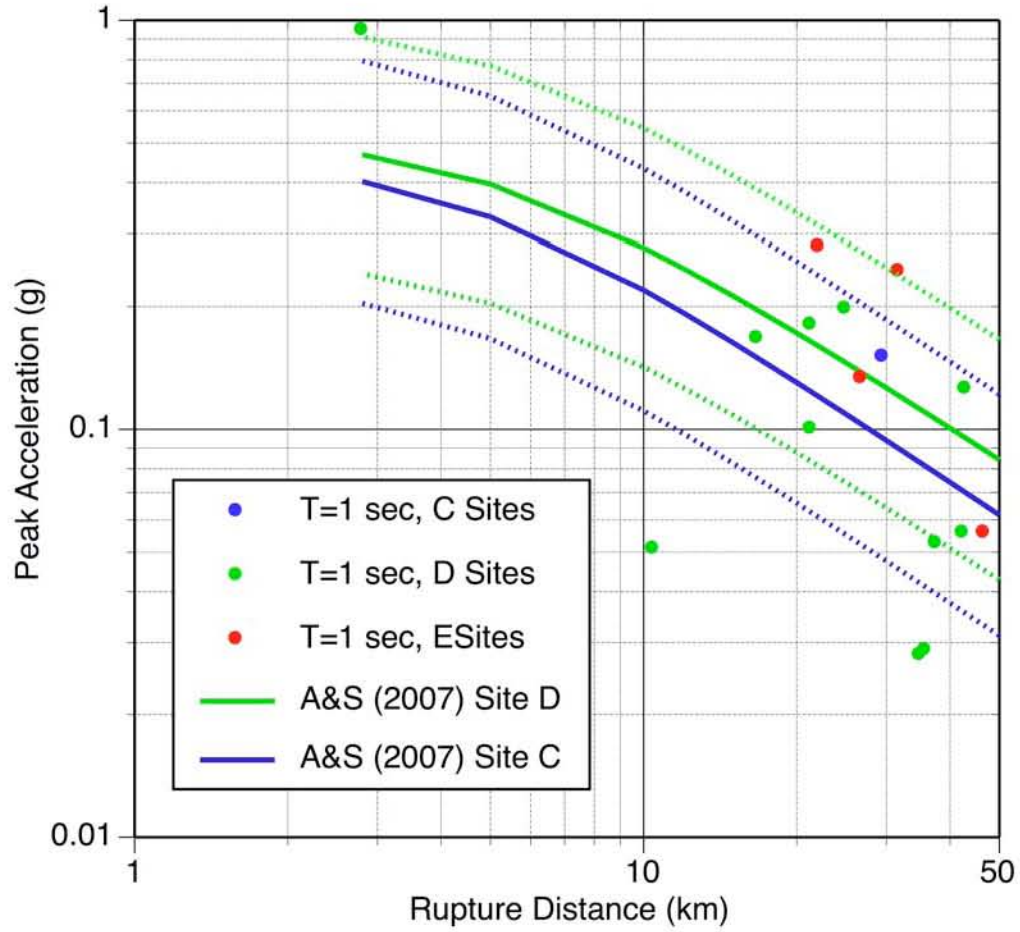


Figure 2.9c: T=1.0 sec attenuation based on the northwest dipping source model. The Abrahamson and Silva model is for the FW since most recording are on the FW side.



Fig. 2.10: Aerial Photograph of Kashiwazaki-Kariwa Nuclear Power Plan Area (GSI, 2007)

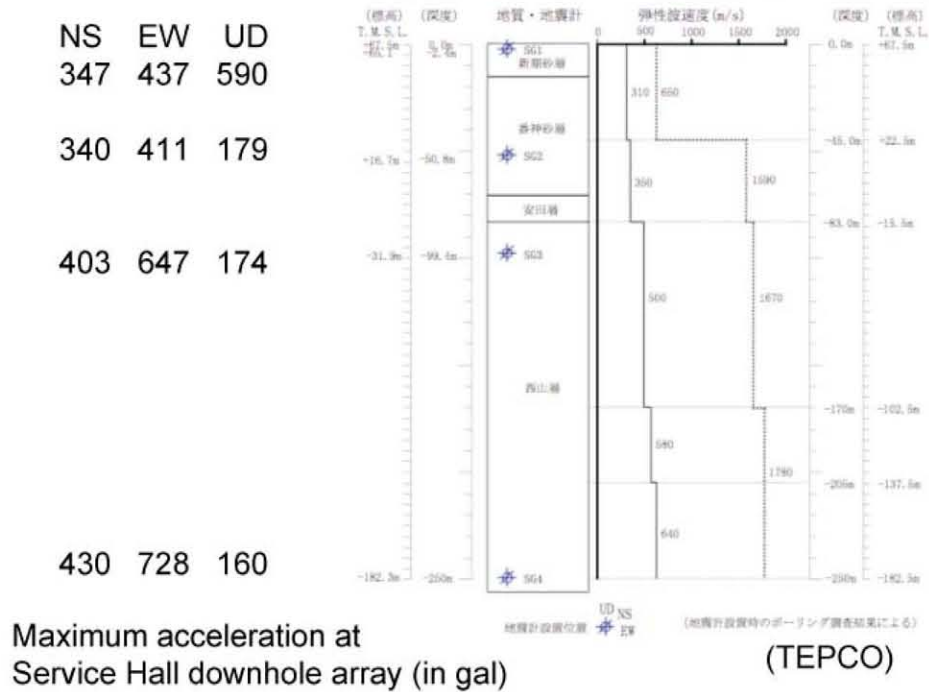


Fig. 2.11: Peak accelerations at Service Hall downhole array (after TEPCO,2007)

Recorded Maximum Acceleration in EW direction (in gal)

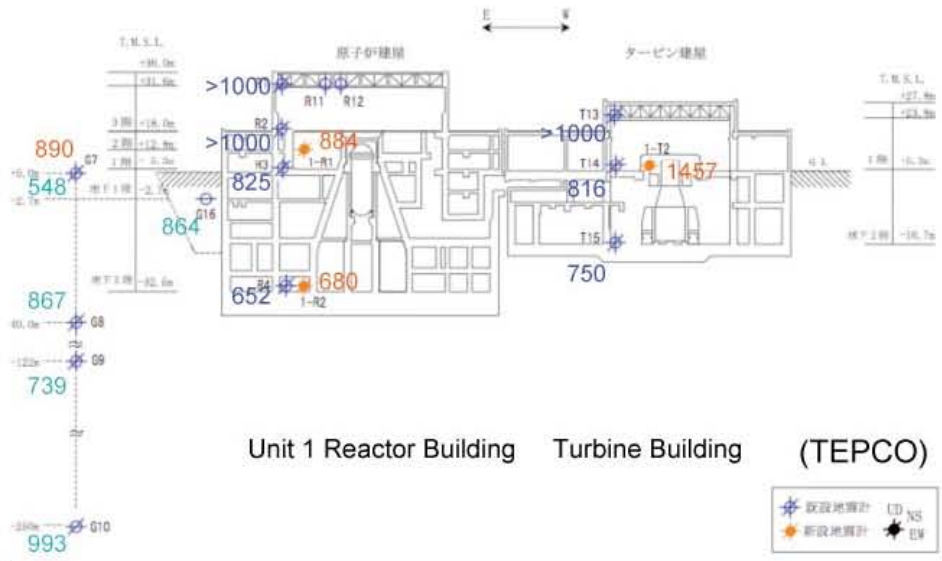


Fig. 2.12: Peak accelerations in and around Unit 1 (from TEPCO, 2007)

Recorded maximum Acceleration in EW direction (in gal)

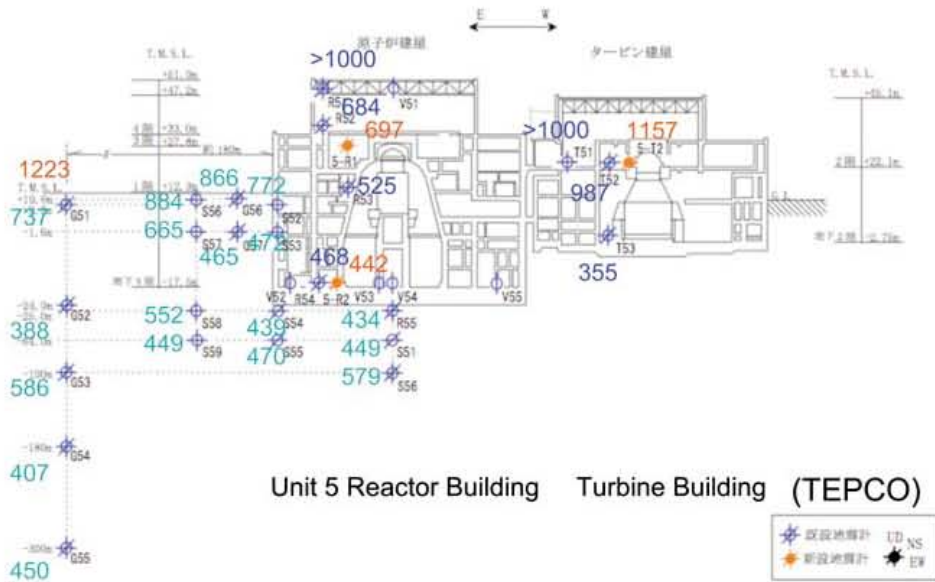


Fig. 2.13: Peak accelerations in and around Unit 5 (From TEPCO, 2007)

Section 3 - Landslides

Landslides caused by the earthquake consisted of shallow translational slides, debris slumps, and deep-seated rotational slides. Although the area had experienced a recent typhoon, soils were generally not sufficiently wet to cause debris flows.

In general, landslide activity was focused near the coast, with many steep ($50^{\circ} +$) slopes experiencing shallow landsliding of overlying colluvial debris and residual soils (Figs. 3.1 - 3.4). Additional landslides also occurred some distance away from the main damaged areas (~10 km northeast of Kashiwazaki and 7 km east of the Kashiwazaki-Kariwa Nuclear Power Plant) in an upland, mountainous region. These slides also generally consisted of shallow translational events, but with at least one debris slump. Where transportation lines crossed areas of steep terrain, landslides often blocked or destroyed whole sections of roadways and railways. Three major transportation routes were blocked by landsliding in the region - the coastal road (Route 353) to the north of the Kashiwazaki-Kariwa Nuclear Power Plant (Fig. 3.2), the railway to the south of Kashiwazaki, at the Oumigawa train station on the Shin-etsu Line (Fig. 3.5) and Highway 8, north of the intersection with Route 252 located inland from the coast (Fig. 3.6).

An area of dense landslide activity not investigated by the field reconnaissance team, but identified through helicopter reconnaissance by the Japanese Public Works Research Institute (PWRI - a research agency under the Japanese Ministry of Infrastructure) was identified approximately 20 km to the southeast of Kashiwazaki in the Takayanagi-Machi region. Their photos identify at least 10 landslides in this area and were graciously lent to the reconnaissance team for study. According to the images, each of the slides appears to be relatively shallow and translational in movement and occurred within heavily vegetated upland areas. Because this area is located a significant distance away from other observed landslides from the earthquake, it is anomalous to the general pattern of observed seismic-induced geotechnical and structural damage and should be investigated more thoroughly.

Shallow coastal landslides were observed to be between 0.5 to several meters deep in colluvial and residual soils and ranged from 5 m^3 to several thousand cubic meters in volume. Typical slope surface and failure plane inclinations were between 50° and 70° , failing in translation as debris slides and slumps. These types of landslides were of sufficient size to close major transportation routes in the region, among them, the southern, coastal rail line and the coastal road (Route 352) located north of the Nuclear Power Station.

A large, deep, rotational slide occurred in weak mudstones and colluvial materials fairly far (~10 km) inland from the coast. The Ozumi Senbon landslide (Fig. 3.6) consisted of approximately $150,000 \text{ m}^3$ of total displaced material and led to destruction of a large road section on Route 8. According to on-site construction personnel, the slide plane was located at a depth ranging between 6 and 11 meters. Nearby to this site, several debris slumps/colluvial slides were also observed, however these required only

minimal grading efforts and maintenance to keep channels open for rice farming irrigation (Fig. 3.7).

Embankment failures were typical in road fills along the coast (Fig. 3.8), and were also observed at three sites located further inland (e.g. Figs. 3.9 - 3.10). Embankments underwent from 10 cm up to one meter of vertical displacement (Fig. 3.8), extending between 10 and to 60 meters in length. Three embankment failures required full closures of roads, and/or protection with tarps to reduce rainfall infiltration and the associated potential for additional movement. Among these was a 15-meter high, 97.5-meter wide, earth-fill dam located to the east of the region (Fig. 3.9), where cracking through the midpoint of the crest was observed. However, the dam was not storing water at the time of our visit and the reservoir had not been filled recently. Further, from on-site design documents, it appears that the normal water level is typically 8 meters below the crest of the dam. At a water supply dam located southwest of the city of Kashiwazaki (Fig. 3.10), cracking of the crest was also observed along with minor concrete cracking and spalling on the upstream side. Here, the reservoir water level was within several meters of the dam crest at the time of observation.



Figure 3.1: Shallow colluvial landslide located just north of the Kasashima Fishing Village, Site RK22/SA10; N37.33802° E138.46995°, photos taken 7/20/07 15:57 (top) and 7/21/07 13:35 (bottom). Dimensions are approximately 36 m wide, 24 m tall, 2 m thick. The lithology is composed of 24 m of weak mudstone overlying 6 m of more indurated, brecciated mudstone, which outcrops at the road. A 10 m tall concrete seawall leads down to the brecciated mudstone shore platform. The slide occurred in weak mudstone/colluvium, sliding over the brecciated mudstone, onto the road, and over the edge of the concrete seawall, spilling debris onto the shore platform at ocean's edge.



Figure 3.2: Coastal landslides on Highway 352 north of Kashiwazaki-Kariwa Nuclear Power Plant at road closure south of Route 373 (Site RK34; N37.48455° E138.62435°, photos taken 7/22/07 at approx. 10:45). This area consisted of at least eight individual slides. The landslide shown in the bottom photo consists of a slide in an area of previous instability - a shotcrete stabilization system is in effect for the bottom 50 m of this slope (total slope height is ~115 m), and overlain with a wire-mesh rock deflection system. The slide is approximately 50 to 60 m wide, 65 m long, and less than 1 meter thick. The landslide initiated above the shotcrete slope, moved into the wire-mesh and caused failure of the meshing and pull-out of the steel supports. The wire-mesh restrained most of debris, depositing the majority on the road, with only a slight quantity of the debris sliding over the road edge. The failure plane inclination is approximately 60°.



Figure 3.3: Coastal landslides on Highway 352 north of Kashiwazaki-Kariwa Nuclear Power Plant at road closure south of Route 373 (Site RK34-Slide 4; N37.48455° E138.62435°, photos taken 7/22/07 at approx. 10:45). This landslide is typical of many of those observed along the coast, and in this case did not damage transportation lines. Slide is approximately 10 m wide, 25 m long, and 0.5 m thick. Failure plane has approximate 50° inclination.



Figure 3.4: Yoneyama Landslide, located south of Kashiwazaki (Site YT17; N37.32223° E138.43828°, photos taken 7/21/07 at approximately 15:20). This slide marked the southwest-most limit of observed landslides along the Sea of Japan coast. The slide extended to the full height of the slope and blocked a paved coastal access road.



Figure 3.5: Landslide at the Oumigawa Train Station on the Shin-etsu Line (Site RK20/SA9/YT16; N37.34200° E138.48888°, photos taken 7/21/07 12:48 (top) and 7/24/07 15:00 (bottom)). This was among the largest of the coastal landslides to the south of Kashiwazaki. Site access was not possible due to construction repairs. Note that slope stability in this area has been a problem, as seen by the railway tunnel protection structure immediately behind (to the south) of this landslide. Many more smaller landslides were observed to the north and south of this location.



Figure 3.6: Ozumi Senbon Landslide at Highway 8 north of intersection with Route 252 (Site RK1/YT1; N37.41422° E138.71347°, photos taken 7/20/07 10:24 (top) and 7/23/07 13:04 (bottom)). This slide is approximately 150 meter wide, 100 meters long and 10 meters deep. According to construction personnel at the site during the reconnaissance, the slide plane occurred near the colluvial/bedrock interface, at a depth of between 6 and 11 meters. Signs of rotational movement were noted from back-rotated guardrails at the toe of the slide. This landslide forced closure of both lanes of traffic along Highway 8, just north of the intersection with Route 252, however both lanes had been reopened as early as 8 days following of the earthquake when reconnaissance team members revisited the site. Bottom photo shows excavated slide and subsurface bedrock lithology and structure.



Figure 3.7: Ozumi-Mishimayamachi Landslides (Site RK2/YT2; N37.44057° E138.70467°, photos taken 7/20/07 at approximately 11:30). These slides occurred on a native hill slope and consisted of debris slumps in mudstone/siltstones and colluvium materials. High-resolution, topographic data was collected of these landslides using the terrestrial LiDAR scanning method.



Figure 3.8: Road embankment failure off Route 8 on the way to Kasashima (Site YT18; N 37.33325 ° E 138.46500°, photos taken 7/21/07 at approximately 15:40). The slope appears to have undergone previous stabilization using slope grading and gabion baskets to support the toe.



Figure 3.9: Embankment cracking and settlement of South Dam near Miyamo Parking Area along Highway 8, Nagaoka-Shi region (Site RK50; N37.43267° E138.73674°, photos taken 7/23/07 at approximately 11:15). The dam is a 15-meter tall, 97.5-meter wide earth fill structure with 3(H):1(V) downstream and 3.5(H):1(V) upstream benched slopes. Crest elevation is 63 meters and normal pool elevation is 55 meters. Observations were made of an embankment slope failure along the crest of this dam, through half the crest width (~4 m). Settlement and deformation occurred along a 10 m long section with up to 4 cm each of lateral and vertical deformation in the down slope direction. Contour-parallel ground cracking (2-4 cm wide, 1-2 m long) along the ground-spillway interface were also observed, two-thirds of the way down the dam face. The reservoir was empty and appeared to not have been filled in some time judging by the height of vegetation growing in the reservoir area.



Figure 3.10: Embankment cracking at the crest of Kawauchi Dam, constructed in 1938. (Site YT19; N37.33635° E138.52410°, photos taken 7/21/07 at approximately 16:20).

Section 4 - Liquefaction

Liquefaction was observed from the southern port of Kasashima to Shiya village, north of the Kashiwazaki-Kawira Nuclear Power Plant. Liquefaction evidence was seen in four general settings, riverbank deposits, beach deposits, dune sand, and placed fill. Locations where liquefaction was observed are noted in the Google Earth file accompanying this report. A photo log showing major sites of liquefaction is included in Figures 4.1 through 4.39.

Along the Sabaishi River, located to the north of the city of Kashiwazaki, liquefaction and lateral spreading features were observed for approximately five kilometers from the river mouth to the village of Shimo-Oshinden. River deposits near the mouth of the river underwent extreme settlement at the Kashiwazaki wastewater treatment plant (Figs. 4.15 - 4.17; Site RK9) on the south bank of the Sabaishi River. Nearby, on the north bank, settlement of the river levee embankment west of the Kai-Un Bridge (Figs. 4.3 - 4.9; Site RK4) led to up to one meter of lateral displacement. On the opposite side of the river, east of the bridge, embankment settlement led to pipe separation of a large water main crossing the river. Extensive evidence of liquefaction was observed in this area with ejecta of the underlying sand and an uplifted underground tank near the base of the water-pipe bridge abutment. Moving inland towards the east and across the river, on the north side, a large lateral spread (Figs. 4.11 - 4.13; Site RK6) along the river bank cut into the neighborhood immediately east of the municipal incinerator (Site RK5). The trend of the head scarp of the lateral spread was in alignment with the edge of the levee settlement on the south side of the river. It may be that the liquefaction observed in this portion of the Sabaishi River occurred along an old meandering channel of the river that now underlies the neighborhoods adjacent to the trained-river.

The U River, located in the southwestern portion of Kashiwazaki City, was further from the epicentral region and exhibited less liquefaction damage. All liquefaction sites along this river were observed within one kilometer of the mouth of the river (Site SA13). In general, these sites experienced relatively small amounts of settlement, with the exception of a localized failure at a bridge located to the north of the nearby JR rail line (SA13), which experienced nearly one meter of settlement.

A long, coast-parallel, surficial unit of dune sand extends north of the city. This deposit was the source of numerous liquefaction failures, particularly along the edge of the modern flood plain. The sand was typically very soft under foot, and may have been reworked in areas by the ancient, meandering Sabaishi River. One site of liquefaction, (Figs. 4.33 - 4.35; Site RK40), had 40 cm of settlement, and minor lateral spreading around the foundation pile cap of a large high-voltage power transmission tower. Though the soil pulled away from the cap, the pile cap and tower had no indication of deformation. On the eastern slope of this dune, south of the tower, a lateral spread damaged a shopping center structure, buckling the floor slab in a compression failure (Figs. 4.36 - 4.39; Site RK41). Approximately one quarter of this warehouse discount shopping center building was damaged by the lateral movement of the ground and closed

to the public.

Sandy fill deposits used for backfill performed poorly throughout the epicentral region. Poorly compacted backfill of the wastewater and storm water drain network resulted in hundreds of uplifted manholes. These failures were localized to the backfilled trench of the drain, and had no apparent impact on surrounding structures. Uplifted manholes were a hazard to drivers and impeded traffic, as one-lane controls and resurfacing were needed to level the road grade around the manhole.

Ports and harbors suffered moderate levels of settlement and liquefaction-related lateral spreading. Following the event, all piers remained operable. In the south harbor of Kashiwazaki (Figs. 4.18 - 4.26; Site RK25/SA25), we saw evidence of caisson movement and lateral spreading towards the harbor. This site was scanned by terrestrial LiDAR for further analysis. At several locations north of the Kashiwazaki-Kawira Nuclear Power Plant (Figs. 4.27 - 4.32; Sites RK35, RK37), I-wall type seawalls founded on liquefied beach sand failed and rotated seaward between 50 and 70 cm. We observed diminishing severity of liquefaction effects as the teams drove away from Kashiwazaki and the nuclear power plant (Site RK33).

Liquefaction Figures

The following photo log is a catalog of example observations of liquefaction within these four settings: riverbank deposits, beach deposits, dune sand, and placed fill.

Site RK16 - Fujii Weir downstream from Tashiou Bridge crossing of river.

N 37.34875° E 138.61670°

Extensive cracking of levee embankment. Repairs were taking place to the levee/weir intersection with sand bags to support an embankment failure. We observed good performance of the weir, with no signs of damage. The control building suffered damage to the foundation with settlement of fill beneath the structure: 15 cm on downstream side of building at the retaining wall, 30 cm at the building, and 30 cm at the upstream side retaining wall that formed contributory channel. Three to four sets of transverse cracks parallel to the river ran through the embankment fill that the structure was built upon. Liquefaction and lateral spreading with ground cracks were observed upstream of the operations building and the contributory channel to the south.



Figure 4.1: Fujii Weir downstream from Tashiou Bridge crossing of river. (Site RK16; N 37.34875° E 138.61670° , visited 7/21/2007 11:28 am UTZ+8). Extensive cracking of levee embankment.



Figure 4.2: Fujii Weir downstream from Tashiou Bridge crossing of river. (Site RK16; N 37.34875° E 138.61670° , visited 7/21/2007 11:28 am UTZ+8). The control building exhibited damage to the foundation with settlement of fill beneath the structure.

Site RK4 - Kai-Un Bridge over Sabaishi River with water pipeline and surrounding area

N 37.39233° E 138.58063°

This area experienced liquefaction, lateral spreading, bridge-ground differential settlement, pavement cracking, structural damage, and embankment failure. We observed approximately one meter of ground extension consisting of several 10-20 cm wide cracks (covered by tarps) in a river levee embankment over a distance of 45 meters associated with lateral spreading. Near an adjacent bridge, we measured pipeline rupture and pipe offsets of 13 cm in the horizontal direction, 10 cm in the vertical direction, and with 40 cm of associated nearby settlement between the pipeline and the ground. In a nearby house to the south, extensive signs of liquefaction were observed with sand boils, uplifted manholes, and large-scale ground cracking. A nearby home had been red-tagged due to distortions that appeared to line up with ground cracks.



Figure 4.3: Kai-Un Bridge over Sabaishi River (Site RK4 N37.39233°, E 138.58063°, 7/19/2007, 1:40 p.m.). A water pipeline rupture was found with pipe offsets of 13 cm in the horizontal direction, 10 cm in the vertical direction, and with 40 cm of associated nearby settlement between the pipeline and the ground.



Figure 4.4: Kai-Un Bridge over Sabaishi River (Site N37.39233°, E138.58063°, 7/19/2007, 1:40 p.m.). A water cistern near the pipeline rupture uplifted in liquefied ground.



Figure 4.5: Kai-Un Bridge over Sabaishi River (Site RK4 N37.39233° E 138.58063°, 7/19/2007, 1:40 p.m.). Liquefaction induced crest cracking on the levee embankment near the northwest side of the bridge.



Figure 4.6: Kai-Un Bridge area Sabaishi River (Site RK4 N37.39233° E138.58063°, 7/19/2007, 1:40 p.m.). Numerous manholes on the southeast bank near the Sabaishi River uplifted in liquefied ground.



Figure 4.7: Kai-Un Bridge area Sabaishi River (Site RK4 N37.39233° E138.58063°, 7/19/2007, 1:40 p.m.). A sub-linear zone of lateral spreading, sand boils and settlement that may be associated with a buried shoestring sand deposit from the former channel of the Sabaishi River resulted in damage in the neighborhood immediately south of the Kai-Un Bridge.



Figure 4.8: Kai-Un Bridge area Sabaishi River (Site RK4 N37.39233° E138.58063°, 7/19/2007, 1:40 p.m.). A sub-linear zone of lateral spreading, sand boils and settlement that may be associated with a buried shoestring sand deposit from the former channel of the Sabaishi River resulted in damage in the neighborhood immediately south of the Kai-Un Bridge.



Figure 4.9: Kai-Un Bridge area Sabaishi River (Site RK4 N37.39233° E138.58063°, 7/19/2007, 1:40 p.m.). A sub-linear zone of lateral spreading, sand boils and settlement that may be associated with a buried shoestring sand deposit from the former channel of the Sabaishi River resulted in damage in the neighborhood immediately south of the Kai-Un Bridge. Here, settlement caused damage to a residential structure.

Site RK6 - Lateral spread on road to Kashiwazaki Incinerator Plant

N 37.39343° E 138.58555°

We observed lateral spreading, liquefaction, slope failures, and associated retaining wall failures at this site. This site was scanned with terrestrial LiDAR for documentation purposes and for further analysis. A massive embankment failure was observed to have occurred from liquefaction and lateral spread slope movement in aeolian sands. Movement was from north to south, from sand quarry area towards river. Vertical displacement of head scarp was a maximum of 2.8 m and diminished in height moving away from road crossing of head scarp. Measurements were made of total lateral displacement along a representative track-line through the failure representing the maximum likely displacement of the failure ~10 m over 55 m distance between head scarp and river edge (approximately 18% strain). The inclination of slope from road to river was measured to be approximately 14°. Nearby, a slope lateral spread caused failure of a 2.6-meter-tall, concrete block, gravity retaining wall, that resulted in the red-tagging of an otherwise undamaged home. The damaged retaining wall section was 25 meters in length and constructed of 40 cm by 30 cm by 100 cm sized concrete blocks. No backfill, drainage, or tieback reinforcement were observed.



Figure 4.11: North side of Kai-Un Bridge area of the Sabaishi River - Lateral Spread on road to Kashiwazaki Municipal Incinerator (Site RK6, N37.39343° E138.58555°, 7/19/2007). A zone of lateral spreading, sand boils and settlement crossing the present-day Sabaishi River, and that may be associated with a buried shoestring sand deposit of a former channel, resulted in failure of a road on the north side of the river adjacent to the Kashiwazaki Municipal Incinerator.



Figure 4.12: North side of Kai-Un Bridge area of the Sabaishi River - Lateral Spread on Road to Kashiwazaki Incinerator (Site RK6, N37.39343° E138.58555°, 7/19/2007). A zone of lateral spreading, sand boils and settlement crossing the present-day Sabaishi River, and that may be associated with a buried shoestring sand deposit of a former channel, resulted in failure of a road on the north side of the river adjacent to the Kashiwazaki Municipal Incinerator.



Figure 4.13: North side of Kai-Un Bridge area Sabaishi River - Lateral Spread on Road to Kashiwazaki Incinerator (Site RK6, N37.39343° E138.58555°, 7/19/2007). Lateral spreading on the north side of the river adjacent to the Kashiwazaki Municipal Incinerator damaged the access road of the facility.

Site RK9 - Kashiwazaki Wastewater Treatment Plant

N 37.38748° E 138.56587°

We observed structural failures to the main building, liquefaction of ground resulting in extensive road damage, and minor tank damage. The main feature at this site was the complete separation of two adjacent, yet integrated, three-story buildings with associated building and ground settlements, as well as pipe breaks between the two sections of the building. Severe road and pavement damage were also observed as a result of liquefaction - nearby areas of sand boils were noted.



Figure 4.15: Kashiwazaki Wastewater Treatment Plant on the south side of Sabaishi River near the Sea of Japan (Site RK9 N37.38748° E138.56587°, 7/19/2007). Damage to the main building from liquefaction of ground resulted in meter-scale ground settlements.



Figure 4.16a: Kashiwazaki Wastewater Treatment Plan on the south side of Sabaishi River near its outlet to the Sea of Japan (Site RK9 N37.38748° E138.56587°, 7/19/2007). Damage to the main building from liquefaction of ground resulted in the complete separation of two sections of the adjacent, yet integrated, three-story buildings with associated building and ground settlements.



Figure 4.16b: Kashiwazaki Wastewater Treatment Plan on the south side of Sabaishi River near its outlet to the Sea of Japan (Site RK9 N37.38748° E138.56587°) Pipe breaks are due to separation of two adjacent building sections (Photo taken at 7/21/07 9:15)



Figure 4.17: Kashiwazaki Wastewater Treatment Plant on the south side of Sabaishi River near its outlet to the Sea of Japan (Site RK9 N37.38748° E138.56587°, 7/19/2007). Liquefaction features were abundant near the wastewater treatment facility.

Site RK25/SA25 - Kashiwazaki Harbor - South area

N37.36713° E138.53210°

This area experienced ground damage from liquefaction induced lateral spreading. We observed sand boils in the grassy area behind the port office building and on the west end of the pier between separated pier slab sections. Some areas of concrete had 15 cm of vertical and 20 cm of lateral displacement. A track-line measurement was performed with a cloth tape. Measurements indicate that 0.7 m of lateral displacement occurred over 79 meters resulting in 0.9% strain, as measured between the seawall on the west to the edge of the pier to the east. The displacement direction was inland to the east. Terrestrial LiDAR scanning was performed at this site.



Figure 4.18: Kashiwazaki Harbor - South area experienced ground damage from liquefaction induced lateral spreading and settlement of separated pier slab sections (Site RK25, N37.36713° E138.53210°, 7/20/2007).



Figure 4.19: Kashiwazaki Harbor - South area experienced ground damage from liquefaction-induced lateral spreading and settlement immediately adjacent to the pile-supported port office building. (Site RK25, N37.36713° E138.53210°, 7/20/2007).



Figure 4.20: Kashiwazaki Harbor - South area experienced ground damage from liquefaction-induced lateral spreading resulting in separated pier slab sections (Site RK25, N37.36713° E138.53210°, 7/20/2007).



Figure 4.21: Kashiwazaki Harbor - The southern area experienced ground damage from liquefaction-induced lateral spreading and settlement. A harbor-front caisson rotated toward the harbor, to the left of the photo, initiating lateral displacement of the soil behind it, between the caisson and port building (Site RK25, N37.36713° E138.53210°, 7/20/2007).



Figure 4.22: Kashiwazaki Harbor - The southern area experienced ground damage from liquefaction-induced lateral spreading and settlement. We observed settlement immediately adjacent to the pile supported port office building. (Site RK25, N37.36713° E138.53210°, 7/20/2007).



Figure 4.23: Kashiwazaki Harbor - The southern area experienced ground damage from liquefaction-induced lateral spreading and settlement. A harbor-front caisson rotated toward the harbor, uplifting the asphalt and tiled section shown here and initiating lateral displacement of the soil behind it, between the caisson and port building (Site RK25, N37.36713° E138.53210°, 7/20/2007).



Figure 4.24: Kashiwazaki Harbor - South area experienced ground damage from liquefaction-induced lateral spreading and settlement, here seen from a mound of riprap (Site RK25, N37.36713° E138.53210°, 7/20/2007).



Figure 4.25: Kashiwazaki Harbor - South area experienced ground damage from liquefaction-induced lateral spreading and settlement. A harbor front caisson rotated toward the harbor, to the left of the photo, initiating lateral displacement of the soil behind it, between the caisson and port building. Settlements can also be seen in this photo. (Site RK25, N37.36713° E138.53210°, 7/20/2007)



Figure 4.26: Kashiwazaki Harbor - South area exhibited surficial features of liquefaction on all sides of the port building. (Site RK25, N37.36713° E138.53210°, 7/20/2007).

Site RK35 - Road and Seawall Failure

N37.48497° E138.62645°

Liquefaction of beach sand led to lateral spreading of a road embankment and both rotation and translation of a 30-meter-long segment of concrete seawall. Deformations were on the order of 25 cm vertical, and up to 64 cm horizontal, with a component of rotation as measured by 32 cm lateral deformation at the base of wall and 64 cm lateral deformation at 2m height of wall.



Figure 4.27: Liquefaction of beach sand led to lateral spreading of a road embankment and both rotation and translation of a 30-meter-long segment of concrete seawall. (Site RK35, N37.48497° E138.62645°, 7/22/2007).



Figure 4.28: Liquefaction of beach sand resulted in lateral spreading, above, in front of a 30-meter-long segment of concrete seawall. (Site RK35, N37.48497° E138.626°, 7/22/2007)



Figure 4.29: Liquefaction of beach sand led to lateral spreading of a road embankment and both rotation and translation of a 30-meter-long segment of concrete seawall. (Site RK35, N37.48497° E138.62645°, 7/22/2007). Deformations were on the order of 25 cm vertical, and up to 64 cm horizontal, with a component of rotation as measured by 32 cm lateral deformation at the base of wall and 64 cm lateral deformation at 2 m height of wall.



Figure 4.30: Concrete seawall deformations were on the order of 25 cm vertical (failed section up), and up to 64 cm horizontal, with a component of rotation as measured by 32 cm lateral deformation at the base of wall and 64 cm lateral deformation at 2 m height of wall. (Site RK35, N37.48497° E138.62645°, 7/22/2007).

Site RK37 - Seawall Failure

N 37.45478° E138.60927°

Embankment failure and lateral spread from liquefaction of beach sands at toe of seawall. We measured 21 cm of vertical displacement and 55 cm of horizontal displacement of a wall section from an adjacent non-failed wall section. The total length of failed sections was 40 m.



Figure 4.31: Seawall Failure as a result of embankment movement into a seawall founded on top of liquefied beach sands. (Site RK37, N37.45478° E138.60927°, 7/22/2007).



Figure 4.32: Lateral spreading related ground cracking in front of seawall. (Site RK37, N37.45478° E138.60927°, 7/22/2007).

Site RK40 - High Voltage Transmission Line Tower and Railroad Tracks

N 37.41633° E138.60792°

Liquefaction and lateral spread of dune sand adjacent to tower footings. We measured 40 cm of vertical displacement and 12 cm of horizontal displacement over a 20-meter track-line moving away from the footing for 0.6% of measured ground strain.



Figure 4.33: Liquefaction and lateral spread of ground adjacent to High Voltage Transmission Line Tower (Site RK40, N37.41633° E138.60792°, 7/22/2007).



Figure 4.34: Lateral spreading in dune sand down slope of high voltage power transmission tower. We measured 0.6% of ground strain at the site. (Site RK40, N37.41633° E138.60792°, 7/22/2007).



Figure 4.35: Settlement of ground adjacent to grade beam between footings of a high voltage transmission line tower (Site RK40, N37.41633° E138.60792°, 7/22/2007).

Site RK41 - Plant 5 Store

N37.41468° E138.60840°

We observed structural damage and ground settlement of a large warehouse-type department store. The interior columns were deformed and leaning, and the interior floor slab reinforcing bars had buckled and were exposed. Reinforcing bars and concrete also failed at a corner of the building. Ground settlement was observed around the building and an underground storage tank had been uplifted (this was the only obvious sign of liquefaction).



Figure 4.36: Plant 5 Store - Ground settlement in dune sand was observed around the building and an underground storage tank had been uplifted (Site RK41, N37.41468° E138.6084°, 7/22/2007).



Figure 4.37: Plant 5 Store showing foundation corner area of failed reinforced concrete. (Site RK41, N37.41468° E138.60840°, 7/22/2007).



Figure 4.38: Plant 5 Store - Ground settlement in dune sand was observed around the building and an underground storage tank had been uplifted (Site RK41, N37.41468° E138.60840°, 7/22/2007).



Figure 4.39: Plant 5 – Failure of slab on grade with buckled reinforcing bars. (Site RK41, N37.41468° E138.60840°, 7/22/2007).

Site YT24 – Deep-seated Lateral Flow of Kashiwazaki Downtown Nishi-Honmachi Area
N 37.36896° E 138.54829° at center

Damage to old wooden houses were concentrated in the downtown area of Kashiwazaki City where the old sand dune deposit is thought to cover the most of the area. Because of strong shaking in these sand deposits with water level at some depth below the surface, a deep seated lateral flow of ground appears to have occurred, resulting in various surface ground distortions in the Nishi-Honmachi area. This hypothesis was first presented by Prof. Konagai of Univ. of Tokyo who conducted a reconnaissance of the area immediately after the quake (July 17, 2007). Yellow markers in Fig. 4.40 show the locations where EERI & GEER team identified signs of ground lateral flow. Photos of each of these areas can be viewed in the Google Earth database available through the USGS website. The ground movement occurred typically from areas of higher elevation to lower elevation, and we observed open tension cracks at higher ground and compressive heaves in lower ground. Fig.4.41 (SiteYT24_YT_19 as shown in Fig. 4.40) shows the ground distortion near a department store building that seems to be supported by deep foundation and shows no major structural damage. The road on the hill side (northern side) settled and moved downwards to result in the large opening and distortion at the road side.

The reconnaissance was made to define the extent of such a deep-seated lateral flow from ground surface distortions. Fig. 4.42 (Site YT24-YT_03 in Fig. 4.40) shows damage at the north-western limit, whereas Fig. 4.43 (Site YT24-YT_14 in Fig. 4.40) shows damage at the south-eastern limit. Thus, the area covered between Fig. 4.42 and Fig. 4.43 may have suffered deep seated lateral flow from higher ground to lower ground. The damages due to such lateral flow extend to the north-eastern direction of downtown. The arcaded street next to (east) Fig. 4.43 (Site YT24-YT_14 in Fig. 4.40) was closed because of heavy structural damages of shops along the street.



Fig. 4.40: Downtown Kashiwazaki Lateral Spread Overview (Adapted from Google Earth[®])



Fig. 4.41: Downtown Kashiwazaki Lateral Spread (SiteYT24, N37.36949°, E138.5541°, photo taken 7/22/07, SiteYT24_YT_19 as shown in Fig. 4.40).



Fig. 4.42: Downtown Kashiwazaki Lateral Spread (SiteYT24, N37.36963°, E138.5486°, photo taken 7/22/07, SiteYT24_YT_03 as shown in Fig. 4.40).

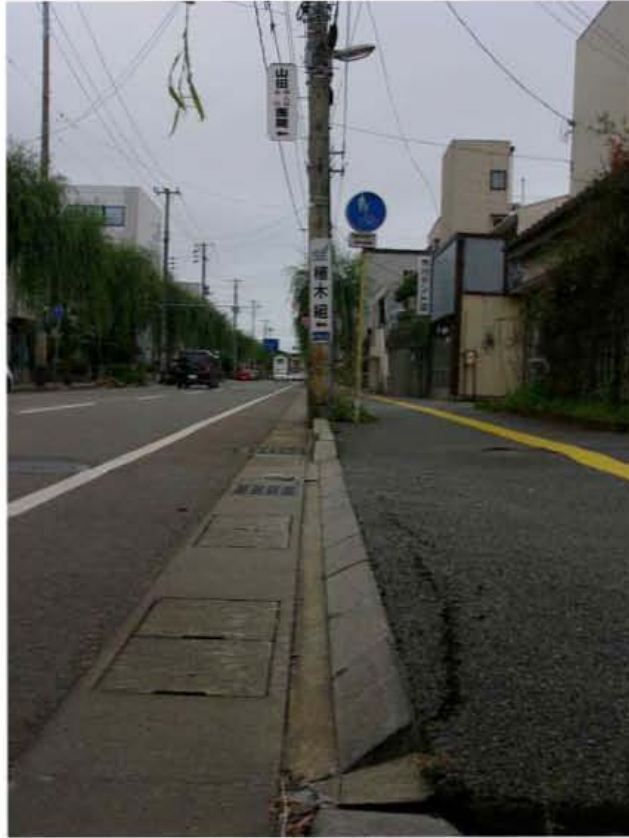


Fig. 4.43: Downtown Kashiwazaki Lateral Spread (SiteYT24, N37.36731°, E138.5522°, photo taken 7/22/07, SiteYT24_YT_14 as shown in Fig. 4.40).

Section 5 - Building and Industrial Structures

5.1 Introduction

The Earthquake of July 16 2007 caused the collapse of nearly eleven hundred houses in the Niigata prefecture in Japan. This section concentrates on observations made by a team of researchers sponsored by JAEE, EERI, and PEER on the response of engineered building structures, the Kashiwazaki-Kariwa Nuclear Power Plant and a smokestack at a recycling facility. Damage to one-to-three story wood buildings was observed along the 30-kilometer-long coastal region between Hatsusaki, to the south, and Shiya, to the north. Damage extended inland to western Nagaoka, 12 kilometers west of the coast.

On the fringes of the damage zone, damage to tile roofs and isolated collapses of residential storage structures and older houses were observed. Kashiwazaki reported the highest number of collapses in the region. Table 5.1 provides information on the distribution of fatalities and damage reported by the local press.

Table 5.1. Distribution of fatalities and damage reported by the local press

Town	Impact on Population		Impact on Housing		
	Fatalities	Injuries	Total Collapse	Partial Collapse	Other Damage
Niigata		12		1	28
Nagaoka		243	8	281	2694
Sanzyo		32			347
Kashiwazaki	10	1339	908	1912	20198
Oziya		40			99
Tokamachi		8		5	58
Tsubame		10	2	4	628
Myoko		0		2	26
Zyoetsu		132	13	43	2220
Uonuma		6			2
Minamiuonuma		4			4
Izumosaki		10	17	84	719
Kariwa	1	105	148	347	436
Kamo		0			
Yuzawa		1			
Mitsuke		14			341
Sado		0			
Agano		0			1
Itoigawa		1			6
TOTAL	11	1957	1096	2679	27807

5.2 Observations

The Kashiwazaki-Kariwa Nuclear Power Plant (Sites SP35-SP39)

Kashiwazaki is home to one of the largest nuclear power plants in the world (Figs. 5.1 and 5.2). The plant is owned by Tokyo Electric Power Corporation (TEPCO) and, with an operational capacity of 8,200 megawatts, can provide electricity for 2 to 3 million households. The power plant is located 10 to 20 km above the potential plane of

the fault dipping southeast (see the fault plane solutions from Section 2 of this report, and the Google Earth map that accompanies this report and is available at EERI’s website.). The NW dipping plane is about 3 km below the site.

Initial reports on the performance of the facility were mixed, with reports of fire and radiation leaks, and reports of successful shutdown of reactors. The reported fire was in an electrical transformer located in the periphery of one of the seven reactors that make up the plant. Radiation leaks were caused by spilling of water from spent fuel pools, failure of joints in exhaust pipes, and the falling of drums containing low-radiation nuclear waste. Some of these drums lost their lids when they fell (<http://www.world-nuclear-news.org>, TEPCO news releases).

Acceleration records obtained at the site indicated that the peak acceleration at the bases of these structures reached values as high as about 0.69g. Figures 2.11 and 2.12 show that accelerations measured away from the structures and at foundation level varied from 388 to 867 cm/sec/sec over a distance of approximately 1.7 kilometers. Table 5.2 shows peak accelerations measured at the bases of the reactors. Observe that, at least in one instance, accelerations varied by more than 50% between bases of adjacent reactors (located approximately 200 m from one another). Bases of reactors sit on bedrock at depths of 45 m (Unit No.1), 44 m (Unit 2), 43 m (Units No.3-4), 36 m (Unit 5) and 26 m (Units No.6-7) below the surface and the buildings that house the reactors reach approximately 31 m to 39 m above ground. Table 5.2 also shows estimates of peak acceleration reported to have been used in the design of the reactors. Observe that the measured values are as much as 3.6 times larger than the assumed values. The discrepancy between the measured and the assumed, and the apparent absence of structural damage indicate that the designs resulted in redundant structures with large “overstrength”. A large fraction of the overstrength is attributable to the use of an “importance factor” equal to 3 in the equivalent static design procedure used in Japan.

Table 5.2. Values of peak acceleration at bases of reactors reported by TEPCO

Reactor	PEAK ACCELERATION								
	MEASURED			DESIGN			RATIO MEAS/ASSUMED		
	NS	EW	UD	NS	EW	UD	NS	EW	UD
	cm/sec/sec								
1	311	680	408	(274)	(272)	(235)	1.1	2.5	1.7
2	304	606	408	(167)	(167)	(235)	1.8	3.6	1.7
3	308	384	311	(192)	(193)	(235)	1.6	2.0	1.3
4	310	492	337	(193)	(194)	(235)	1.6	2.5	1.4
5	277	442	205	(249)	(254)	(235)	1.1	1.7	0.9
6	271	322	488	(263)	(263)	(235)	1.0	1.2	2.1
7	267	356	355	(263)	(263)	(235)	1.0	1.4	1.5
					MAX		1.8	3.6	2.1
					MEAN		1.3	2.1	1.5
					MIN		1.0	1.2	0.9

One of the authors of this report (Prof. Kabeyasawa of the University of Tokyo) is a member of The Working Group for Building Structures in Japan's Nuclear and Industrial Safety Agency and, as such, was granted access to the immediate vicinity of the reactors. Damage was observed, but it appeared to be related almost exclusively to problems with the soils (Figs. 5.3 through 5.6).

We observed signs of liquefaction (sand boils near the shore), distorted roads, tilted isolated footings, and a small landslide in a man-made hill that separates reactors 1-4 from reactors 3-7 (this hill was constructed with soils excavated to construct the plant). In a two-story steel building used for administration, drop-ceilings fell and windows broke (<http://www.world-nuclear-news.org>) (Fig. 5.7). Joints of piping resting on isolated footings and expansion joints in covered pathways failed. Access through doors was impaired by ground settlements of up to 40 cm. And underground pipes supplying fire retardant to reactors broke because of the relative movement between the soils that surrounded the pipes and the foundations of the reactors.

In summary, there were problems at the TEPCO power plant, but official accounts indicate that the main structures did not suffer damage. There was no loss of life and the emergency shutdown system, which had been set to be triggered by accelerations exceeding 120 gal, operated successfully.

The Failure of a Reinforced Concrete Tower (Stack) at the Kashiwazaki Municipal Recycling Plant (Site SP31)

The stack is one of the tallest reinforced concrete structures in the area, and its failure was noticeable from afar (Fig. 5.8). The structure was 59 m tall. It had a square cross section with 4.6-meter sides. The thickness of the walls was 18 cm at the top and 36.6 cm at the bottom. At the bottom of the east face, a large frame reinforced an opening for a gate. Through its west face and at a sixth of its height, the stack was connected to the adjacent plant by a large duct. The failure took place at a height of approximately 17 m, where the longitudinal reinforcing bars were lap spliced (Fig. 5.9). The failure caused the upper part of the stack to fall 6 to 7 meters. Some transverse reinforcing bars, which also had lap splices, were observed to have ruptured.

Apparently, the stack was designed in accordance with modern design standards. Current Japanese standards require lap splices to have a length equal to forty times the diameter of the largest bar spliced. Splice failures in similar conditions have been reported to have caused the collapse of a stack in Turkey during the 1999 Kocaeli Earthquake (Kilic and Sozen, 2003).

Houses

The earthquake caused the collapse of nearly eleven hundred houses in the Niigata prefecture in Japan. Damage to one-to-three story wood buildings was observed along the 30-kilometer long coastal region between Hatsusaki, to the south, and Shiya, to the north. Damage extended inland to western Nagaoka, 12 kilometers west of the coast. The city of Kashiwazaki reported the highest number of collapses in the region. The

structures that collapsed were almost exclusively wooden structures (Fig. 5.10) and unreinforced masonry fences. Preliminary estimates of collapse rate were between 5 and 7% for buildings and houses in the vicinity of the K-NET instrument in Kashiwazaki. One team documented more than 200 collapses of houses, fences, sheds, and canopies near this location. Photos of all of the sites visited are linked to the Google Earth map available through the USGS link provided in this report. The direction of collapse or permanent displacement for many of these sites can be queried through the site map, although no clear trend is visible regarding overall displacement direction.

A large fraction of the houses affected were of old-style heavy clay-tile kawara roofs with walls constructed of wood, and walls of soil and bamboo-lathe known in Japanese as *tsuchi-kabe* or “soil wall” (Fig. 5.11). The clay-wood combination can be used effectively if provided with braces for lateral strength and stiffness, however in general, results in heavy and brittle building components. Soft story collapses were observed in buildings with open businesses on the ground floor. The business arcade of Higashi-Honcho Dori was particularly hard hit, accompanied by ground movement/settlement on the south side of the street that was located on the shoulder of sand dunes.

Dense concentrations of structural damage to houses located on slopes of sand dunes as well as flat artificial reclaimed/alluvial sandy deposits that cross the Kashiwazaki-Kariwa area were observed. Many houses suffered from soil performance problems such as those caused by soil liquefaction, vertical settlement, and dynamic displacements of structures built on the slopes of these deposits. An example of residential houses affected by soil-related damage is found in the district of Nishi-Honmachi. There, collapse or large deformation of old temples and houses occurred, both, along the steep north-slope and along a more gentle slope towards the south. Nishi-Honmachi experienced deep-seated ground movements from high to low elevations and collapses of homes were due to the softening or liquefaction of the underlying sand deposits (e.g. see Site YT24, 37.36712°, 138.54590°).

Steel Structures

In Kashiwazaki, steel structures were not as common as concrete structures at the time of our visit. None of the few steel structures we saw collapsed. One of these structures was a gymnasium built in the 1950's (Site SP2), located 1.1 km away from the K-NET NIG018 station. The structure was composed of a series of 2D trusses running in the EW direction. Trusses running NS connected the EW trusses at the roof (Fig. 5.12). Finishes did not allow viewing of additional structural elements. But windows along the NS direction made it evident that, at least in this direction, the structure was provided with no braces. The structure survived the earthquake with an estimated permanent drift ratio of 2.5% to the north.

Another example of a surviving steel structure is illustrated in Fig. 5.13 (Site SP29). This structure was located at approximately 270 m from the K-NET NIG018 station, which measured PGV=100m/s. The two-story structure included nine, one-bay

frames parallel to the EW direction. The five frames closer to the front of the structure had no moment connections. The four frames closer to the back did have moment connections. The frames were connected to one another by a concrete slab cast on a steel deck at the second level and presumably by the roof. The slab had a step in the span that connects the moment resisting frames in the back and the gravity frames in the front. Braces were visible along the NS walls of the structure. The braces were connected to the webs of columns in the front frames through brackets as shown in Figure 5.13.

We inspected another gymnasium (Fig. 5.14 - Site SP7) with a steel structure. In this structure, located 430 m from the K-NET station, we observed buckling of steel braces in the lower of the two stories in the structure. The braces had T-shape cross sections with a thickness of 12 mm. The flange measured 150 mm, and the stem 45 mm. The braces had a slope of 2/3 with respect to the horizontal. Four pairs of braces reinforced each story in the NS direction. The floor plan was approximately 20 m in the EW direction and 33 m in the NS direction.

The storage at site RK41 was affected by large ground distortion (see Section 4). At this site, we observed buckling of flanges of beams at bolted connections (Fig. 5.15).

Steel frames are commonly used in the area to strengthen reinforced concrete structures. In the structures that use this system and we visited, the steel-concrete marriage seemed fruitful. Nevertheless, in one of these structures (Site SP30), spalling of plaster and concrete, and damage to architectural elements at construction joints caused disruption of operations.

Reinforced Concrete Structures

Initial reports did not mention damage to reinforced concrete structures. This was surprising initially given the measured ground motion intensity and the fact that, according to the Japan Building Disaster Prevention Association, the Niigata prefecture has one of the lowest rates of completion of mandated strengthening schedules in Japan. We therefore investigated in detail a number of reinforced concrete structures in the vicinity of the K-Net station at Kashiwazaki. We concentrated on public buildings because they had relatively regular floor plans and because they were accessible. We were allowed by the local government to inspect all public schools in the city. Photographs of each building inspected are linked to the Google Earth map accompanying this report.

We observed 1-mm thick inclined cracks in a column and 1 to 2.5-mm-thick inclined cracks in reinforced concrete walls in the Kashiwazaki High School (Site SP11), located at 100 m from the K-NET NIG018 station. The high school facilities included two reinforced concrete buildings (Figs. 5.16 to 5.20). We observed the south building to be a four-story building with shear walls in the NS direction and moment-resisting frames in the EW direction. The walls with cracks filled bays in one of the frames parallel to the EW direction in the south building and had a thickness of 12 cm. These walls were reinforced with bars with a diameter of 10 mm, spaced at 20 cm in the vertical and

horizontal directions. The inclined cracks described had the same orientation in the column and the walls, and indicated movement of the second level towards the west. The wall with the largest cracks had a door opening (bay 3-4). Refer to the Google Earth map accompanying this report for additional information.

The column observed to have an inclined crack had a clear height of 1.3 m. Other columns in the building had clear heights ranging from 1.3 to 3 m. The column with an inclined crack was located at the intersection of column lines C and 19. The cross section of column C-19 was rectangular with dimensions of 70 cm and 55 cm in the EW and NS directions, respectively (Fig. 5.21). Ties were specified to be 13 mm in diameter and to have an even spacing of 10 cm. A maximum tie spacing of 10 cm has been mandatory in Japan since 1972. In drawings of buildings built before 1972, one may find specifications calling for larger tie spacing (30cm). Cross ties with a diameter of 9 mm were to be provided every 50 cm. Column C-19 supported a single level (a slab that serves as roof beyond column line 18). Averages obtained for buildings from the same vintage indicate that concrete strength is likely to be close to 3 ksi. The yield stress of the reinforcement is estimated to be $f_y = 45$ ksi.

Inclined cracks were also observed in walls in the Kashiwazaki City Hall (Site SP 26), located 100 m from the K-NET NIG018 station and in a government building in Kariwa (Fig. 5.22 - Site SP33), which sits right next to the Kariwa JMA recording station. The building in Kariwa also showed damage to a sliding door and broken windows. Disruption of the soil surrounding the foundation was observed in this and other sites.

In general, the performance of the reinforced concrete buildings we visited was satisfactory with one exception. A three-story building used as a karaoke parlor in downtown Kashiwazaki suffered shear failures of columns in its first story (Figs. 5.23 and 5.24). From Figs. 5.23 and 5.24 it appears that the spacing of ties exceeded the specified maximum of 10cm.

The buildings we surveyed are not new buildings. The east wing of Kashiwazaki's Jr. High School 2 (Site SP3), for instance, was built in the 1960s. Nevertheless, the reinforced concrete structures we inspected performed well, except for the karaoke parlor. But in general, it is fair to say that the performance of reinforced concrete building structures was far superior to that of buildings in other seismic events. In an attempt to provide tangible information for interpretation of our observations, the ratios of column areas to total floor areas were computed for buildings inspected in or near Kashiwazaki (Table 5.3). The mean ratio of column to floor area is 0.59%.

Table 5.3. Ratios of column areas to total floor areas.

Building	Site	Average Tributary Length		Typ. Column Dimensions		Number of Stories	Ratio of Column to Floor Area
		Longitudinal Direction	Transverse Direction	Depth	Width		
		m	m	cm	cm		
Kariwa Government Building	SP33	7.5	5	90	90	3	0.72%
Kashiwazaki City Hall	SP26	4.5	5.5	80	80	5	0.52%
Technical High School	SP40	5	4	80	50	4	0.50%
Kashiwazaki High School	SP11	4.5	5	70	55	4	0.43%
Kashiwazaki Jr. Hi. #2 West Bldg.	SP1	4.5	4.5	80	67	3	0.88%
Kashiwazaki Jr. Hi. #2 East Bldg.	SP3	4.5	4.5	65	40	3	0.43%
Kashiwazaki Jr. Hi. #1	SP8	8.5	4	80	80	3	0.63%

It is worth noting that the Kashiwazaki High School and buildings surrounding the K-NET NIG018 station featured large reinforced concrete spandrels built integrally with girders and columns. These spandrels are common in Japan among buildings built before 1982. The spandrels in the high school had thickness varying from 12 to 30 cm and total depths (including the depth of the girder) ranging from 1.2 to 2.2 m. The longitudinal reinforcement in the spandrels (D10 bars at 10 cm from one another) runs through the column and flexural cracks in the spandrels suggested that they acted as integral parts of the girders.

5.3 References

Kilic, S., Sozen, M., (2003). Evaluation of Effect of August 17, 1999, Marmara Earthquake on Two Tall Reinforced Concrete Chimneys, ACI Structural Journal, Vol. 100, No. 3.



Figure 5.1: Layout of the Kashiwazaki-Kariwa nuclear reactors and locations of sites visited by the reconnaissance team within and near the facility.



Figure 5.2: TEPCO Nuclear Power Plant (Sites SP35-SP39).



Figure 5.3: Damaged road at power plant.



Figure 5.4: Cracks in reinforced concrete element at ground level.



Figure 5.5: Failure of joint in exhaust pipe.



Figure 5.6: Rotation of isolated footings for equipment at nuclear power plant.



Figure 5.7: Ceiling damage in administration building of nuclear power plant.



Figure 5.8: Failure of reinforced concrete stack (Site SP31, N37.3939° E138.5840°).



Figure 5.9: Details of failure of reinforced concrete stack (Site SP31, N37.3939° E138.5840°).



Figure 5.10: Collapse of house (N37.367°, E138.567°).



Figure 5.11: Traditional Japanese tsumi-kabe (“soil wall”) construction technique (Site SP13, N37.37056°, E138.55694°).

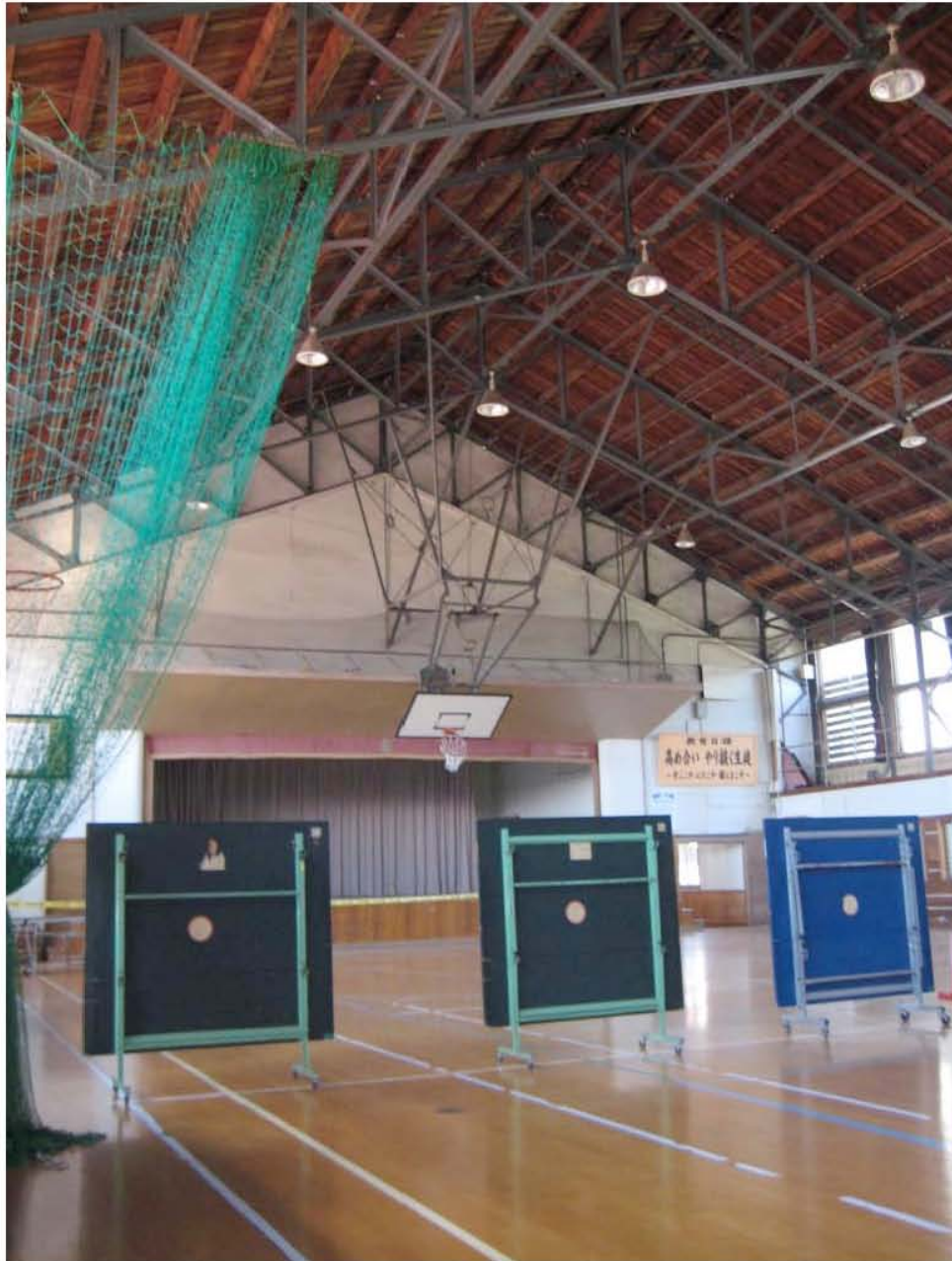


Figure 5.12: Gymnasium at Jr. High School No. 2, Kashiwazaki (Site SP2, N37.3728° E138.5709°).



Figure 5.13: Parking structure in Kashiwazaki (Site SP29, N37.3707° E138.5566°).



Figure 5.14: Buckling of braces in gymnasium in Kashiwazaki (Site SP7, N37.3755° E138.5541°).



Figure 5.15: Buckling of beam flanges (Site RK41, N37.41472° E138.60833°, photo by Peter Yanev).



Figure 5.16: Kashiwazaki High School, south building (Site SP11, N37.3721° E138.5569°).

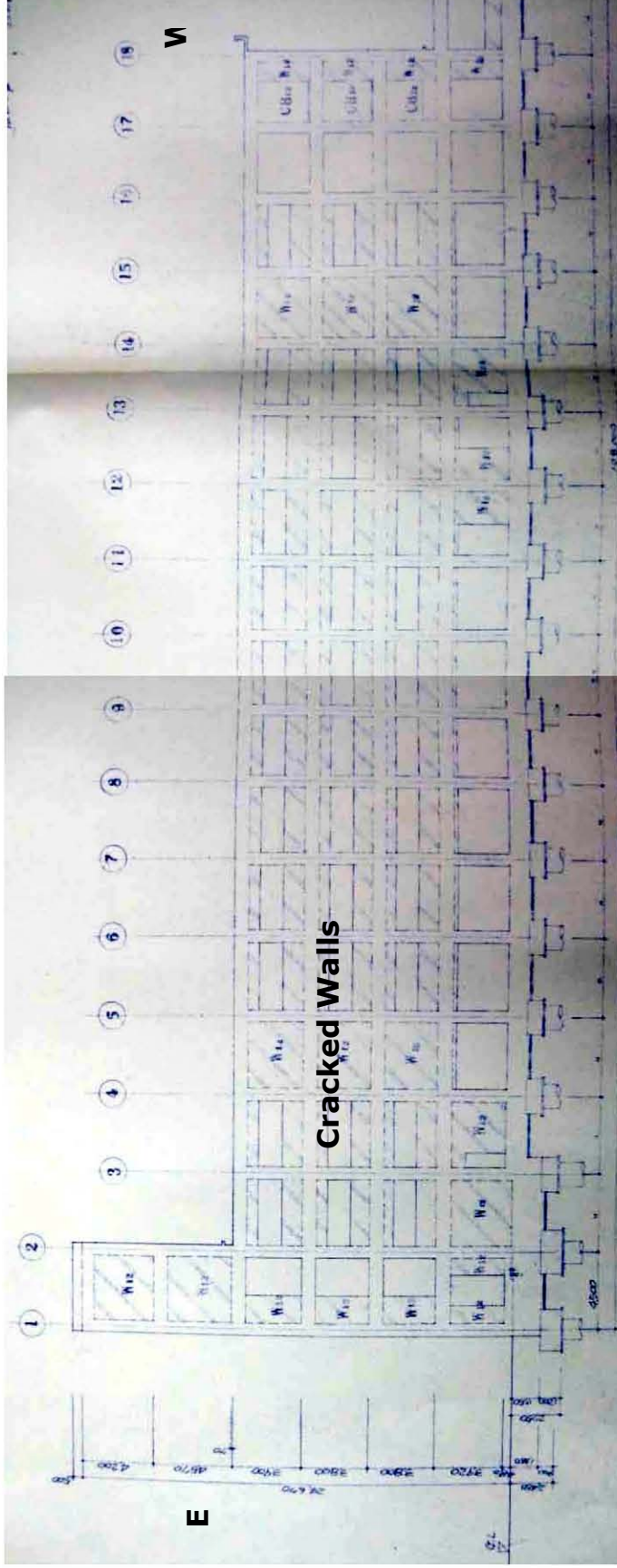


Figure 5.17: Kashiwazaki High School design drawings, vertical section, column line C.

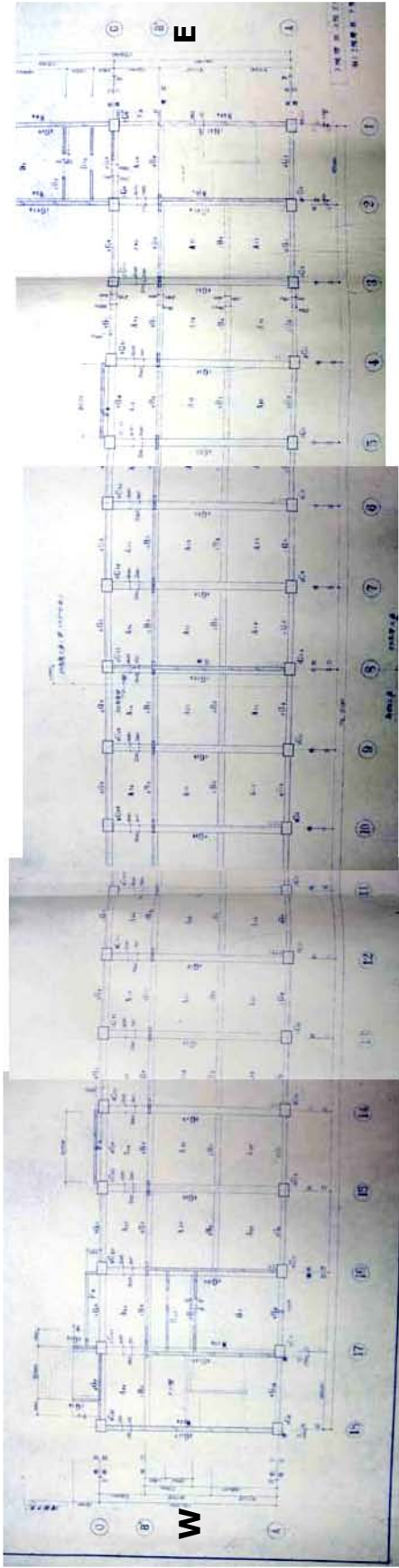


Figure 5.18: Kashiwazaki High School design drawings for typical floor plan.

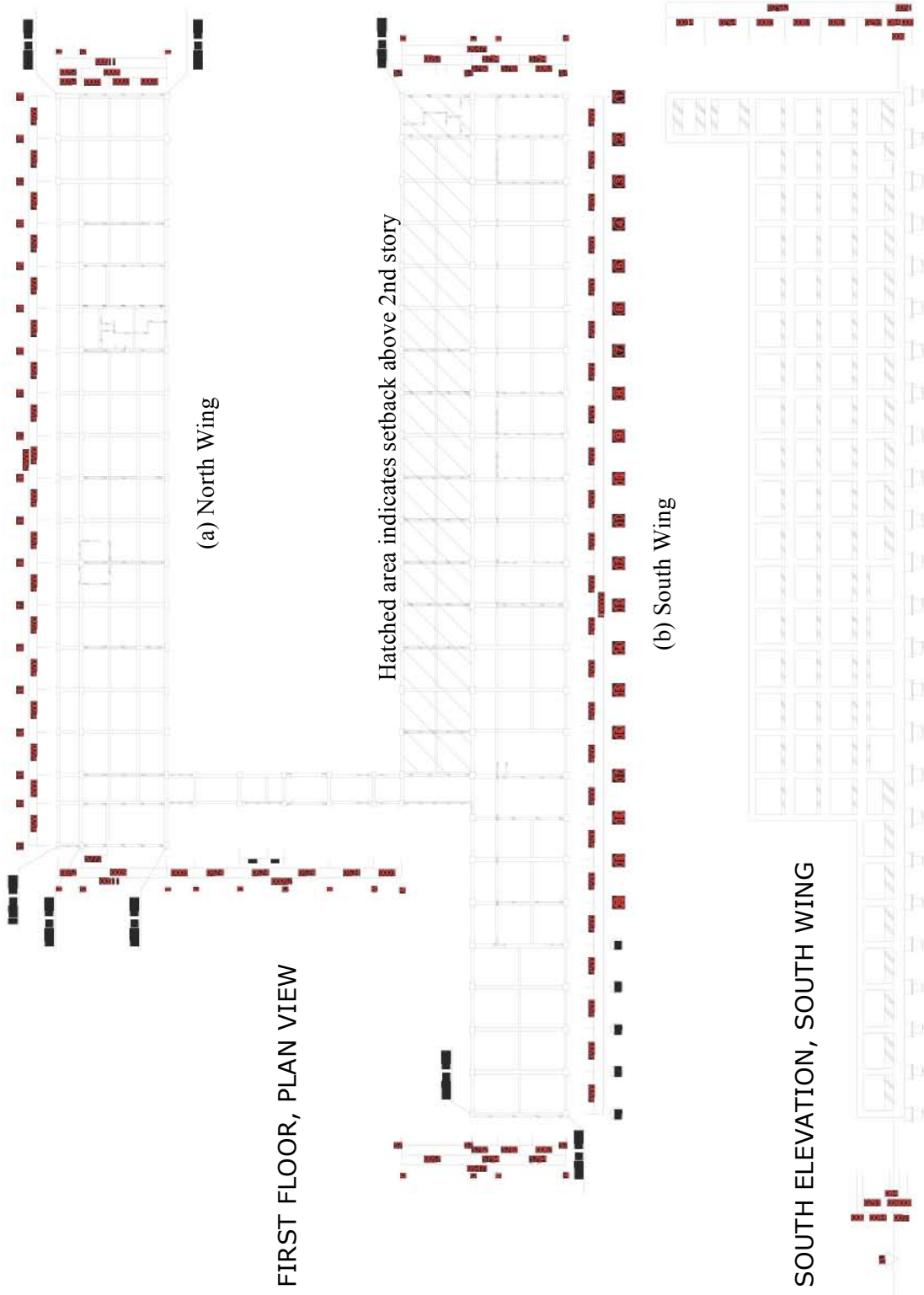


Figure 5.19: Kashiwazaki High School, plan view and vertical section.

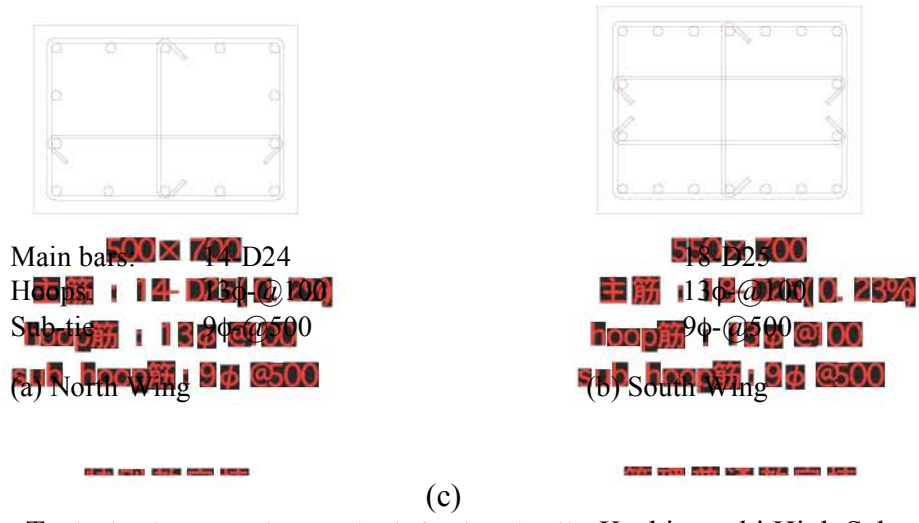


Figure 5.20: Typical column sections and reinforcing details, Kashiwazaki High School.

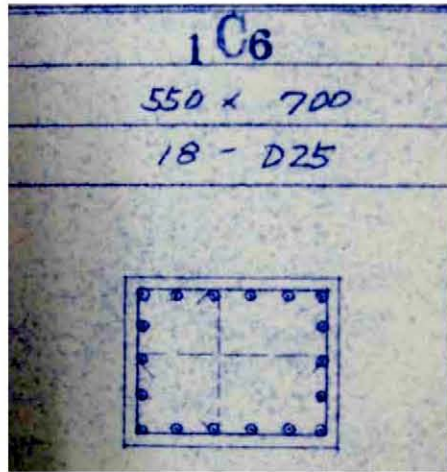


Figure 5.21: Column in first story of The Kashiwazaki High School, cross section and observed crack pattern (Site SP11, N37.3721°, E138.5569°).



Figure 5.22: Disruption of soil surrounding a government building in Kariwa (Site SP33, N37.4223° E138.6222°).



Figure 5.23: Karaoke parlor (Site NIT-81, N37.37000° E138.55825°, photo by Peter Yanev)



Figure 5.24: Shear failures of reinforced concrete columns (Site NIT-81, N37.37000° E13855825°, photo by Peter Yanev)

Section 6. Bridges

The GEER and the TCLEE teams investigated bridge damage on the Hokuriku Expressway, on National Highway 8, on bridges crossing the Sabaishi and the U Rivers, and on prefectural and city bridges. Most of the damage was the result of problem soils that caused lateral spreading or settlement to bridge approaches, making it impossible to use the bridge until repairs could be made. Damage to the bridges consisted of some combination of cracks in the abutments, vertical offsets at the approaches, and lateral offsets in the bearings. On longer bridges, there was also some damage to structural elements. Nearly every bridge was in service at the time of the investigations.

Table 6.1: Bridges observed during reconnaissance.

Name	Latitude (deg)	Longitude (deg)	Length (m)	Liquefaction	Landslides	Lateral Spreading	Bearing Distortion	Approach Offset	Severe Bridge Damage	Moderate Bridge Damage	Minor Bridge Damage	No Bridge Damage
Hachisaki Bridges	N37.315°	E138.437°	5-span 185 m			x	x	x		x		
Omigawa Bridges	N37.343°	E138.482°	3-span 300 m				x				x	
Yoshiigawa Bridges	N37.399°	E138.625°	7-span 200 m					x			x	
-	N37.4225°	E138.6412°	130 m					x				
Toyota Bridges	N37.389°	E138.592°	3-span 160 m				x	x	x	x		
Route 522	N37.364°	E138.570°	2-span 10 m						x			
Ugawa River Bridge	N37.3605°	E138.549°	2-span 60 m				x					
Yoneyama Bridge	N37.346°	E138.488°	5-span 280 m		x						x	
Yonahime Bridge	N37.3168°	E138.4348°	1-span 120 m		x		x			x		
Ansei Bridge	N37.3864	E138.5693	106 m			x		x				
Heishi Hashi	N37.3894°	E138.5742°	22 m	x		x	x	x			x	
Heishi O-Hashi	N37.3888°	E138.5767°	118 m	x		x	x	x			x	
Kaiun Bridge	N37.3918°	E138.5806°	111 m	x		x	x	x			x	
Railway Bridge	N37.3917°	E138.5899°	65 m									x
Nagoma Bridge	N37.3904°	E138.5908°	112 m	x		x	x	x		x		
Uehara Ni Bridge	N37.3900°	E138.5960°	65 m			x	x	x		x		
Uehara Ichi Bridge	N3895°	E138.5966°	100 m			x	x	x		x		
Tsurugi Bridge	37.3921°	E138.6008°	43 m			x		x		x		
Genji Bridge	N37.3845°	E138.6017°	95 m			x	x	x		x		

Rinko Yasaka	N37.3675°	E138.5433°	81 m			x	x	x		x		
Yasaka Bridge	N37.3658°	E138.5438°	62 m			x						
Ukawa Bridge	N37.3641°	E138.5462°	66 m			x						
Osu Bashi	N37.3635°	E138.5478°	66 m			x	x	x		x		
Railway Bridges	N37.3619°	E138.5493°										x
Steel Bridge	N37.3547°	E138.5515°										x
Other Bridges												
Railway Bridge	N37.36896°	E138.56530°	20 m									x
Rte 352 by NPP	N37.4248°	E138.6076°	20 m					x				
Highway 116 Bridge	N37.446°	E138.638°	20 m					x				

6.1 Hokuriku Expressway

The Hokuriku Expressway is owned by the Japanese government and operated by NEXCO (the East Nippon Expressway Company Limited). There was considerable damage to this highway during to the earthquake. However, four hours after the earthquake, emergency repairs were completed and the emergency traffic could use the expressway, and 56 hours later, it was reopened to ordinary traffic This helped with the transfer of people and goods to the earthquake- affected area. There were at least 17 locations where damage was severe enough to temporarily close parts of the expressway. There was damage to bridges, tunnels, roads, and to other highway facilities. The damage extended from 338 KP to 416 KP, for a distance of 78 kilometers.

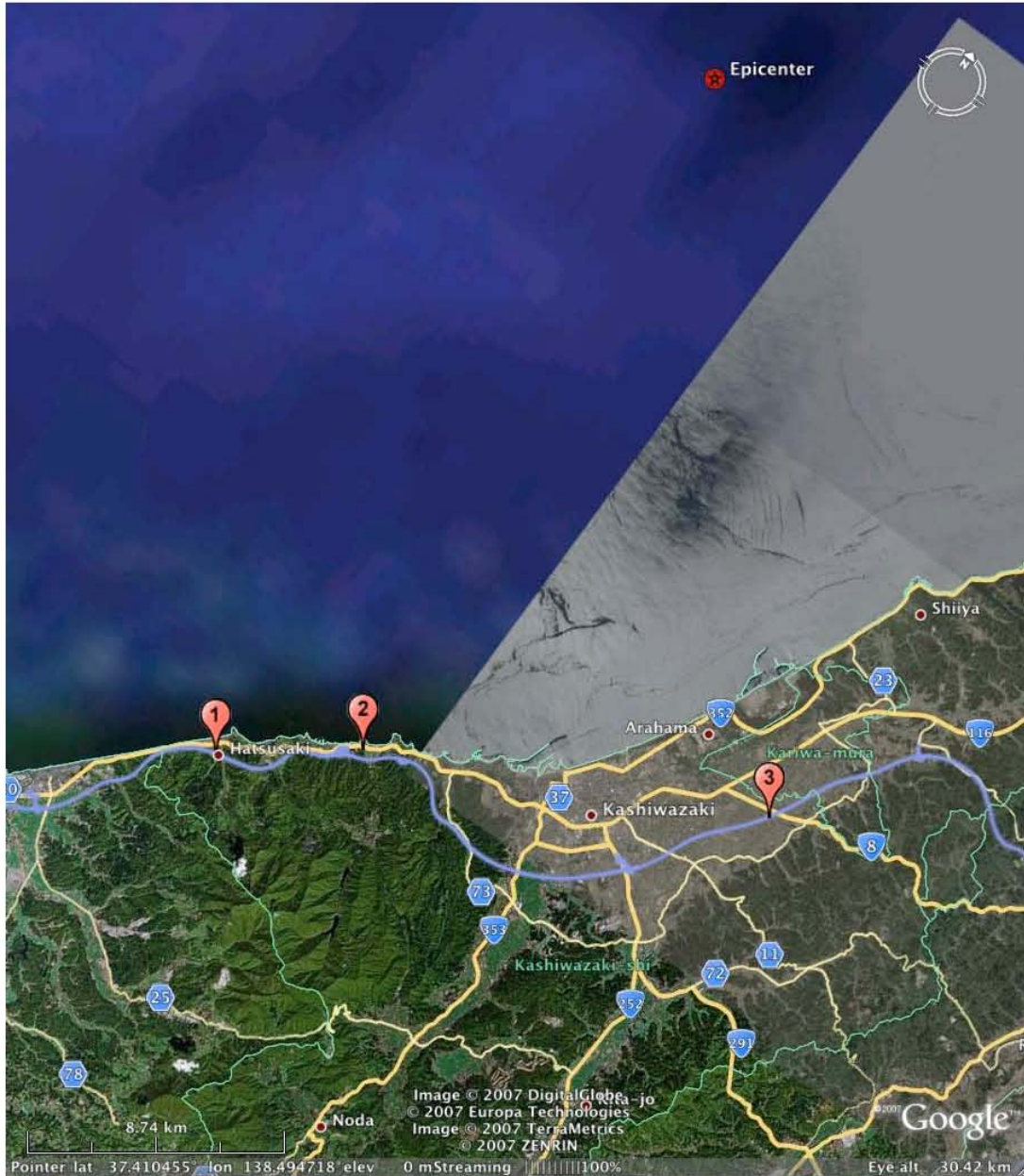


Fig. 6.1 Locations of Bridge Damage on the Hokuriku Expressway.

(1) Hachisaki Bridges (380.4 KP) N37.315° E138.437°

These are two parallel five-span concrete ‘I’ girder bridges on seat-type abutments and tall (30m+) pier walls (Fig. 6.2). The three northern spans are continuous over steel bearings with an expansion joint at the end of the third span. The piers are on piles except where there is rock near the surface. The bridges are just north of the Yoneyama tunnel, which was also damaged. Our team went under the bridge to study the bottom of the piers but the undergrowth was so thick we couldn’t get close to them.

During the earthquake, the embankments moved downhill, exposing the wingwalls (Fig. 6.3). The girders are supported by fixed bearings at the abutment and it is thought that the

shear force exceeded the shear strength of girder at the bearing connection. There was a spall at the bottom of the girders about 0.6m from the abutment backwall and on the other side of the bearing. Perhaps, as the abutment moved downward, large shear forces in the girders caused them to spall (Fig. 6.4). The damage occurred at the north end of the west bridge (small cracks were observed on the east bridge).



Fig. 6.2. Looking south at the Hachisaki Bridges.

When we arrived at the scene (on August 5th), both directions of traffic had been diverted to the east bridge, they had finished driving sheet piles around the abutment to stabilize the soil, and were casting a large pad at the west bridge so that they could jack up the southern three spans and repair the girders and bearings.



Fig. 6.3. Damage at north end of the west Hachisaki Bridge.



Fig. 6.4. Closer view of girders on the west Hachisaki Bridge.

(2) Omigawa Bridges (386.3 KP) N37.343° E138.482°

These are two haunched, three-span, segmentally-constructed cast-in-place, concrete box girder bridges on very tall hollow, reinforced concrete piers (Fig. 6.5). Like several other bridges in the same area, the superstructures moved enough during the earthquake to break the fixed steel bearings (Fig. 6.6). Perhaps the weakest member, in this case the

steel bearings, acted as fuses to protect the structure from more catastrophic damage. Jacking up these long, continuous superstructures is no easy task, and jacking them back transversely is also a lot of work, but it's also one of the most common types of bridge damage that occurs during earthquakes.



Fig. 6.5. Omigawa Bridges on the Horukiru Expressway.

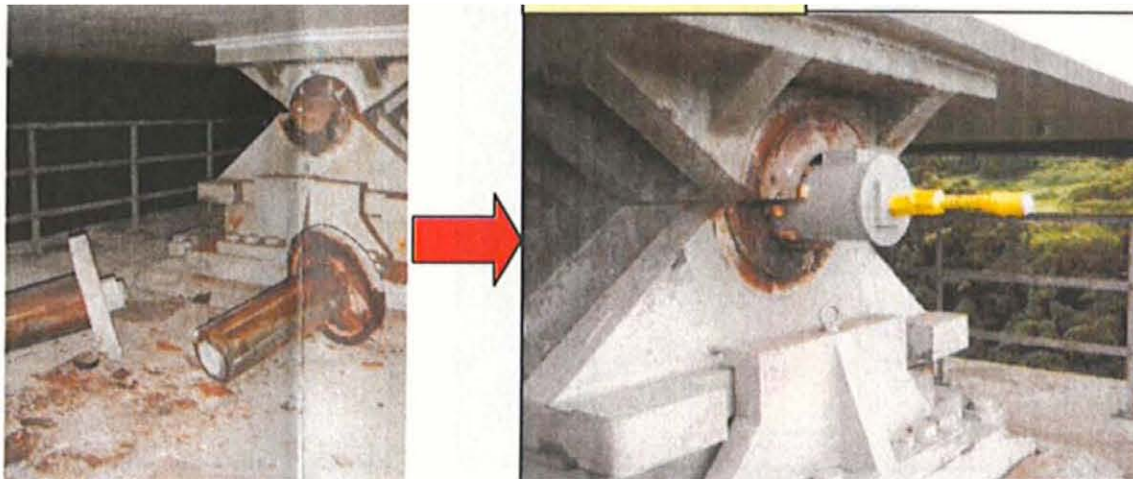


Fig. 6.6. Damage and Repair to Omigawa Bridge (photo courtesy of the Nippon Expressway Company.).

(3) Yoshiigawa Bridges (402.2KP) N37.399° E138.625°

These are two, long steel I girder bridges on single column bents and seat-type abutments. The bridges were being retrofit at the time of the earthquake (Fig. 6.7). Expressway bridges are built with an approach slab that is pinned to the abutment backwall, but this connection broke due to the ground shaking combined with the approach settlement (Fig. 6.8). The only other noticeable damage was the grout plate that

the steel abutment bearing was seated on had shattered as the steel girders banged against the steel longitudinal keys that were to limit movement (Fig 9).



Fig. 6.7. Looking under the Yoshiigawa Bridges (and at the piers being retrofitted).



Fig. 6.8. Damage to approach slab and embankment at Yoshiigawa Bridges.



Fig. 6.9. Bearing at south abutment of Yoshiigawa Bridges.

Sand was placed at the back of the approach slab and new asphalt was placed to create a gentle ramp back onto the bridge (Fig. 6.10). There was a lot more of this kind of approach damage on the Hokuriku Expressway and on many other roads and highways, especially where they crossed rivers.



Fig. 6.10 Repaired embankment and approach slab at Yoshiigawa Bridges.

There was a lot of approach settlement damage but the expressway was reopened (with some lane limitations to traffic) 56 hours after the earthquake, which allowed emergency vehicles to use the expressway.

6.2 National Highway 8.

National Highway 8 runs north along the coast until it reaches Kashiwazaki where it goes eastward through foothills to Nagoaka. The highway had damage along 60 km of its length during the earthquake. There were several landslides and slip-outs as well as damage to long-span bridges and river crossings. The landslides were at much further distance from the epicenter, suggesting that it takes much less ground shaking to disturb unstable rocks and soil.

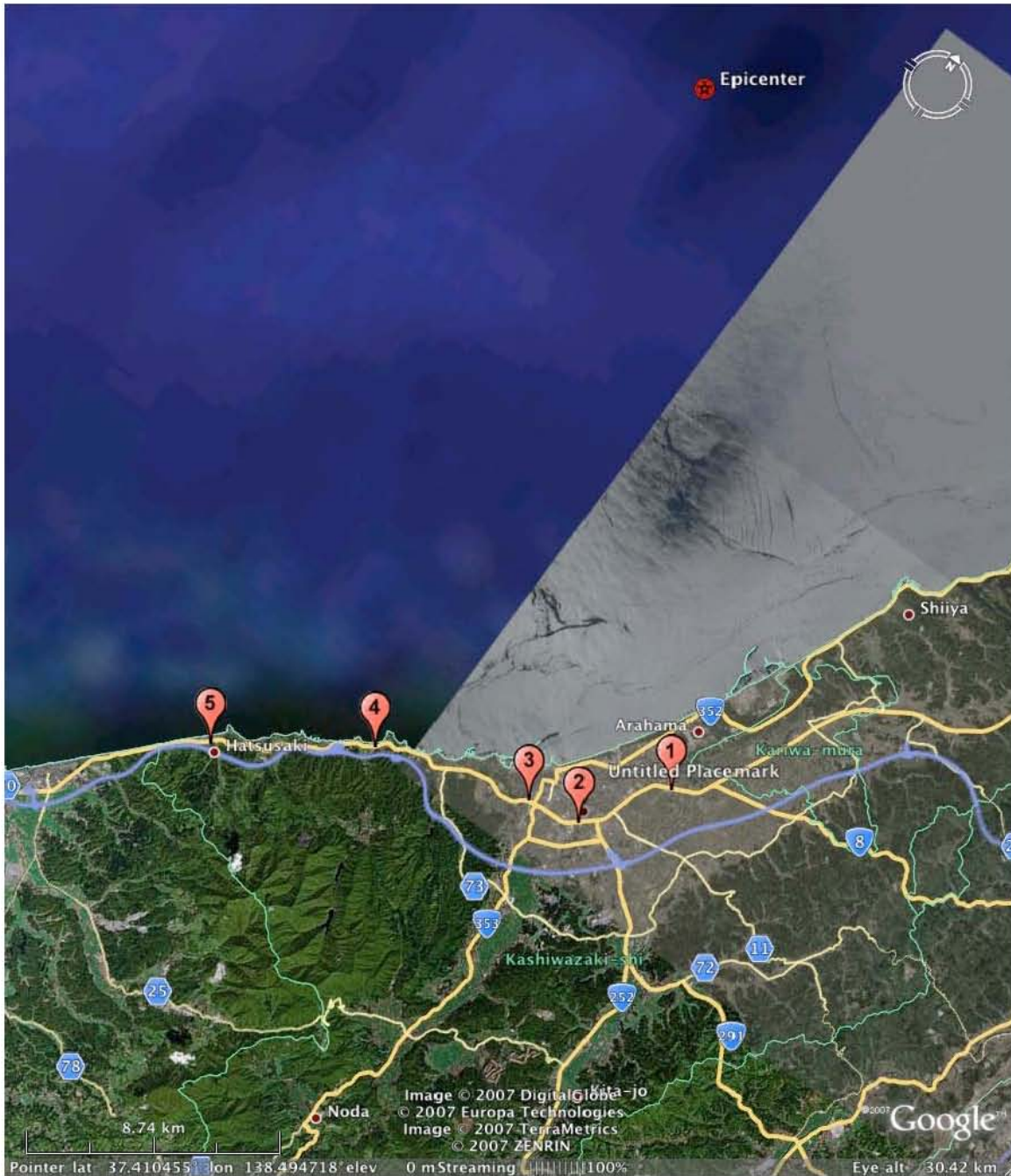


Fig. 6.11. Locations of Bridge Damage on National Highway 8.

(1) Toyota (Sabaishi River) Bridges (N37.389° E138.592°)

Two structures carry vehicles up and over the Sabaishi River on Highway 8. The river crossing has a 3 span continuous steel (highly skewed and curved) I girder superstructure on seat-type abutments and single column bents (Fig. 6.12). The deck is 160m long with a 12m width and is supported on tall elastomeric bearings with transverse shear keys and concrete backwalls to limit movement. The embankment behind abutment #1 (on the west end of the bridge) is supported by mechanically stabilized retaining walls that were undamaged by the earthquake. However, both bridge approaches settled about half a meter during the earthquake. A rigid box structure, that allowed vehicle access through the west bridge embankment, was now half a meter above the road surface, closing the highway (Fig. 6.13). The riverbanks and abutments moved towards the river and the superstructure moved to the northwest (Fig. 6.14). As a result of this movement the elastomeric bearings experienced some shear (Fig. 6.15). However, because the bearings take up to 70% shear strain for temperature change, 150% for a mild earthquake, and 250% for large earthquake they still have much more shear capacity.



Fig. 6.12. Three span steel girder Toyota Bridge over Sabaishi River.



Fig. 6.13. Settlement of west embankment (courtesy G. Watanabe, Tokyo Institute of Technology).

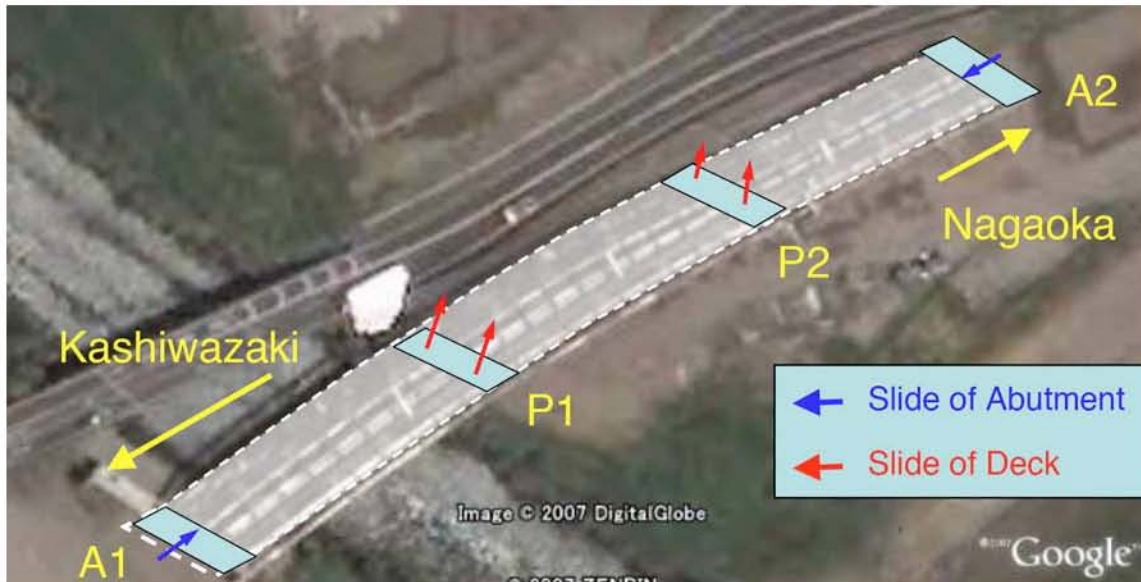


Fig. 6.14. Movement of Toyota Bridge (courtesy G. Watanabe, Tokyo Institute of Technology).

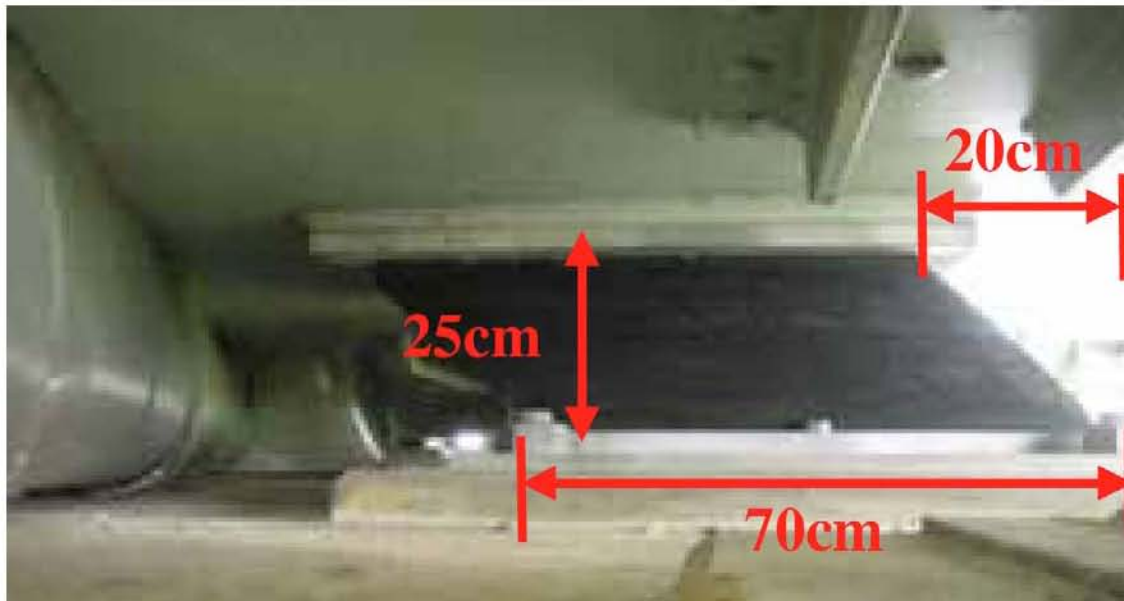


Fig. 6.15. Displacement of Bearing Bridge (courtesy G. Watanabe, Tokyo Institute of Technology).

(2) Highway 8 (Railroad & Rte 522) Bridges N37.364° E138.570°

In downtown Kashiwazaki, on Highway 8 there are a couple of older bridges that are beginning to be maintenance problems. However, the only noticeable damage from the earthquake was some embankment damage behind the abutments on the Route 522 and the Japan Rail Bridges (Fig 6.16 and 6.17).



Fig. 6.16. Damage and repairs where Highway 8 crosses Route 522 Bridge (courtesy G. Watanabe, Tokyo Institute of Technology).



Fig. 6.17. Damage and repairs where railway crosses Highway 8 Bridge (courtesy G. Watanabe, Tokyo Institute of Technology).

(3) Highway 8 over the Ugawa (N37.3605° E138.549°)

This is a two-span concrete I girder bridge on a pier wall and seat-type abutments (Fig. 6.18). Although bridges closer to the mouth of the Ugawa River sustained damage due to lateral spreading, this bridge (about 1.2 km upstream) had just a little bit of embankment

settlement that was quickly repaired (Fig. 6.19). Just north of the bridge were several manholes raised above another roadway's surface and a nearby stonecutter's shop had toppled statuary suggesting a $PGA > 0.25g$, and that liquefaction was a problem at this site. However, the embankment settlement was only about 10cm and continued to decrease upstream, suggesting better soil and/or weaker accelerations.



Fig. 6.18. Highway 80 Bridge across the Ugawa.



Fig. 6.19. Slight (10cm) settlement at bridge approaches.

(4) Yoneyama Bridge (N37.346° E138.488°)

This is a 280 meter long steel girder bridge (the longer spans are steel boxes and the shorter spans are steel stringers) supported on tall, four-legged steel towers, shorter two-legged piers, and seat-type abutments (see Fig. 6.20 and 6.21).

The bridge had been retrofit before the earthquake, which may have helped reduce the amount of damage that occurred. Lateral and vertical restrainers and stoppers were added at the superstructure (Fig. 6.22). The steel towers had been filled with concrete and stiffeners and doubler plates had been added to make the towers very stiff and strong. The bearing damage was very slight. It was just the failure of the stopper key element and deformation of the pin-cap, which did not affect the bearing function (Fig. 6.23). Other damage occurred as a result of the superstructure pounding against the abutment backwall.

Shikegi Unjoh (from Japan’s Public Works Research Institute) said, ‘The Yoneyama bridge had seismometers but they were out-of-order (no maintenance for a long time). There was another new seismometer at ground level that recorded the free field motion during the 7/16 main shock. Dr. Iwasaki of the Public Works Research Center (PWRC) wrote that it recorded a PGA of 0.65g. Dr. Iwasaki also mentioned that he wrote several papers about this bridge after the 1964 Niigata earthquake (Iwasaki, 1972) (Kuribayashi, 1967). One paper, “Response Analysis of Civil Engineering Structures Subjected to Earthquake Motions” is at: <http://www.fujipress.jp/JDR/open/DSSTR000100020012.pdf>.

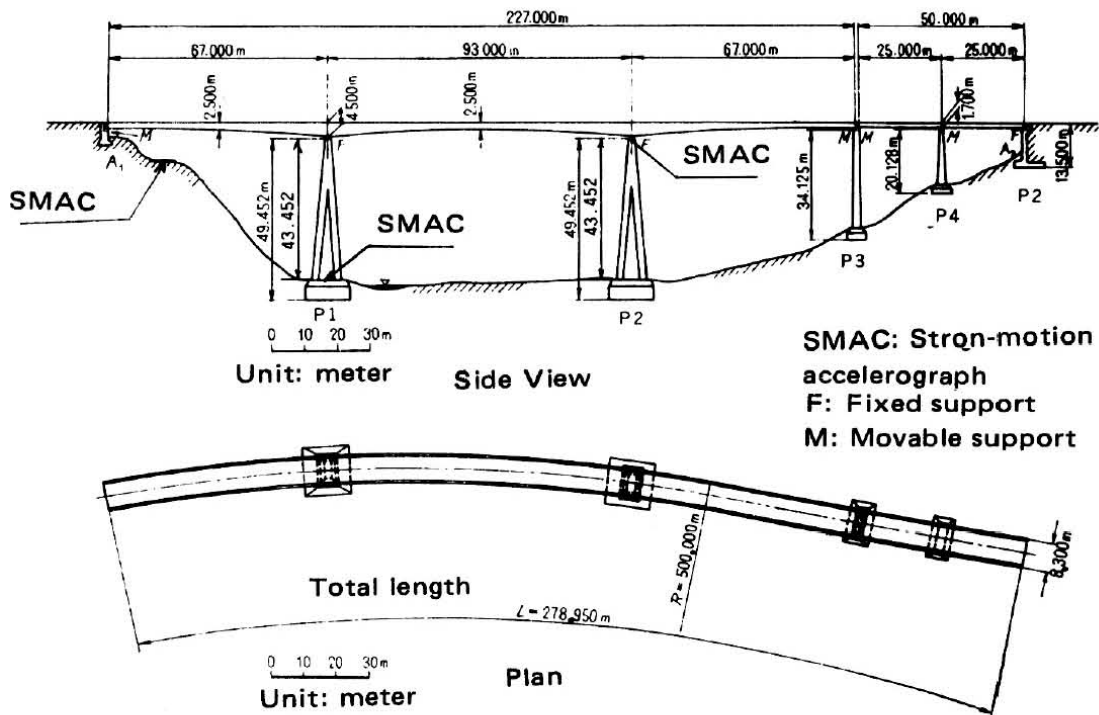


Fig. 6.20 Elevation and Plan Drawings for Yoneyama Bridge (Iwasaki, 1972).



Fig. 6.21. Yoneyama Bridge and landslide.



Fig. 6.22. Retrofitted bent cap at Yoneyama Bridge (courtesy of S. Unjoh, PWRI).



Fig. 6.23. Deformation of Bearing Pin-Cap caused by uplift force (courtesy of S. Unjoh, PWRI).

(5) Yonahime Bridge (N37.3168° E138.4348°)

This is a 120 m long through truss arch, crossing over a narrow canyon (Fig. 6.24) south of Kashiwazaki. We saw a landslide scarp on the uphill side of this bridge, and because it is supported by spread footings, it was probably a combination of ground movement and strong shaking that caused it to rack during the earthquake.



Fig. 6.24. Looking at the struts and cross-bracing of the Yonahime Bridge.

When we visited the bridge (on Aug. 4th) we saw many of its members had buckled (Fig. 6.25) and some of its connections were damaged (Fig 6.26) along with its bearings (Fig. 6.27). Still, the bridge remained in service. Metal boxes were placed around the bearings to support the bridge in case a strong aftershock occurs. This is a very common bridge type. However, the struts and bracings need to be designed against lateral wind force and lateral earthquake force. It appears that the earthquake force during this earthquake exceeded the design force. A deck arch bridge, the Agewa Bridge immediately to the north was undamaged by the earthquake (Fig. 6.28). It might be possible to retrofit the Yonahime bridge for large earthquakes, possibly by supporting it on isolation bearings. Certainly, these fixed bearings, which we saw damaged on several of the longer span bridges, are a lot of trouble to replace.



Fig. 6.25. Buckled cross bracing on Yonahime Bridge.



Fig. 6.26. Torn cross bracing connection on Yonahime Bridge.



Fig. 6.27. Damage of set bolts and the additional steel box support to prepare the aftershocks)



Fig. 6.28. Undamaged Agewa (Deck Arch) Bridge just north of damaged Yonahime Bridge.

6.3 Sabaishi River Crossings

The bridges along the Sabaishi River consisted primarily of continuous steel I-girder superstructures resting on elastomeric bearings on reinforced concrete piers and abutments. Lateral spreading pushed the abutments toward the river, causing a permanent offset in the elastomeric bearings with the bottom of the bearing moving toward the river relative to the top of the bearing. Offsets in the bearings ranged from 7 cm to 17 cm, and in some cases the bearings had become unbonded from the steel plates in a small region near the edges of the connections. In some cases, some small transverse bearing displacements were evident, though the primary mode of deformation was longitudinal. Cracks up to 1-cm wide were observed in many of the concrete abutments at the 90° angle where the back wall connects to the horizontal platform on which the bearings are connected. Vertical offsets at the approaches of the damaged bridges ranged from about 5 cm to 30 cm, and asphalt or gravel backfill was often placed to permit cars to traverse the bridge. Some bridges that had settlement of the approach soils were functional without any repair required at the approach because the settlement occurred such that the approach soil ramped up onto the bridge rather than forming a vertical offset. Utilities attached to the side of the bridge were often damaged near the abutments. Several of the bridges crossing the Sabaishi River in Kashiwazaki (Fig. 6.29) had settlement of their approaches due to lateral spreading of the river banks. Typically the abutments (on piles) would remain at their original height, but they were pushed against the superstructure by the lateral movement of the surrounding soil.



Fig. 6.29 Map of Sabaishi River Bridges

The bridge carrying National Highway 352 traffic across the river had little damage from the earthquake. However, the next two bridges (Heisei and Heisei O'Hashi) crossed onto an island (Fig. 6.30) composed of loose fill which liquefied during the earthquake.



Fig. 6.30. An island in the meander of the Sabaishi River liquefied.

Heisei Hashi (N37.3894° E138.5742°)

The smaller of the two bridges crossing the island, Heisei Hashi is on the north end. It is a single-span concrete box girder bridge on seat-type abutments.

During the earthquake, the south bridge embankment settled as the bank spread into the river. The wingwalls weren't attached to the abutment (which was on piles) and moved with the embankment (Fig. 6.31). The lateral spread was the result of liquefaction of the island (Fig. 6.32). Figure 33 shows about 400 cm settlement of the south embankment.



Fig 6.31. Looking southeast at Heisei bridge abutment, settled embankment, and the island.



Fig. 6.32. Looking northwest at liquefaction of island and the Heisei Bridge.



Fig. 6.33. Looking north from island at Hashi bridge deck.

Heisei O'Hashi (N37.3888° E138.5767°)

This is a continuous, two-span, concrete box girder bridge supported on seat abutments and a pier wall (Fig. 6.34). During the earthquake, the north bridge embankment settled about 40 cm (Fig 6.35). There were also signs that the bridge underwent shaking and pounding (Fig. 6.36). Although the abutments were on piles, the bearings were distorted, indicating that the abutments had been pushed toward the river (Fig. 6.37).



Fig. 6.34. Heisei O'Hashi



Fig. 6.35. Settlement of north bridge approach.



Fig. 6.36. The superstructure and bearings moved back and forth, cracking the abutment.



Fig. 6.37. Signs of movement of the abutments included distortion of bearings.

Note that unlike the north Heisei Bridge, there are apparently piles under the short wingwalls on the south Heisei Bridge. Figures 6.38 and 6.39 show the wingwalls at the same height as the abutment and they also show signs of pounding between them.



Fig. 6.38. Pounding between abutment and wingwall.



Fig. 6.39. Settlement of north bridge abutment.

Kaiun Bridge (N37.3918° E138.5806°)

About 1/2 km upstream from the Heisei Bridges sits the four span Kaiun Bridge (Fig. 6.40), which had a 1 meter settlement of the south approach (Fig. 6.41).



Fig. 6.40. The four, steel 'I' girder span Kaiun Bridge on pier walls and seat abutments.



Fig. 6.41. About one meter settlement of south Kaiun bridge approach.

Like the other Sabaishi bridges, this settlement was caused by the riverbank spreading toward the river (Fig. 6.42). Although the expansion joint, the abutment, and the bearings should have been isolated from this movement by the pile supports, they were distorted as shown in Fig. 6.43 during the earthquake, perhaps due to the ground shaking.



Fig. 6.42 The soil around the south abutment moved towards the river during the earthquake.



Fig. 6.43. Distortion of expansion joint, bearings, and abutment on Kaiun Bridge.

Nagomi Bridge (N37.3904° E138.5908°)

This is a three span steel girder bridge on pier walls and seat-type abutments (Fig. 6.44). There was evidence of fine grain soil being ejected at depth to the ground surface (along with settlement) at the saturated riverbanks (Fig. 6.45). There was damage to the abutment backwall (Fig. 6.46) and to the bridge approaches (Fig. 6.47).



Fig.44. Nagomi Bridge (photo courtesy of Scott Brandenburg).



Fig. 6.45. Soil settled around pier in riverbank (photo courtesy of Scott Brandenburg).



Fig. 6.46. Distorted bearing and cracked abutment backwall (photo courtesy of Scott Brandenburg).



Fig 47. Repairs to bridge approach on Nagomi Bridge (photo courtesy of Scott Brandenburg).

Genji Bridge (N37.3845° E138.6017°)

This is the last Sabaishi River bridge that had a big approach settlement (Fig. 6.48).



Fig 6.48 Genji Bridge (photo courtesy of Scott Brandenburg).

6.4 U River Crossings

Unlike the Sabaishi River (which had lateral spreading for about 5 km upstream), the banks of the Ugawa (a river south of the Sabaishi in Kashiwazaki) laterally spread for only one km from the mouth of the river (Fig. 6.49). This may be due to the more meandering path of the Sabaishi which resulted in more sediment being dropped along the banks. Also, the Sabaishi travels along a large sand dune with poorly compacted soil.

Another difference between these two rivers is that the Ugawa has at least 8 meter high levees built up along the banks and much greater flood protection (pumps and gates). Perhaps it is this tendency of the Ugawa to flood that periodically cleans its banks of loose sediment. At any rate, the tall dikes meant that when the banks spread, they carried more material, and caused damage to the slope paving and flood control facilities.

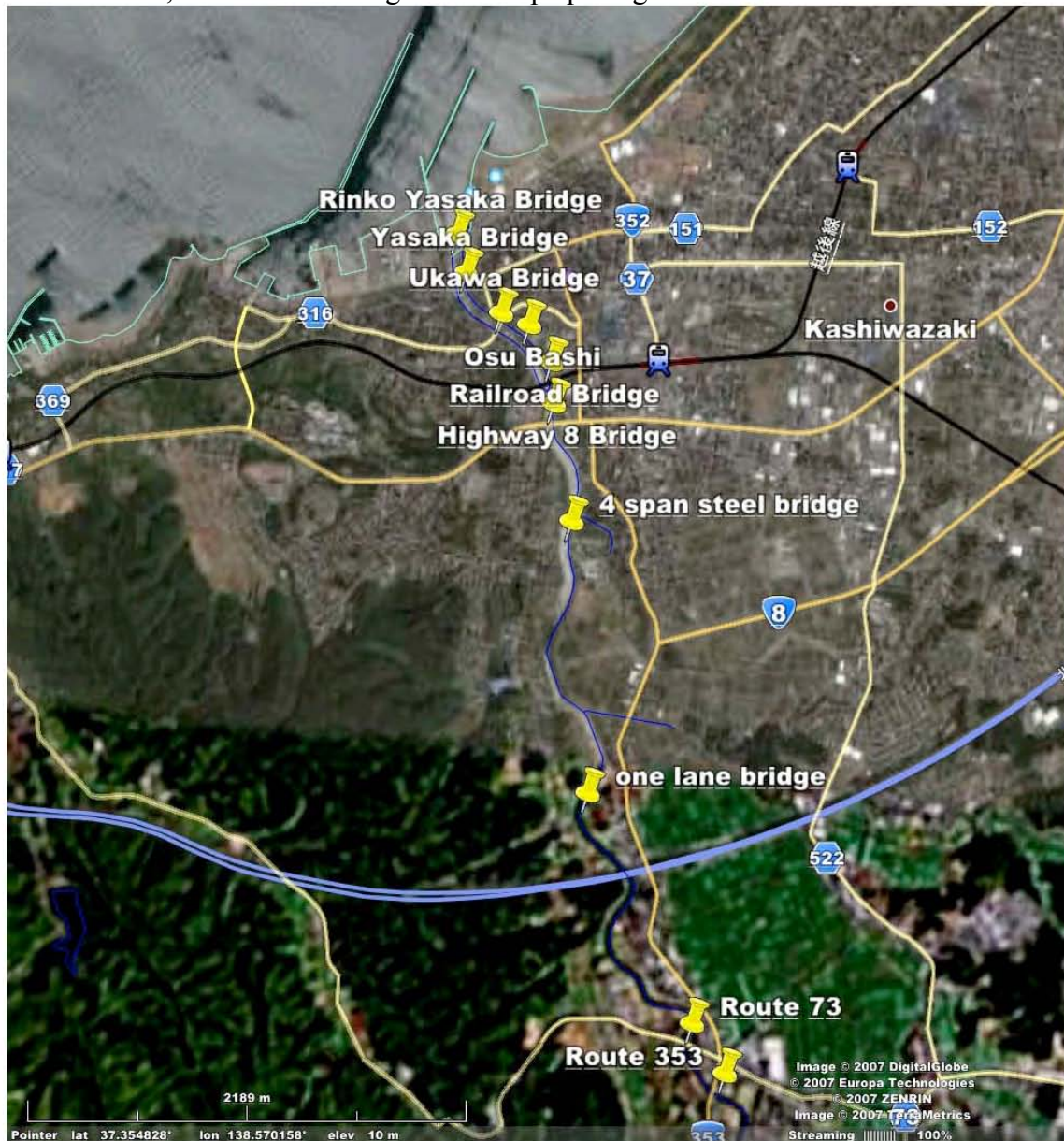


Fig. 6.49 Map of U River Bridges.

Rinko Yasaka Bridge (N37.3675° E138.5433°)

This is a two span concrete I girder bridge on seat abutments and a single column bent with a hammerhead cap at the mouth of the Ugawa. This location had the most lateral spreading on the Ugawa. The entire levee was dragged toward the river (Fig. 6.50) and the abutment was damaged and separated from the wingwall (Fig. 6.51).



Fig 6.50. Rinko Yasaka Bridge at the mouth of the Ugawa.



Fig. 6.51. Abutment and wingwall damage from the earthquake.

The concrete I girders broke the abutment backwall (Fig. 6.52), the bridge approaches were damaged but quickly repaired (Fig. 6.53), and it appeared that repair work was going on at the center pier (Fig. 6.54).



Fig. 6.52. Backwall-Diaphragm damaged by earthquake.

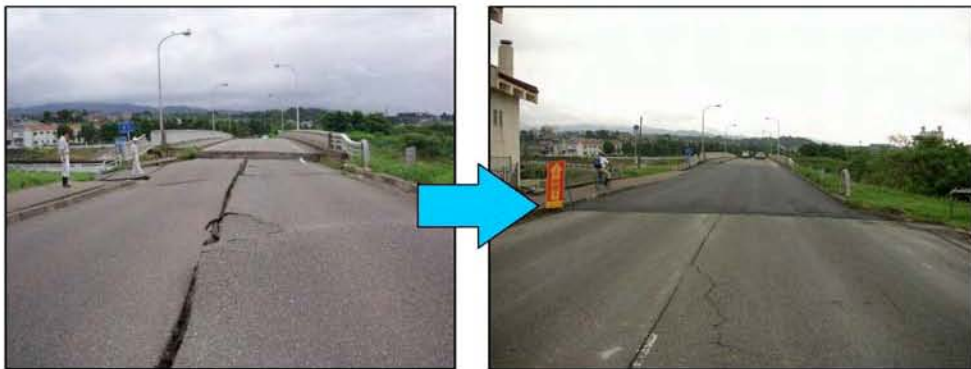


Fig. 6.53. Before and after views of approach and bridge deck.



Fig. 6.54. Pier supporting Rinko Yasaka Bridge.

Yasaka Bridge (N37.3658° E138.5438°)

Like most of the bridges over the Ugawa, this is a two span, simply-supported river crossing, but with steel girders, and supported on a pier wall and seat-type abutments (Fig. 6.55). It is about 200 meters from the more heavily damaged Rinko Yasaka Bridge, but the soil was much firmer at this site, there was less than 100 cm of settlement at the approaches, and no damage to the abutments or wingwalls (Fig. 6.56).



Fig. 6.55. The Yasaka Bridge.



Fig. 6.56. Approach and deck of Yasaka Bridge.

Ukawa Bridge (N37.3641° E138.5462°)

Continuing to walk upstream another 300 meters, we came to the third bridge crossing the Ugawa. The Ukawa bridge is a two (simple) span 'I' girder bridge supported by a pier wall and seat-type abutments (Fig. 6.57). All of these bridges are about 60 meters long. As seen in Figure 6.58 the only damage was some settlement of the sidewalk on the south end of the bridge.



Fig. 6.57. The Ukawa Bridge.



Fig. 6.58. Approach to Ukawa Bridge.

Osu Bashi (N37.3635° E138.5478°)

The fourth crossing, a narrow (6 m wide) two-span concrete box girder bridge on a single-column bent and tall and short abutments (Fig. 6.59) had more damage. Although the south levee moved very little, the embankment between the levee and the bridge settled a meter (Fig. 6.60) and there was damage to the abutment including a leaking waterline (Fig. 6.61). Figure 6.62 provides a closer view of the settled embankment.



Fig. 6.59. Looking east (upstream) at the Osu Bashi.



Fig. 6.60. Looking north at the south approach to Osu Bashi.



Fig. 6.61. The superstructure is supported on a single bearing (note waterline).



Fig. 6.62. Closer view of settlement at south abutment.

Railway Bridges (N37.3619° E138.5493°)

These are two through girder bridges on steel rocker bearings, seat-type abutments, and a pier wall 200 meters upstream from Osu Bashi (Figures 63 and 64). They are much beefier than the road bridges we had previously studied. When we arrived on August 6th, rail crew were re-attaching the rails and there was new ballast on the approaches. However, they went off to lunch before we could ask them if they were repairing earthquake damage. The rails were rusty, suggesting they hadn't been used in awhile, but its possible that the railway was closed due to damage down south at Omigawa Station. The bridge was built in 1997.



Fig. 6.63. Looking under the Railway Bridges.



Fig. 6.64. Looking at rails on the west bridge where rail crew had left their tools.

Four-span steel bridge (N37.3547° E138.5515°)

This was the last bridge across the Ugawa where we saw any sign of approach settlement. It's a four-simple span steel 'I' girder bridge that crosses over the river, the levees, and a river road. We walked past a lot of flood control facilities along the river including the flood gate seen in Figure 6.65. This bridge has a long embankment on the south side. Figure 6.66 shows a very slight settlement at the north approach.



Fig. 6.65 View looking south across the Ugawa River at this steel bridge.



Fig. 6.66. Looking at the north approach.

6.5 Observations and Recommendations

Almost all of the damage to transportation systems and facilities was a result of problem soils. Recorded ground shaking was fairly high and caused landslides, liquefaction, and lateral spreading, but very little damage to bridges. The 2004 Earthquake near Nagaoka caused more shaking around Kashiwazaki city, but without causing much damage during that earthquake. Why this is so will require more study.

The July 16, 2007 earthquake caused about \$100 million US dollars in damage to the transportation systems. However, Japan's robust construction industry was able to make most repairs within a few hours of the earthquake. There was only one section to take a week for reopen on Route 8 (the slope failure at the road to Nagaoka). Other locations were completed within a day. On the expressway, it took four hours for emergency vehicle access and 56 hours to reopen it to the public. The longest closures to roads was due to landslides.

Because of the considerable expense of soil remediation techniques, it is not clear whether this is a cost-effective technique for bridges with problem soils. It requires the remediation of a large area, its expensive, and is not always effective. Perhaps a better idea based on boring data, is to strengthen the foundation structurally. Although most bridge owners are only concerned to prevent loss of life on their facilities for large earthquakes, it may be cost-efficient to spend some money to improve functionality following earthquakes, especially in highly seismic regions like Niigata Prefecture. Still, transportation structures, in general performed well for this earthquake, which may be close to the maximum earthquake at this site. There were no casualties or collapses and repairs were made very quickly.

US engineers, especially those using HAZUS as a tool to estimate bridge damage should study this report carefully. We routinely saw lateral spreading greater than 50 cm with almost no bridge damage, which HAZUS would typify as major bridge damage.

Also, engineers will sometimes propose spending millions of dollars to retrofit bridges for lateral spreading that is usually not justified, at least from a life-safety perspective. It is the authors' hope that the examples shown in this chapter will be carefully studied by researchers, and used to help bridge owners make better decisions about liquefaction hazards.

Section 7 -Tanks

The reconnaissance team observed numerous tanks during the field investigation, however in-depth structural inspections of these structures were generally not performed. Despite only a cursory observation of many tanks, often performed from facility perimeters, our collective, general insights may be useful for subsequent investigation teams. Underground storage tanks were not inspected, however several instances of “floating”, uplifted tanks due to liquefaction were observed in areas such as gasoline service stations and near water distribution systems. Overall, the seismic performance of above-ground tanks was good with only one observed exception. In several instances tanks were observed at sites with minor to moderate ground settlement yet the tanks performed well. Specific examples include:

- Wastewater tanks at a site of extensive liquefaction. Both concrete and steel tanks were observed at the Ansei-Chou waste water treatment plant adjacent to the Sabaishi River (Figure 7.1). Sand boils and ground settlement adjacent to the tanks were observed, however the concrete tanks appeared undamaged. A large steel tank exhibited a section with very minor ripples along the wall that may have been due to the earthquake (Figure 7.2). Overall it appeared to be in good condition and maintained full operation.
- Failure of two cement-plant storage tanks. Buckling failure of the tank bases was observed in an area of extensive liquefaction damage (Figures 7.3 and 7.4). Mast-structures perched above the tanks also failed at the mast-tank connection. The tanks, although recently painted and appearing to be operational, were also empty at the time of investigation, possibly indicating that the tanks were not currently in use or maintained.
- Asphalt storage tank located in the western portion of the Port of Kashiwazaki (Take Naka Facility). The facility was in operation at the time of the reconnaissance and the inspection focused on the performance of a large, insulated asphalt holding tank (Figure 7.5). The tank is secured at its base by a bolt and flange detail (Figure 7.6). Many of the flanges were bent, however none of the bolts appeared to have failed. No “elephant’s foot” bulking of the tank was noted, although the exterior of the tank is covered with a layer of insulation which prohibited a more thorough inspection (Figure 7.7). The tank structure and appurtenant pipes appeared to be undamaged except for minor failures of the tank anchor system. This structure is also addressed in the section on Port and Harbors.
- Cement tanks located at the Kashiwazaki Port (Taiheiyo Cement Tanks). This facility is located in the backland portion of the terminal and it is the site of two large cement tanks. Inspection of the tank foundations revealed minor ground settlement of 5 cm to 12 cm adjacent to the tank foundations (Figures 7.8 and 7.9). Liquefaction effects were negligible in this area. The tanks and

pipe system appeared to be in good shape with negligible damage. This structure is also addressed in the section on Port and Harbors.

- Sake factory storage tanks. While old sake production warehouses were completely collapsed, modern facilities such as steel tanks were not damaged (Site YT22).
- Spherical natural gas tanks at several locations. Numerous large radius, spherical, natural gas tanks were observed in the field area (Sites SD13/RK57, SD18, RK31). cursory inspections were made at four sites around the Kashiwazaki city limits. In all cases, the tanks appeared to be undamaged. At two sites, the skirts at the base of the tanks that protect the piping system were opened, exposing the pipes. There did not appear to be any damage to the piping system. Extensive inspections were being conducted at Site SD13/RK57 at the time of the investigation (Figure 7.10). At this site, it appeared that trenching had been performed for below grade pipes, however no above grade damage of the tanks or distribution pipes was observed (Figure 7.11). Permanent ground deformations in the vicinity of the site were very minor to negligible. This site is also discussed in the Lifeline Systems section.
- Cylindrical oil storage tanks. Several oil storage tanks were investigated from the facility perimeter and appeared to be in good condition with no observable damage (Fig. 7.12 - Site RK55).

Possible tasks for subsequent investigation include:

- Further investigation of silos and tall tanks.
- Request data from Tokyo Gas or Chiba Gas on the performance of their natural gas tanks.
- Gather data on petroleum tanks in the region.
- Focus on tanks located north of the central Kashiwazaki City area.



Figure 7.1: Steel tank at the Ansei-Chou waste water treatment plant (Site RK9, N37.38748°, E138.56587°, photo taken 7/20/07 16:40). Sand boils and slight overturning of the support member to the far-most right of the photograph were observed, as was extensive lateral spreading and road damage. Indications of minor distress of the tank was identified but for the most part appeared in good service.



Figure 7.2: Steel tank at the Ansei-Chou waste water treatment plant (Site RK9, N37.38748°, E138.56587°, photo taken 7/20/07 16:40). Minor distress to the wall was observed roughly 3 m above the base of the tank.



Figure 7.3: Damage to steel tanks at the cement plant located adjacent to the mouth of the Sabaishi River (Site RK10, N37.38795°, E138.56508°, photo taken 7/20/07 17:10). Tank damage likely caused by the cumulative effects of inertial loading, ground failures, and lateral loads due to the failure of appurtenant structures.



Figure 7.4: Close-up of damage to steel tanks at the cement plant located adjacent to the mouth of the Sabaishi River (Site RK10, N37.38795°, E138.56508°, photo taken 7/20/07 17:20). Buckling at the base of the tanks is evident.



Figure 7.5: Kashiwazaki Port - Asphalt storage and transport facility located in the western portion of the port (Located near Site RK25, N37.36713° E138.53210°, photo taken 7/21/07 15:58).



Figure 7.6: Kashiwazaki Port - Anchorage of asphalt storage tank (Located near Site RK25, N37.36713° E138.53210°, photo taken 7/22/07 12:37).



Figure 7.7: Kashiwazaki Port - Anchorage of asphalt storage tank (Located near Site RK25, N37.36713° E138.53210°, photo taken 7/22/07 12:37).



Figure 7.8: Kashiwazaki Port (Taiheiyo Cement Facility) - Evidence of minor to moderate settlement of sandy fill adjacent to one of the large diameter tanks (Site SD 9, approximately N37.36665° E138.53983°, photo taken 7/22/07 15:48).



Figure 7.9: Kashiwazaki Port (Taiheiyo Cement Facility) - Evidence of minor to moderate settlement of sandy fill adjacent to one of the large diameter tanks (Site SD 9, approximately N37.36665° E138.53983°, photo taken 7/22/07 15:48).



Figure 7.10: Steel natural gas tanks undergoing inspection by the operator and engineering consultants (Site SD13/RK57, N37.37253°, E138.59488°, photo taken 7/23/07 12:37). Trenching and below grade inspections had already taken place prior to the field investigation. No damage was observed to the tanks, pipe connections, or mains, however observations were made from the perimeter of the facility, a short distance from the structures.



Figure 7.11: Steel natural gas tanks undergoing inspection by the operator and engineering consultants (Site SD13/RK57, N37.37253° E138.59488°, photo taken 7/23/07 12:31).



Figure 7.12: Oil storage tanks (Site RK55, N37.38917° E138.63377°, photos taken 7/23/07 12:30). No damage was observed at this site.

Section 8 - Ports and Harbors

The coastal location of this earthquake has provided the opportunity to assess the performance of port and coastal infrastructure to a moderate-sized event. Several members of the reconnaissance team have focused on the seismic performance of waterfront structures and the occurrence of ground failures at ports, harbors, and other coastal environments. The coordinated field inspection of ports, marinas, and fishing facilities was initiated from the southwest, at the small village of Kasashima, and progressed to the northeast into and past the city of Kashiwazaki. A brief overview of the field observations at waterfront sites is provided in order to assist subsequent earthquake investigation teams interested in this aspect of the event.

The Kasashima harbor exhibited negligible to very minor evidence of ground deformation and seismic effects to coastal infrastructure (e.g. quay walls, seawalls, breakwaters). Trace remnants of very small, localized ground deformations were observed, and it appears that the ground motions in this area were just strong enough for incipient lateral deformation of the ground and waterfront earth retention structures (Figure 8.1). This site is useful for investigating the regional extent of liquefaction-induced ground failure at ports located southwest of the meiseismic region. Lateral spreading of 7 cm to 12 cm was observed in beach deposits with lateral deformation of short concrete quay walls of 1 cm to 2 cm. No movement of larger caisson-type quay walls or breakwaters was observed. Settlement of paved aprons of roughly 10 cm to 12 cm was noted behind the short quay wall (Figures 8.2 and 8.3). The investigation team did not inspect coastal facilities located southwest of Kasashima harbor. It is possible that very minor evidence of liquefaction occurred to the west, however in the absence of significantly different site effects, the impact on coastal infrastructure is likely minimal. The investigation team did not receive reports of significant damage to coastal facilities west of Kasashima, despite the occurrence of several moderate to large landslides in cut slopes for highways and rail routes in this area.

From Kasashima the reconnaissance moved eastward toward the epicentral region. The Kashiwazaki Marina was inspected and considered a site of minor damage. Evidence of ground deformation was observed in the form of minor lateral movement (generally 2 cm to 7 cm) of short quay walls and maximum ground settlements adjacent to quay walls of roughly 7 cm to 15 cm (Figures 8.4 and 8.5). Small sand boils were observed in isolated portions of the boat storage yard. The alignment of the quay walls was very good indicating fairly uniform, minor lateral movement. Estimates of maximum lateral wall movement are 6 cm to 10 cm. Minor ground cracking and lateral deformation was observed around the perimeter of the marina property. Paved and unpaved parking areas located in filled areas adjacent to the facility exhibited very minor cracks with cumulative displacements on the order of 3 cm to 5 cm. A park with a multi-story observation structure is located immediately to the west of the marina property (Onodachi Seaside Park). The structure appears to be located on fill, although the foundation type is not currently known to the team. The sloping, grass-covered fill at this site exhibited very minor cracking indicating incipient ground failure.

The Port of Kashiwazaki is relatively large in lateral extent (i.e. along the coastline) and for the sake of this investigation it is subdivided in roughly 4 main portions, with two lesser sections that are located between more active berths. These sections of the port are divided as follows:

Westernmost section – From the landward portion of this section of the port to the outer harbor this area includes; (a) an older portion of the berth that appears to be relatively unused, (b) an asphalt heating and pumping facility, (c) a new facility that includes sightseeing boat mooring and a single-story office building, (d) an outer harbor-front quay wall, and (e) the major seawall and breakwater that extends from the beach into the harbor a total length of approximately 2.4 km. The landward portion of the berth (a) appears to include both concrete caissons and a wharf deck supported by vertical concrete piles (Figure 8.6). No lateral movement of this portion of the wharf was noted and no damage to the piles was noted, although only the waterfront row of piles was visible during the investigation. The Take Naka asphalt facility (b) exhibited very little damage (Figures 8.7 - 8.9). The facility was in operation at the time of the reconnaissance and the inspection focused on the performance of the large, insulated asphalt holding tank. The tank is secured at its base by a bolt and flange detail. Many of the flanges were bent, however none of the bolts appeared to have failed. No “elephant’s foot” bulking of the tank was noted, although the exterior of the tank is covered with a layer of insulation prohibiting a more thorough inspection. The asphalt distribution pipe, which is slightly elevated above the ground, did not exhibit signs of distress despite extensive ground failure along the adjacent area near the sightseeing facility (Figure 8.10).

The new sightseeing facility (c), including a new single-story structure, associated pedestrian areas, and wharf, were subjected to the effects of widespread liquefaction, lateral spreading and settlement. The structure performed very well, but did exhibit minor distress along two pedestrian-accessible roof areas on either side of the main structure. It is believed that the distress is due to adjacent lateral spreading and differential settlement between the ground and structure. The paved areas and walkways surrounding the building were extensively damaged (Figure 8.11). Settlements exceeded 30 cm in many areas and a pronounced graben formed between the building and the waterfront quay wall. The quay wall has moved laterally and tilted a minor amount (Figure 8.12). This area was extensively investigated by the team and it was the focus of a ground-based LiDAR survey.

The outer quay wall area has been subjected to large lateral ground deformation and settlement due to liquefaction (Figures 8.13 and 8.14). The seawall/breakwater was inspected landward from the beach adjacent to the asphalt handling facility to the outer quay area. The breakwater exhibited negligible to very minor displacement adjacent to the beach. The waterfront side of the seawall is armored with concrete tetrapods. The tetrapods appear to be unreinforced and numerous units showed damage due to rocking during the earthquake (Figure 8.15). This type of damage to tetrapods and other wave armor units was noted throughout the Kashiwazaki Port and long seawall located northeast of the Sabaishi River.

Southwestern pier – The portion of the Port of Kashiwazaki referred to herein as the “southwestern pier,” appears to be a shallow water terminal used along one berth as a staging area for a dredging barge and on the opposite side of the terminal as a fishing and/or light cargo handling area. This berth exhibited extensive liquefaction-induced damage. Lateral movement of the quay wall (anchored sheetpile wall) along the western face was approximately one meter with settlements of roughly 0.5 m to 0.6 m (Figures 8.16 and 8.17). The quay wall tilted roughly 5°. The lateral deformation along the eastern face was much less pronounced (roughly 0.3 m), although the settlement of the backfill was equally severe (0.6 m) (Figure 8.18). It appears that the eastern portion of the terminal has been constructed of concrete caissons. It is believed that a portion of the difference in the observed lateral quay wall movement is due to the use of different structures during construction of the terminal. The heights of the sheetpile walls and caissons could not be discerned during the reconnaissance.

Steel Scrap Handling Facility – Moving eastward along the port complex the next major industrial facility is a steel scrap handling and transport wharf. Sand boils, ground cracks and liquefaction-induced settlement were pervasive throughout this facility, particularly around the waterfront perimeter. Waterfront settlements up to approximately 35 cm were noted and lateral wall movements varied between 2 cm and 30 cm depending on the orientation of the quay wall (Figures 8.19 and 8.20). Pronounced pavement disruption and ground cracks in the landward section of the facility indicated lateral deformation of the anchor system for the sheetpile walls (Figure 8.19). Lateral movement and rotation of near-shore concrete blocks with bollards and damage to wave armor units were also observed.

Interior, north facing quay wall (end of Coast Guard Berth) – This landward and short length of quay wall is located between the Steel Scrap Handling Facility and the terminal that was being used at the time of the reconnaissance by the Japan Coast Guard described in the following subsection. The water depth in this portion of the port is relatively small although the exact depth of water and height of caissons was not determined during the investigation. The caissons were laterally displaced roughly 30 cm to 45 cm (Figure 8.21). The caissons are approximately 4.5 m wide.

Japan Coast Guard/Japan Self Defense Forces Staging Berth – The largest terminal area at the Port of Kashiwazaki was being used by the Japanese Coast Guard and Japanese Self Defense Forces. The north facing berth of this terminal is approximately 400 m in length. At the time of the investigation the terminal served as a staging area for military assistance personnel and stockpile area for construction materials being used in the recovery and rebuilding efforts. A large pile of steel scrap from operations conducted prior to the earthquake was located immediately adjacent to the western quay wall. This western portion of the terminal was being utilized by the Coast Guard. Only very minor liquefaction effects, lateral displacement, and settlement were observed in this area. Small sand boils were noted and lateral displacements of the quay wall were very small (≤ 5 cm) (Figure 8.22). Apron settlements of roughly 2 cm to 7 cm were observed. Maximum settlements adjacent to bollards were roughly 7 cm.

The west end of the north facing quay was also utilized by the Japan Coast Guard. This portion of the quay exhibited negligible lateral displacement (≤ 4 cm) and minor settlement (Figures 8.23 and 8.24). Overall, the seismic performance of this portion of the terminal was very good. The middle to eastern end of the quay was being used to berth a ship of the Japan Self Defense Forces at the time of the survey. The effects of liquefaction were similarly minor with localized apron cracking and minor lateral displacement along much of the berth (Figure 8.25). It is interesting to note however that the evidence of liquefaction-related ground failure and quay wall displacement increased along the berth to the east (i.e. closer to the eastern boundary of the berth at the mouth of the U River, Figure 8.26). Within roughly 100 m of the U River the effects of liquefaction became pronounced. Significant damage was observed to the quay wall with lateral displacement and failure of the upper portion of the wall (Figures 8.27 and 8.28).

Taiheiyo Cement Tanks – This facility is located in the backland portion of the terminal and it is the site of two large cement tanks. Inspection of the tank foundations revealed minor ground settlement of 5 cm to 12 cm adjacent to the tank foundations (Figures 8.29 and 8.30). Liquefaction effects are negligible in this area. The tanks and appurtenant piping appeared to be in good shape with negligible damage.

The eastern boundary of the Port of Kashiwazaki is located at the mouth of the U River. None of the breakwater structures located offshore of the port complex (west bank) or the levee and breakwater structures along the east bank near the river mouth were investigated during this reconnaissance. The Minatomachi Seaside Park, bounded to the west by the U River, was entirely occupied by Self Defense Forces and being used for temporary housing and staging areas for relief efforts. The area is generally open parkland and a very cursory walk-through inspection was made. Evidence of liquefaction was prevalent throughout the park. Ground cracks, sand boils, and damages to paved surfaces were widespread. Numerous sand boils and extensive ground cracks associated with lateral spreading were observed on the beach. No structural inspections were performed to assess the performance of building foundations in this area. The oceanfront from this park to the mouth of the Sabaishi River, located roughly 2.5 km to the northeast, consists of two public beaches then a long reach of waterfront wave armor units backed by concrete seawalls. A long portion of the seawall extending southwest from the Sabaishi River was inspected by the reconnaissance team.

The mouth of the Sabaishi River is protected along its southwest bank by a wall constructed of sheet piles with concrete filling (Figure 8.31). Negligible lateral movement of the riverfront wall was noted and roughly 5 cm to 7 cm of settlement was noted adjacent to the sheet pile wall. Evidence of approximately 30 cm of lateral spreading in the sand deposits behind the sheet pile shore protection was observed. Minor lateral deformation and damage to the concrete slope armor panels was observed across the river from this site.

Along the waterfront to the southwest of the Sabaishi River and transverse to the riverfront sheet pile wall previously described, is a seawall that extends southwest

roughly 2.0 km towards the Minatomachi Seaside Park. This seawall was inspected for over a 1 km length. Observations were made from the river mouth southwest to an armored rockfill breakwater located roughly 900 m from the cement plant site. The initial portion of the seawall is located along a narrow beach with wave armor units. This portion of the seawall exhibited lateral deformation, rotation, and structural damage along the counterfort ends of several of the individual wall sections (Figure 8.32).

There is a seaward step in the seawall located immediately southwest of the cement plant site. This point was the location of a seawall failure that included a collapsed section of wall, significant settlement and cracking of the backfill, and settlement of the concrete panels located behind the seawall (Figure 8.33). The backfill adjacent to the seawall is composed of clean, rounded cobbles (diameter > 15 cm) (Figure 8.34). The lateral wall movement in this area was roughly 0.6 m.

The area located behind the seawall has been developed with a benched, earth embankment composed of sandy clay and clayey sand that extends almost the entire distance to the beaches near the Minatomachi Seaside Park. The seawall exhibited an increased seaward tilt as the investigation moved to the southwest (Figure 8.35). The lateral deformation was crudely estimated to be approximately 1.5 m to 2.0 m. The actual lateral movement is very difficult to estimate in the field due to the contributions of lateral spreading, levee slumping, and foundation failure. The embankment exhibited pervasive longitudinal cracks along the crest and side slopes, and a less well-developed set of transverse cracks. The longitudinal cracks were noted on both sides of the embankment however the deformations in the seaward direction were much more pronounced (Figure 8.36). The embankment is discontinuous and is bisected by several unpaved access roads. At these sections it is clear that the embankment has experienced significant differential settlement, transverse cracking, and longitudinal cracking extending through the entire earth structure (Figure 8.37). The radial pattern of longitudinal cracks observed at the base of one of the embankment sections clearly demonstrated the extent of foundation failure and differential settlement of the embankment. No liquefaction features (e.g., sand boils, vented sand) were observed in the embankment fill or in tension cracks. Several large voids (> 1 m³) were exposed near the toes of failed portions of the embankment.

The lateral ground deformation associated with these embankment and foundation failures impacted the seawall and contributed to the development of larger displacements (Figure 8.38). At one location near the southwestern end of this area ground settlement and lateral movement of the seawall was accompanied by the failure of the top of the wall (Figure 8.39). The inspection of the seawall was terminated at the location of an armored groin structure (possibly an outfall structure). At the time of the investigation a track-hoe was being utilized to move rockfill between the seawall and the concrete armor blocks that overlie the rockfill offshore (Figure 8.40).

Oceanfront inspection was made by the reconnaissance team along a roughly 8.25 km portion of the coast extending northeast from the mouth of the Sabaishi River including the Kariwa nuclear power plant. At the TEPCO Nuclear Power Plant ground

settlement and tilting of a building were observed near the shore on the west of Unit 5 (Figs. 5.4 and 5.5, SP39). Some sand boils observed nearby suggested that soil liquefaction of reclaimed sand did occur in this area.

The next coastal observations were made at site located roughly 1.8 to 2.0 km northeast of the nuclear power plant facility (Site RK37). Minor displacement of the seawall and landward embankments, very likely due to liquefaction of beach sands at the toe of the walls, was observed (Figure 8.41). Displacements of 21 cm vertical, and 55 cm horizontal were measured between displaced seawall sections and adjacent wall sections that performed well. The total length of the failed seawall was 40 m (Figure 8.42).

Approximately 3.5 km northeast (direct line) of this site liquefaction of beach sand led to lateral spreading of the road embankment and failure (rotation and translation) of the concrete seawall. Deformations were on the order of 25 cm vertical, and up to 64 cm horizontal, with approximately 9° of rotation (Figures 8.43 and 8.44). This site marked the northeastern-most extent of the coastal investigation.



Figure 8.1: Minor ground failure along the waterfront at Kasashima (Site RK21, N37.33702° E138.46680°, photo taken 7/21/07 14:49). The limited extent of the ground cracking indicated incipient lateral movement.



Figure 8.2: Kasashima Harbor - Ground settlement and minor lateral deformation adjacent to quay walls (Site RK21, N37.33702° E138.46680°, photo taken 7/21/07 14:40).



Figure 8.3: Kasashima Harbor - Settlement of fill behind quay walls (Site RK21, N37.33702° E138.46680°, photo taken 7/21/07 14:48).



Figure 8.4: Kashiwazaki Marina - Evidence of minor lateral movement of quay walls and associated settlement of the paved apron (Site SD3, N37.36093° E138.52027°, photo taken 7/22/07 12:59).



Figure 8.5: Kashiwazaki Marina - Evidence of minor settlement behind quay walls (Site SD3, N37.36093° E138.52027°, photo taken 7/22/07 13:12).



Figure 8.6: Kashiwazaki Port - Older, undamaged pile-supported wharf located in the western portion of the port facility (Site RK25/SA25/YT4, N37.36713° E138.53210°, photo taken 7/21/07 16:12).



Figure 8.7: Kashiwazaki Port - Asphalt storage and transport facility located in the western portion of the port (Located near Site RK25, N37.36713° E138.53210°, photo taken 7/21/07 15:58).



Figure 8.8: Kashiwazaki Port - Anchorage of asphalt storage tank (Located near Site RK25, N37.36713° E138.53210°, photo taken 7/22/07 12:37).



Figure 8.9: Kashiwazaki Port - Anchorage of asphalt storage tank (Located near Site RK25, N37.36713° E138.53210°, photo taken 7/22/07 12:37).



Figure 8.10: Kashiwazaki Port - Seawall and exposed end of the elevated asphalt pipe (Located near Site RK25, N37.36713° E138.53210°, photo taken 7/21/07 15:51).



Figure 8.11: Kashiwazaki Port - Liquefaction-induced damage to the sightseeing wharf (Site RK25/SA25/YT4, N37.36713° E138.53210°, photo taken 7/21/07 16:03).



Figure 8.12: Kashiwazaki Port - Liquefaction-induced damage to the sightseeing wharf with minor displacement of the caisson quay wall (Site RK25/SA25/YT4, N37.36713° E138.53210°, photo taken 7/21/07 16:09).



Figure 8.13: Kashiwazaki Port - Evidence of lateral ground deformation adjacent to the outer quay wall (Located near site RK25/SA25/YT4, N37.36713° E138.53210°, photo taken 7/21/07 15:49).



Figure 8.14: Kashiwazaki Port - Evidence of ground failure adjacent to the seawall at the outer quay wall area (Located near site RK25/SA25/YT4, N37.36713° E138.53210°, photo taken 7/21/07 15:50).



Figure 8.15: Kashiwazaki Port - Likely earthquake-related damage to tetrapod wave armor units (Located near site RK25/SA25/YT4, N37.36713° E138.53210°, photo taken 7/21/07 15:53).



Figure 8.16: Kashiwazaki Port - West facing portion of the “Southwestern Pier” showing displacement of the sheet pile wall and ground settlement due to liquefaction of sandy backfill (Site SD5, N37.36532° E138.53213°, photo taken 7/22/07 13:57).



Figure 8.17: Kashiwazaki Port - West facing portion of the “Southwestern Pier” showing displacement of the sheetpile wall and ground settlement due to liquefaction of sandy backfill (Site SD5, N37.36532° E138.53213°, photo taken 7/22/07 13:58).



Figure 8.18: Kashiwazaki Port - East facing portion of the “Southwestern Pier” showing pronounced ground settlement (Site SD5, N37.36532° E138.53213°, photo taken 7/22/07 14:05).



Figure 8.19: Kashiwazaki Port - Steel Scrap Transport Facility showing evidence of ground failure due to liquefaction of sand fill and damage to concrete aprons (Site SD6, N37.36668° E138.53565°, photo taken 7/22/07 14:46).



Figure 8.20: Kashiwazaki Port - Steel Scrap Transport Facility showing caisson displacement (Site SD6, N37.36668° E138.53565°, photo taken 7/22/07 14:56).



Figure 8.21: Kashiwazaki Port - North facing, landward quay wall exhibiting lateral movement and rotation of caissons (Site SD7, N37.36593° E138.53692°, photo taken 7/22/07 15:12). The Taiheiyo Cement Tanks are in the background.



Figure 8.22: Kashiwazaki Port - Minor ground cracks located parallel to the western quay wall used as the berth for the Japan Coast Guard (Site SD8, N37.36680° E138.53825°, photo taken 7/22/07 15:17).



Figure 8.23: Kashiwazaki Port - Evidence of very minor lateral movement of quay walls and minor settlement located along the northern face of the terminal used as the berth for the Japan Coast Guard (Site SD8, N37.36680° E138.53825°, photo taken 7/22/07 15:22).



Photo 8.24: Kashiwazaki Port - Evidence of minor settlement adjacent to a pile-supported (?) bollard anchorage located along the northern face of the terminal used as the berth for the Japan Coast Guard (Site SD8, N37.36680° E138.53825°, photo taken 7/22/07 15:21).



Figure 8.25: Kashiwazaki Port - Evidence of very minor lateral movement of quay walls and minor settlement located along the northern face of the terminal used as the berth for the Japan Self Defense Force (Site SD8, approximately N37.36680° E138.53825°, photo taken 7/22/07 15:24).



Figure 8.26: Kashiwazaki Port - Evidence of more extensive lateral caisson displacement and ground settlement adjacent to the quay wall located along the eastern end of the north face of the terminal (Site SD8, approximately N37.36680° E138.53825°, photo taken 7/22/07 15:36).



Figure 8.27: Kashiwazaki Port - Significant liquefaction-related damage to the quay walls located at the eastern edge of the terminal adjacent to the mouth of the U River (Site SD8, approximately N37.36680° E138.53825°, photo taken 7/22/07 15:32).



Figure 8.28: Kashiwazaki Port - Significant liquefaction-related damage to the quay walls located adjacent to the U River (Site SD8, approximately N37.36680° E138.53825°, photo taken 7/22/07 15:36).



Figure 8.29: Kashiwazaki Port (Taiheiyo Cement Facility) - Evidence of minor to moderate settlement of sandy fill adjacent to one of the large diameter tanks (Site SD9, approximately N37.36665° E138.53983°, photo taken 7/22/07 15:48).



Figure 8.30: Kashiwazaki Port (Taiheiyo Cement Facility) - Evidence of minor to moderate settlement of sandy fill adjacent to one of the large diameter tanks (Site SD9, approximately N37.36665° E138.53983°, photo taken 7/22/07 15:48).



Figure 8.31: Mouth of the Sabaishi River showing the erosion control measures (Site SD 1, approximately N37.38868° E138.56508°, photo taken 7/22/07 11:07). The Ansei Bridge (Sites SA6/SD2/RK8) is visible in the background.



Figure 8.32: Eastern end of the seawall located adjacent to the damaged cement plant and mouth of the Sabaishi River (Site SD1, approximately N37.38868° E138.56413°, photo taken 7/22/07 10:56). Lateral spreading behind the wave armor units, as well as ground settlement and minor sea wall damage was widespread.



Figure 8.33: Partial collapse of a portion of the seawall located at the lateral, seaward step in alignment just west of the damaged cement plant (Site SD1, N37.38868° E138.56413°, photo taken 7/22/07 11:18).



Figure 8.34: Close-up of the collapsed portion of the seawall showing the clean cobble backfill (Site SD1, N37.38868° E138.56413°, photo taken 7/22/07 11:23).



Figure 8.35: Evidence of seawall rotation, ground settlement, and longitudinal cracking of the benched embankment (Moving southwest of Site SD1, approximately N37.38868° E138.56413°, photo taken 7/22/07 11:25).



Figure 8.36: Representative cracking and lateral displacement of the clayey earth embankment adjacent to the seawall (Location is southwest of Site SD1, photo taken 7/22/07 11:35).



Figure 8.37: Ground deformations adjacent to the embankment and seawall (Location is southwest of Site SD1, photo taken 7/22/07 11:41).



Figure 8.38: Ground deformations adjacent to the embankment and seawall (Location is southwest of Site SD1, photo taken 7/22/07 11:42).



Figure 8.39: Lateral displacement, rotation, and structural damage to the seawall (Location is southwest of Site SD1, photo taken 7/22/07 11:45).

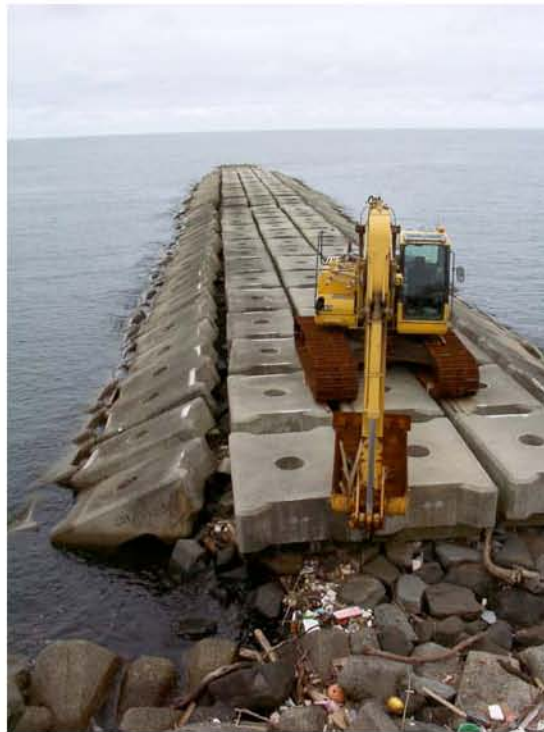


Figure 8.40: Repair of an armored, rockfill breakwater (possibly an outfall structure). (Location is southwest of Site SD1, photo taken 7/22/07 11:49).



Figure 8.41: Evidence of minor liquefaction and lateral spreading in sandy beach deposits adjacent to the seawall (Site RK37, N37.45478°, E138.60927°, photo taken 7/23/07).



Figure 8.42: Rotation and lateral displacement of the concrete seawall (Site RK37, N37.45478°, E138.60927°, photo taken 7/23/07).



Figure 8.43: Liquefaction-induced damage to the seawall and adjacent roadway (Site RK35, N37.48497°, E138.62645°, photo taken 7/23/07).



Figure 8.44: Lateral spreading associated with liquefaction of beach sand (Site RK35, N37.48497°, E138.62645°, photo taken 7/23/07).

Section 9 - Transportation Systems

9.1 Roads

Transportation systems were disrupted by landslides, lateral spreads, embankment slumping and spreading, bridge approach settlement, liquefaction of utility trench fills, and post-earthquake sub-grade construction recovery efforts. In many cases, roadways were blocked by landslide debris, in others the roadfill and foundation failed requiring extensive repair. Despite the numerous road closures and pavement damage, the reconnaissance team found that driving throughout Kashiwazaki was relatively easy. Furthermore, significant progress was made toward repairing critical damaged roadways during the time of the reconnaissance.

The most striking damage to the transportation network was caused by large landslides destroying sections of roads. The Ozumi Senbon Landslide (Fig. 9.1 - Site RK1) closed both lanes of Highway 8 just north of the intersection with Route 252. The roadway traversed the landslide at approximately its mid-elevation, and the roadway moved down slope with the slide. The landslide geometry and roadway damage were clearly observed on Friday, July 20th, and by Monday, July 23th, the landslide and roadway had been repaired almost completely, including asphalt, yellow-center striping, and guard rails, permitting two-way passage of traffic through the affected region. A roadway approaching the Kashiwazaki municipal waste incinerator plant was destroyed by a liquefaction-induced lateral spread (Fig. 9.2). The head scarp of the lateral spread traversed a section of the roadway, causing a vertical offset of approximately 2.5 meters at one section of road. The pavement was heavily damaged on the portion of the roadway affected by the lateral spread.

Embankment failures affected transportation access, closing partial to whole lanes. In most cases, one lane remained open despite longitudinal ground cracks in many pavement sections that required cars to progress slowly and carefully over the damaged roadway. Figs. 9.3 and 9.4 are typical cases where one lane was closed to traffic due to slumping and spreading of roadway embankments. Fig. 9.5 is typical of pavement cracks that caused traffic to move more slowly than normal. In general, the severity of pavement and embankment damage was noticeably greater nearer to the city of Kashiwazaki (e.g. on the coastal road north of Kashiwazaki, compare Fig. 9.3 which was taken more than four kilometers southward from Fig. 9.4)

Settlement of soils at bridge approach fills caused vertical offsets at many bridges by as much as one meter (Figs 9.6 and 9.7, additional details are provided in the “Bridges Section”). The offsets required placement of gravel or asphalt pavement to maintain a smooth transition for traffic flow onto the bridges. At the beginning of the reconnaissance mission during July 20-24, 2007, fill had been placed at nearly all of the bridges requiring such repair and only two bridges remained closed. It is not clear how the bridge offsets affected traffic during the first three days following the earthquake.

Near the beginning of the reconnaissance mission (Friday, July 20th), the main Kashiwazaki exit from the Hokuriku Expressway was closed for cars exiting into Kashiwazaki, but access to the Expressway was permitted for those leaving the city. By the end of the reconnaissance mission on July 24th, traffic control officers permitted some vehicles to exit the Hokuriku Expressway at Kashiwazaki. This closure was apparently not due to damage to bridges or pavement at the Expressway exit, but rather to permit access only to residents and recovery personnel in order to lower the number of vehicles within the city.

Two tunnels were closed to through traffic during the time of the reconnaissance. A tunnel along the coastal road at Site SD4 was open on July 20th, and subsequently closed on July 22nd (Fig. 9.8). The cause of tunnel closure was believed to be due to shallow landsliding adjacent to the portal. A tunnel along Route 352 north of the nuclear power plant was closed for reasons that are unknown.

A common cause of pavement damage was liquefaction of utility trench fills, and/or uplift of buried utilities due to buoyancy in liquefied ground. Fig. 9.9 is an example of this widespread pavement damage mechanism. Such damage typically caused closure of one lane of traffic, and in only a few cases were closure of entire roadways necessary due to utility trench fill liquefaction failures.

9.2 Rail

Damage to railways was caused by landslides, settlement of foundation soils, spreading and slumping of railway embankments, and in some cases, damage was observed at sites without apparent ground failure presumably due to transient ground shaking. Some damage occurred to trains carrying passengers at the time of the earthquake - news reports immediately following the earthquake indicated that a stationary train derailed at Kashiwazaki Station but that no one was injured.

Cursory yet pertinent examples of the damage to rail lines include those described by the following sites. A large landslide at the Oumigawa Train Station on the JR Shinetsu line (Site RK20 - Fig. 9.10) overran the tracks, damaging both the tracks and related infrastructure at the station. All train travel through this station was halted as a result of the failure. A LiDAR survey was conducted at this site on July 24th for further analysis of the slide geometry. At the time of the LiDAR survey, construction operations were underway to remove landslide debris and repair the train tracks.

Damage to other rail lines and stations was scattered throughout the region. Liquefaction at Arahama Station caused significant damage to rail infrastructure, including the platform and power lines (Fig. 9.11). Horizontal track offsets of 30 cm were observed in the tracks at Arahama Station (Fig. 9.12), and whereas liquefaction damaged the platform and power lines, there was no evidence that it played a role in the track offsets. It is surmised that surface wave effects may have contributed to the rail deformations observed at this site. Fig. 9.13 shows another site of lateral rail deformation with no signs of liquefaction, but that experienced lateral embankment displacement leading to the deformed tracks. At another site (Site SA24), vertical deformations were

observed in the railway (Fig. 9.14). Numerous other rail disruptions due to foundation settlement and permanent ground deformations were observed by the reconnaissance team. In most cases the deformations were minor, yet significant enough to preclude rail traffic during the period of the reconnaissance. During this time, rail crews were observed making inspections of several rail lines in order to place them back into service.



Figure 9.1: The Ozumi Senbon Landslide (Site RK1, N37.41422° E138.71347°), located along Highway 8 just north of the intersection with Route 252, closed both lanes of traffic. The upper photo, taken 7/20/07 at 11:30, four days after the earthquake, shows the displaced roadway which ran from the distance vehicles to the upper right of the photo to just in front of the investigation team members in the lower right. The bottom photo, taken 7/23/07 at 13:00, shows the nearly completed landslide and roadway repair, complete with guard rails, pavement, and center striping, just three days later.



Figure 9.2: Road to Kashiwazaki municipal waste incinerator plant (Site RK6, N37.39343° E138.58555°, photo taken 7/24/07 18:06). Liquefaction-induced lateral spreading led caused the roadbed and associated slope to move southwards towards the Sabaishi River. Photos show formation of a 2.5 meter tall head scarp at the west end.



Figure 9.3: Road damage from fill embankment failure on coastal road north of Kashiwazaki Nuclear Power Station (Site RK38, N37.44927° E138.60572°, photo taken 7/22/07 13:04). Such damage tended to increase with distance toward the epicenter, often requiring traffic controls to guide cars across the one open lane.



Figure 9.4: Site RK34 - Road damage from fill embankment failure on coastal road north of Kashiwazaki-Kariwa Nuclear Power Plant (Site RK34, N37.48455° E138.62435°, photo taken 7/22/07 09:56).



Figure 9.5: Typical road damage near epicentral region (Site RK30, N37.45727° E138.65328°, photo taken 7/22/07 09:46). Cracks of 5 to 10 cm were often quickly paved over in high-traffic areas, within one or two days of the earthquake. On local community roads with alternate traffic routes, this damage was not immediately repaired.



Figure 9.6: Vertical offset at the approach of Kai-Un Bridge that has been temporarily repaired with gravel fill to permit access (Site YT3, N37.39232° E138.58063°, photo taken 7/20/07 12:42). A vertical offset of 33 cm was measured at the adjacent abutment (left of this photo).



Figure 9.7: Vertical offset at approach of rural bridge that has not yet been repaired (Site SA22 N37.38439° E138.60083°, photo taken 7/21/07 15:00).



Figure 9.8: Tunnel was initially open to traffic following earthquake, but subsequently closed as of July 22nd (Site SD4, N37.38439° E138.60083°, photo taken 7/22/07 13:36). Damage to tunnel was not observed, but landsliding and toppled monuments on top of the tunnel was observed.



Figure 9.9: Pavement damage caused by utility trench liquefaction (Site SA21, N37.38950° E138.59662°, photo taken 7/21/07 14:57).



Figure 9.10: Landslide at Oumigawa Train Station impacted Shin-etsu line railway (Sites RK20/YT16/SA9, N37.34490° E138.48435°, 7/21/07 13:52).



Figure 9.11: Liquefaction-induced damage at Arahama Station (Site RK13, N37.40555° E138.60197°, 7/21/07 09:42).



Figure 9.12: Lateral deformation of train tracks at Arahama Station (Site RK13, N37.40555° E138.60197°, 7/21/07 09:52).



Figure 9.13: Lateral railway buckling (Site RK28, N37.37037° E138.56475°, 7/21/07 18:01).



Figure 9.14: Vertical deformation in train tracks (Site SA24, N37.39323° E138.59520°, 7/21/07 15:44).

Section 10 - Lifeline Systems

In a general sense, lifeline systems represent the civil infrastructure that is necessary for the response and recovery of affected areas following natural disasters. For the sake of this preliminary reconnaissance report, the lifeline systems have been broadly categorized following the convention of the ASCE-Technical Council on Lifeline Earthquake Engineering. This includes the following systems; water and wastewater, gas and liquid fuels, electric power and communication, transportation, and ports. A cursory overview of the seismic performance of the components of the water, gas, and electric systems is provided in this section. The latter lifelines systems have been addressed in separate sections of this report.

Detailed, system-wide evaluations of the seismic performance of lifelines systems were generally not possible during this initial investigation due to the field-oriented nature of the EERI-GEER investigation and the need for extensive background data required for most lifelines assessments (e.g. maps of distribution systems, documentation and statistics on damage patterns and the duration of loss of service, re-routing strategies and system flexibility, and the effectiveness of recovery efforts). The EERI-GEER reconnaissance team was primarily charged with gathering field data of geologic, geotechnical, and structural interest that was considered perishable. This led to a very good overall sense of damage patterns exhibited by several of the lifeline systems and the performance of a limited number of key facilities, however a full investigation of a given lifeline systems was outside the scope of this reconnaissance. These cursory observations are intended to assist subsequent investigation teams as they plan and conduct more focused evaluations of specific lifelines.

10.1 Water and Wastewater

Observations of the seismic performance of water and wastewater distribution systems were made in conjunction with in-depth bridge inspections, site visits to industrial facilities, and during more general visual surveys of the region around Kashiwazaki city conducted by car. Pertinent general observations include the following:

- Water pipe breaks were widespread. Not unexpectedly, these failures were primarily located in areas of soil liquefaction or in areas that were likely underlain by very soft soils (e.g., irrigated agricultural fields such a rice paddies, sites near streams, marshy areas) leading to permanent ground deformations. In response to the large number of pipe breaks numerous emergency water supply stations were established within the Kashiwazaki city limits.
- Ground settlement associated with uncompacted trench fill, loosely placed road fill, and/or liquefaction resulted in elevated manholes, storm drains, and pipes throughout the Kashiwazaki area (Fig. 10.1). Settlement associated with densification of lightly compacted trench backfill during cyclic loading was

conspicuous throughout the region affected by the earthquake. This likely contributed to the damage suffered by the water distribution systems.

- Numerous water and gas pipes were observed at stream crossings. Many unsupported pipes were observed spanning small, channelized streams. No pipe breaks were observed at the small to moderate stream crossings despite evidence of minor lateral and vertical ground deformations (Fig. 10.2).
- Several pipe failures were observed at sites where pipes were attached to bridge structures crossing major streams (Sites RK4/YT3, RK7). At these sites, ground deformations of levees, embankments, and approach fills adjacent to pile supported bridge abutments resulted in stress concentrations and rupture of at least one pipe (Fig. 10.3).
- The site of the Ansui-Chou waste water treatment plant (Site RK9) located adjacent to the Sabaishi River exhibited widespread liquefaction-induced ground deformation. The facility was out of operation at the time of the field survey due to extensive structural damage to the facility. Lateral spreading resulted in separation of one building (Fig. 10.4). Despite this level of ground deformation (vertical and lateral) the initial inspection revealed no rupture of pipes located at grade or in elevated pipe racks. No trenching had been performed at the time of the investigation therefore the performance of buried pipes could not be assessed. No surface evidence of buried pipe breaks was noted. This is an important location for subsequent investigation.
- No other waste water treatment facilities were inspected by the team.

It is very likely that the city or prefecture will prepare maps of pipe breaks in the near future. This information will be very useful for assessing the regional performance of the water distribution system and efforts associated with restoring the full operation of the water supply system.

Possible tasks for subsequent investigations include:

- Investigate the performance of the water supply system (municipal wells and/or water supply reservoirs). Information on the collection, storage, conveyance, and distribution of municipal water in the Kashiwazaki region is severely lacking at this time. It should be noted that minor damage to moderate-sized (30 meter high) earth fill dams was observed in an area northeast of the Kashiwazaki (Site RK50, RK46, see Landslides Section for additional background).
- Extend observations of the water and wastewater systems to the region north of Kashiwazaki.
- Revisit the Ansui-Chou wastewater treatment plant to confirm the performance of the buried pipes.

- If maps exist at the time of the next investigation, attempt to correlate the location and pattern of pipe damage to geologic conditions. This exercise may direct investigators to areas not covered by the initial EERI-GEER team.
- Information on various pipelines materials, dimensions, and layouts may be useful. Data on pipe material, diameter, joints, and other specifics would be beneficial for enhancing empirically-based methods for estimating the occurrence of pipe breaks and system fragility.

,



Figure 10.1: Example of an elevated manhole caused by settlement of road fill. The depression caused by densification of lightly compacted trench backfill during cyclic loading was evident along extensive sections of the roadway. This area was conspicuous for pipe breaks associated with ground deformation (Site SD11, N37.36650° E138.58868°, photo taken 7/23/07).



Figure 10.2: Example of short span pipes (water and gas) across a channelized stream exhibiting very minor ground deformation. No damage to the pipes was observed (Site SD12, N37.36663° E138.59223°, photo taken 7/23/07).



Figure 10.3: Damage to a water pipe at a stream crossing (Site RK4/YT3, N37.39233° E138.58063°, photo taken 7/20/07).



Figure 10.4: Ansui-Chou waste water treatment plant showing evidence of lateral spreading and extension of the structure (Site RK9, N37.38748° E138.56587°, photo taken 7/20/07).

10.2 Electric Power and Communications

The GEER reconnaissance team did not specifically focus on electrical power and communications aspects of this event. Moderate to large facilities were noted in field logs during the regional reconnaissance, however site visits were not made to facilities such as electrical substations, telecommunications buildings, cellular phone networks, or microwave facilities. Numerous power and communication sites warrant further investigation, the most high-profile of which is the Kashiwazaki-Kawira Nuclear Power Facility. The EERI-GEER team did not have full access to this facility, however given the importance of the power distribution system emanating from this plant to much of central Honshu many of the large high voltage towers were observed during the investigation. The team inspected several of the foundations to the large high tension towers leading from the nuclear power plant. No damage to the foundations or tower structures was noted at any of the sites (RK12, RK39, RK40). At one location (RK40) the tower foundation was located on a shallow slope and ground deformations were observed (Fig. 10.5). Ground settlement of roughly 40 cm and lateral movement of 12 cm was measured. No damage to the tower or its foundation was observed. Other tower sites with weak surficial soils and near-by ground failures were observed (Figs. 10.6 and 10.7) however no evidence of structural damage was noted.

A very general overview of other large facilities includes a large electrical substation that was noted roughly 0.6 km west of the Hokuriku Expressway (3.4 km north-northeast of the expressway exit to Kashiwazaki city; N37°23'23.68", E138°36'27.55"). The EERI-GEER team did not visit the site, however it appeared to be a major facility and worthwhile for subsequent inspection. Numerous smaller substations also exist throughout the city, however we did not obtain GPS coordinates for these sites. It may also be worthwhile for subsequent investigation teams to inquire about the NTT building located in downtown Kashiwazaki (Fig. 10.8). Finally, pipes that appeared to be electrical power or communication conduits were observed on numerous bridges (Fig. 10.9).

Possible tasks for subsequent investigations:

- Continue the inspection of foundations for the high tension power lines leading from the Kashiwazaki-Kawira Nuclear Power Facility.
- Obtain statistics on the pattern and duration of interruption of power and communication systems, if any, immediately after the event.
- Inspect the structural details of the components at the electrical substations.
- Attempt to locate maps of power line failures from system operators.



Figure 10.5: Ground failures at the site of a high voltage tower (Site RK40, N37.41633° E138.60792°, photo taken 7/24/07). No evidence of structural damage to the towers was observed.



Figure 10.6: High voltage power line towers located in the Kashiwazaki area (Site RK12, N37.44113° E138.63390°, photo taken 7/21/07). No evidence of structural damage to the towers was observed.



Figure 10.7: High voltage power line towers located in an area of soft ground (Site RK12, N37.44113° E138.63390°, photo taken 7/21/07). No evidence of ground failure, settlement, or structural damage to the towers was observed.



Figure 10.8: NTT communications building in downtown Kashiwazaki (Site SD20, N37.36847° E138.55813°, photo taken 7/23/07). No evidence of major structural damage to the tower was observed however no information on the performance of the electronics was available at the time of the investigation.



Figure 10.9: Evidence of moderate ground failure in an approach fill. Minor damage to the pipes was observed (Site RK7, N37.38940° E138.57393°, photo taken 7/21/07).

10.3 Gas and Liquid Fuels

The GEER reconnaissance team did not focus specific attention on gas and liquid fuel systems. Because maps of the gas distribution network were not available to the team at the time of the field investigation, the performance of any large underground mains or pipelines that may have existed in the region could not be assessed. Observations were confined to relatively few large, above-ground tanks, as well as numerous, widespread sightings of personnel from Tokyo Gas and Chiba Gas inspecting neighborhood distribution systems, pressure testing buried sections of gas mains, and excavations at sites of ruptured gas lines located throughout the city of Kashiwazaki. A perimeter inspection of an oil storage and distribution facility (Fig.10.10 - Site RK55) was performed with no observed signs of damage. Numerous large-diameter spherical natural gas tanks were observed in the region (Sites RK31, SD13/RK57, SD18) and cursory inspections were made at these sites. In all cases the tanks appeared to be undamaged. At two sites the skirts at the base of the tanks that protect the piping system were opened exposing the pipes. There did not appear to be any damage to the piping system. Extensive inspections were being conducted by an energy engineering company at Site SD13 at the time of the investigation (Fig. 10.11). At this site, it appeared that trenching had been performed for below grade pipes however no above grade damage of the tanks or distribution pipes was observed. Permanent ground deformation was minor

to negligible adjacent to this site. Overall, gas and liquid fuel facilities appear to have performed very well during this event. The reconnaissance team is unaware of any failures at this time.

No data was available on the occurrence of fires following the earthquake, but it should be mentioned that none of the reconnaissance team members observed sites of residential or industrial fires. This may be due to the limited nature of the regional investigation (i.e. extensive general coverage as opposed to block-by-block inspection), the use of automatic gas shut-off valves at structures, or other factors.

Possible tasks for subsequent investigation:

- As with the water distribution system, investigate the performance of the gas supply system. Information on the extent of the distribution system and the seismic performance of natural gas and liquid fuels systems in the Kashiwazaki region is not known at this time.
- If possible prior to the next field investigation, determine the location of regional petroleum and natural gas pipelines. Inspection of distribution facilities may be worthwhile.
- Plan for expanded efforts beyond Kashiwazaki with coverage to the north.
- Confirm the occurrence of fires (if any) that likely resulted from ruptured gas mains.
- Statistics on gas usage before and immediately after the earthquake may be useful for a system-wide perspective on the impact of the event.
- If maps exist at the time of the next investigation, attempt to correlate the location and pattern of pipe damage to geologic conditions. This exercise may direct investigators to areas not covered by the initial reconnaissance team. In light of the ground failures observed throughout the region it seems likely that damage to buried gas pipes was experienced.



Figure 10.10: Oil storage and distribution facility (Site RK55, N37.38917° E138.63377°, photos taken 7/23/07 12:30). No damage was observed at this site.



Figure 10.11: Natural gas tanks being inspected by local engineers (Site SD13/RK57, N37.37253° E138.59488°, photo taken 7/23/07). Very minor ground settlement and later movement near ditches was observed in the vicinity but the no damage was apparent to the tank foundations, appurtenant piping, or the tanks.

Section 11 - Response and Recovery Issues

11.1 Overview

The earthquake struck on a national holiday in Japan, but essential government personnel began reporting for work soon after, as required when an earthquake registers JMA Intensity 6 or greater. Niigata Prefecture's offices are located in the City of Niigata (more than 80 km from the epicenter). Most prefecture personnel were not directly affected by the earthquake and able to report to work relatively quickly. The prefecture activated its emergency task force (ETF) headquarters within the first hour (see Figure 11.1), and the Prefecture Governor held his first press conference at 11:30 am. The prefecture's ETF was open until August 1 (day 16 of the disaster).



Figure 11.1: Niigata Prefecture's Emergency Task Force headquarters, July 26, 2007

Niigata Prefecture has a 2-tier staffing structure in its ETF, with current department representatives supported by those who had held that same position in 2004. In Japan, government employees routinely rotate between departments and jobs every few years. The 2-tier staffing structure helps ensure that knowledge from 2004 is applied in 2007 and it also provides training for the current department representatives. Over the course of the first day, impacted cities and villages also activated their ETF's and began conversing with their prefectural counterparts to register their disaster impacts and needs.

Japan's Disaster Relief Law (similarly to the Stafford Act in the U.S.) spells out the process by which disasters are declared. The Prime Minister officially declared this to be a "very severe" disaster and established a Cabinet-level ETF to coordinate with the

prefecture and affected local governments. Also, similarly to the U.S., the disasters can be influenced by politics. Given that this earthquake occurred two weeks before a very controversial “upper house” election in Japan, there has been very visible and responsive Cabinet and ministerial support. Many national officials visited the impacted area within the first days of the disaster. The Prime Minister’s designation of this earthquake as a “very severe” disaster means that 4/5 of the local government costs of response and repairs to public roads and building will be reimbursed by the national government.

Following the 2004 earthquake, the prefecture helped establish a disaster recovery and research center at Niigata University. Some of the staff there also worked with Kyoto University on the prepared of the prefecture’s comprehensive disaster reduction plan which was adopted in March 2006. Those academic ties are now proving fruitful, as Niigata University, Kyoto University and Fuji Tokoha University are some of the academic institutions providing assistance to the prefecture and local governments in this disaster.

Along with the Niigata GIS Association and ESRI-Japan, some of these universities are helping staff and manage the first-ever, Emergency Mapping Center (EMC) at the prefecture’s offices. The EMC was formed on July 18 at the request of the Prefectural Governor to support the ETF with easy-to-understand maps. The EMC tracked and mapped disaster management operations, utility restoration, and temporary housing site selection, to name a few. Table 11.1 provides a more complete listing of all the map products that have been developed for the prefecture, and Figure 11.2 shows a series of water restoration maps developed by the EMC. These universities are also helping Kashiwazaki city with its damage certification process (see section 11.4).

Niigata prefecture has a dedicated section of its website for information on the earthquake. To accommodate the foreign populations in the prefecture, information has been translated into Chinese, Korean, Russian and English (see <http://www.pref.niigata.jp/seisaku/kokusai/english/emergency>). Some of the EMC maps were also posted on the web for the public to view. They can be found at <http://bosai.pref.niigata.jp/bosaiportal/0716jishin> and <http://chuetsu-gis.jp/chuetsuoki/>.

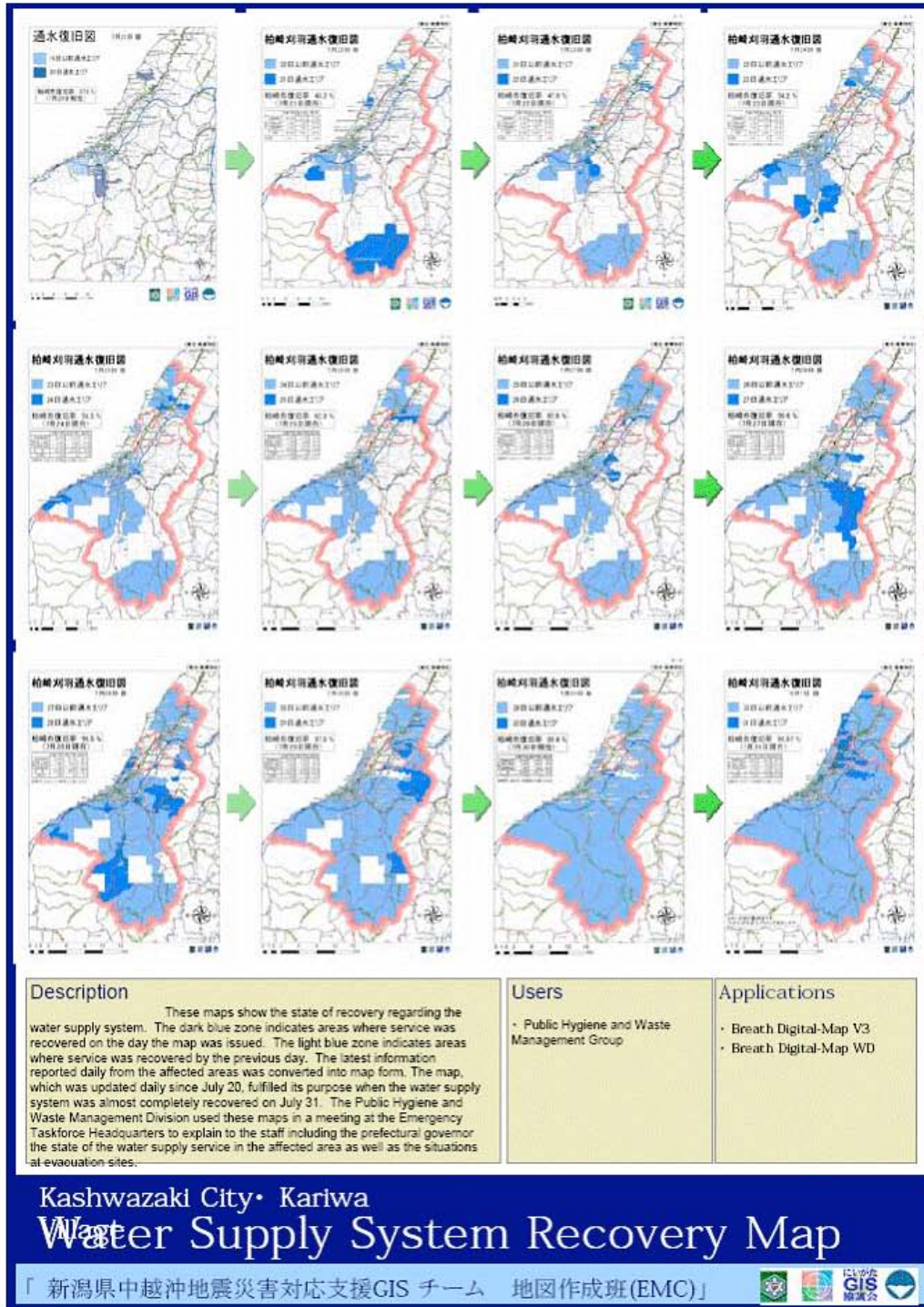


Figure 11.2: A series of maps prepared by the Emergency Mapping Center for Niigata Prefecture, documenting the daily recovery of the region’s water supply system.

Table 11.1. List of Maps Developed by the Emergency Mapping Center, Niigata Prefecture

Administrative/Base Maps
1/25,000 Scale Topographic Map
Municipality Outline Map
Kashiwazaki/Kariwa Regional Map
Aerial Photographs, Orthographic Images, and Charts
Disaster Summary Maps
Chuetsu Offshore Earthquake Disaster Condition Map
Disaster Report Map for the National Government
Recovery Condition Map
Evacuation/Security Maps
Distance Measurement Between Nuclear Power Plant and Earthquake Epicenter
Kashiwazaki Police Jurisdiction Map
Police Unit Deployment Map
Areas under Evacuation Advisory/Order
Evacuation Method Planning Map for Those with Special Needs
Evacuation Site Guide Map and List
Evacuation Site Map and Welfare Institution Location Map
Number of Evacuees and Food Distribution Map
Number of Evacuees and Water Supply Recovery Map
Shelter/Temporary Housing Maps
Evacuation Site and Housing Map
Temporary Housing Location Map
Air Conditioner Placement Planning Map
Housing Map (Regional and key cities)
Building Damage Maps
Map of Building Emergency Danger Level Results
Danger Level Inspection of Damaged Architecture
Damage Verified by Official Inspection
Totally Destroyed Buildings Maps (Regional, by Neighborhood, and with Evacuation Sites)
Residential Zone Damage Condition Map
Property Destruction Level Map
Infrastructure Maps
Locations of Road Closures
Transportation Information Map
Traffic Congestion Information Map
Niigata Airport Map
Shipping Management Map
Akasaka-cho Waterworks Map
Kashiwazaki/Kariwa Water Supply Damage Map
Agricultural Water Supply Damage Map
Water Supply Recovery Maps
Sewage System Damage Maps (Public and Rural Community)

11.2 Early Response and Sheltering

During the first 72 hours (days 1 to 3 of the disaster), the prefecture and its local governments focused on immediate response needs, particularly rescue operations, sheltering and food and water provisions. Most of the damage occurred in the City of Kashiwazaki (population 90,000) and the neighboring towns of Izumozaki (population 6,000) and Kariwa village (population 4,500). There were 11 deaths and nearly 2,000 injuries. Most of these deaths were caused by the collapse of wooden houses. The prefecture reports that more than 1,096 houses collapsed, 2,679 partially collapsed, and another 27,807 had partial damage.

In Japan, local governments (i.e. cities and village) are responsible for providing shelter space, and the prefecture and national governments assist with resources, food and water provisions (see Figures 11.3 a and b). More than half of Japan's public buildings are elementary and junior high schools and under the control of local governments; they fulfill much of the local supply of evacuation and relief sites.

In the immediate aftermath, there were 124 shelter sites in Niigata Prefecture, serving more than 11,000 evacuees. Power was restored to most of the impacted region by July 18 (day 3 of the disaster), but many households lacked gas or running water. Many evacuees returned to their undamaged houses but continued getting emergency food and water. Over 100 locations throughout the prefecture also provided free shower and bathing facilities to disaster victims, including many onsen and hotels.



Figure 11.3: Disaster Relief Area in Kashiwazaki City area on July 27. Self Defense Forces cooking and latrine facilities (a) and evacuees inside community center (b)

Japan's Self Defense Forces (SDF) supported various rescue operations and prefectures and local governments across Japan assisted through mutual aid agreements. The SDF and Coast Guard sent several ships to Kashiwazaki city port to provide drinking water supplies using their desalination systems (see Figures 11.4 and 11.5).

On July 19, Niigata Prefecture issued an official call for volunteers to assist with relief operations. The Prefecture ETF had a Disaster Relief Volunteer Coordination Group that oversaw the volunteer registration and operations centers established in Niigata as well as within the most impacted villages and cities. The prefecture also

provided free shuttle bus services to transport volunteers from the major railway stations in the cities of Nagaoka, Joetsu, and Niigata into the impacted region. This service ran until July 31 when the prefecture discontinued it stating that road conditions and public transportation were sufficiently improved.



Figure 11.4: SDF ship at Kashiwazaki City port, July 27. SDF used desalination systems aboard ships to supply emergency water while local water systems were repaired.



Figure 11.5: SDF filling tanker trucks with water on July 27 to deliver to impacted areas without running water.

11.3 Short-term Recovery and Temporary Housing

Field investigations on July 26 and 27 (days 10 and 11 of the disaster) found that most of the impacted businesses and residents were beyond the emergency phase and

transitioning into recovery. Stores shelves were stocked, windows repaired and doors open for business. Residents were cleaning up, including those whose houses had collapsed, and temporary housing sites were under construction. By July 30 (day 14 of the disaster), running water had been restored to nearly 95% of the households in Kashiwazaki city and Kariwa village, but on 15% of the households had gas restored. As of August 8 (day 24 of the disaster), the prefecture reported 55 shelter sites were still in operation serving 974 evacuees.

In Japan, cities and villages are responsible for designating sites for temporary housing, and the prefectures are responsible for constructing it. Prefectural governments have standing agreements with a consortium of modular housing companies and many such companies were already at designated sites erecting the temporary structures and installing the utilities by the second week of the disaster (see Figure 11.6). Niigata Prefecture plans to construct more than 1,200 temporary units.



Figure 11.6: Construction of temporary housing under way in the Kashiwazaki area, July 27.

11.4 Building Damage Certification Process

At least 2 building damage surveys have been conducted in this disaster (see Figure 11.7). Largely within the first week, teams of engineers and architects inspected

and posted buildings throughout the prefecture with red, yellow and green tags related to the building's safety for occupancy. This system is similar to the rapid, post-disaster survey process, based upon ATC-13, and employed in the U.S. after earthquakes. As within the U.S., the teams are mostly volunteers. But, unlike the U.S., this tagging system is not tied directly to local occupancy regulations. A posting is not legally binding; it is merely informational.



Figure 11.7: A building in Kashiwazaki city that has been through two surveys, with both a green tag as well as a standard yellow notice that the damage certification survey has also been completed.

The second survey system has become more formalized since the 1995 Kobe earthquake. It has been a long-held custom for local governments to issue certificates to disaster victims as evidence of their losses. Following the Kobe earthquake, local governments had to conduct over 500,000 building surveys and issue the certificates.

Later analyses pointed to inconsistencies in the quality and standards of the survey and also estimated that about 30% of the disaster victims challenged local government decisions which had timely and costly consequences.

In 1996, the national government attempted to standardize the local damage certification procedures, developing a very detailed set of guidelines for assessing damage. The guidelines define 5 classes of damage which are determined by a scoring system. Structures that have 50 or more points are classified as ‘heavy damage.’ Figure 11.6 is a translation of a portion of the 1-page form and 5 damage classifications that are being used in the survey of damaged wooden houses in Kashiwazaki city.

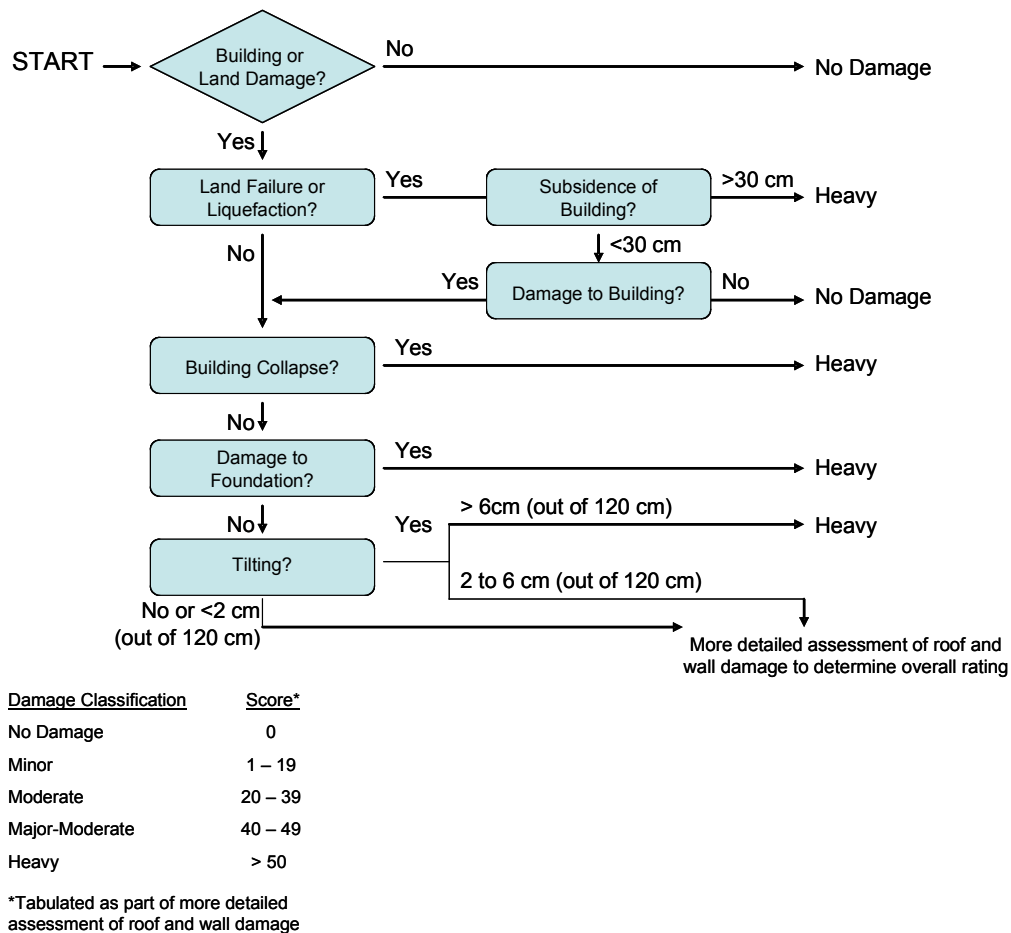


Figure 11.7: Translated portions of the 1-page form for surveying damage to wooden houses in Kashiwazaki city.

The damage certification process is often managed by local tax assessor’s offices and, since 1995, the academic community has helped at least 3 disaster-impacted cities apply the new standards: first in Ojiya city following the 2004 Niigata earthquake, inspecting 20,000 structures; next, in 2007, when 18,000 structures were inspected following the Noto-Hanto peninsula earthquake; and now in Kashiwazaki city. Kashiwazaki city planned to inspect more than 62,000 structures by August 10 and start

issuing certificates on August 17. The city and supporting academic institutions trained 70 teams of two to conduct the surveys. Many of the surveyors came from other cities. Kyoto University has a GIS-based data entry program and is helping manage the survey data entry and creation of an electronic certification database in Kashiwazaki city (see Figures 11.8 and 11.9).



Figure 11.8: Data entry center for the damage certification survey underway in Kashiwazaki city.



Figure 11.9: Close-up view of the GIS-based data entry program developed by Kyoto University that is being used in Kashiwazaki city.

In Japan, national government dollars cannot be spent on private property repairs of houses and businesses. However, local and prefectural governments can direct other funds to residents and businesses. Following disasters, local and prefectural governments have based the apportionment of monetary donations, allotment of temporary housing, and other recovery-related benefits on these certificates. On July 26, Niigata Prefecture announced its disaster aid system for both individuals and houses. Only those with a disaster victim's certificate for the 3 highest-score, damage classes are eligible for the aid (discussed further in the following section).

11.5 Long-term Recovery and Financing

On July 23, the Prefecture Governor released projected damage costs for the 2007 earthquake totaling ¥1.5 trillion (US\$12.77 billion) (see Table 11.2). For comparison, the prefecture provided its loss estimates for the 2004 earthquake which totaled ¥3 trillion (US\$25.5 billion). The 2007 costs include an ¥880 billion (US\$7.5 billion) estimate for unspecific damage costs which are reportedly the indirect economic costs anticipated with the prolonged closure of the nuclear power plant, decreased tourism and other economic impacts of this disaster.

Table 11.2: Projected Damage Costs in Niigata Prefecture for 2007 Earthquake, Compared with Estimated Damage Costs for the 2004 Earthquake

	2007 Earthquake Projected Damage Costs	2004 Earthquake Estimated Damage Costs
Buildings	¥200 billion	¥700 billion
Infrastructure	¥70 billion	¥1,200 billion
Businesses and Factories	¥300 billion	¥300 billion
Agriculture, Forestry, Fishing	¥ 40 billion	¥400 billion
Utilities	¥10 billion	¥100 billion
Other	¥880 billion	¥300 billion
TOTAL	¥1,500 billion	¥3,000 billion

(Source: Policy Division, Governor's Policy Bureau, Niigata Prefecture, July 23, 2007)

News about the earthquake as well as damage at the Kariwa-Kashiwazaki nuclear power plant had an immediate impact on the tourism and fishing industries. Summer is usually a busy time for Niigata's mountain and onsen villages and its beach areas; hotel cancellation increased markedly after the earthquake. As of August 5, Kashiwazaki city's tourist office reported more than 30,000 reservation cancellations for hotel rooms in the city and only half of its 110 lodging facilities were accepting guests. Other facilities in the city were closed either due to damage or because cooking and heating gas had not been restored. The prefecture, especially its tourist office, has undertaken a fairly aggressive public relations campaign to offset the negative press surrounding the nuclear power plant's damage. They are trying to reach both Japanese and international audiences. Niigata airport is a major port of entry for Russian, Taiwanese and South Korean tourists.

In 2004, the national government had a significant role in financing the recovery. The national government covered the costs to repair damaged roads, tunnels and other public infrastructure. The Prime Minister's designation of this earthquake as a "very severe" disaster means that the national government will cover 4/5 of the costs of response and repairs to public infrastructure and buildings and local governments will have to cover the rest.

Public funding for private property repairs and reconstruction is limited, and Niigata Prefecture also has one of the lowest earthquake insurance penetration rates in the country. So, residents and businesses will be challenged to find the necessary recovery dollars.

Under Japan's national aid system, disaster-impacted individuals can receive a grant of up to a ¥3 million (US\$26,000) for temporary living and other daily life expenses. An emergency housing repair program also grants up to ¥500,000 (US\$4,300) for minor repairs to the affected structure, such as replacing broken windows or covering their damaged roofs. Private property owners are generally responsible for costs to cover (e.g. putting tarps on) their damaged roofs as well as demolition. Local governments will remove demolition debris that is in the public right-of-way.

Niigata Prefecture also established a disaster aid system for disaster-impacted individuals and houses. Only those with a disaster victim's certificate for the 3 highest-score, damage classes are eligible for the aid. The prefecture will grant up to ¥2 million (US\$17,200) for temporary living and other daily life expenses, contents replacement, demolition and removal costs, and housing repairs and rebuilding.

On July 26, the prefecture also announced reductions in prefectural taxes. Corporations that have lost more than half of their capital due to the earthquake are eligible for a reduced prefectural tax rate of 5% for one year, until July 15, 2008. Homeowners are also eligible for tax exemptions on housing purchased to replace earthquake-damaged homes. The exemption amount equals the price of 1 square meter of new housing multiplied by the floor area of the damaged section of the formerly-owned housing multiplied by the tax rate. The prefecture is also giving tax exemptions on tuition, public housing and several other recovery-related fees.

On August 1, Niigata Prefecture opened a consultation center in Kashiwazaki city to assist earthquake victims in applying for temporary housing, disposing of demolition debris, making emergency repairs to damaged housing, and getting information on available financial support. The prefecture also announced that it has requested that the national government simplify its application procedure for the national aid system.

11.6 Concluding Observations

In an interview on July 26, the prefecture staff was optimistic about the recovery and the progress that had been made thus far. Compared with the 2004 earthquake, there have been fewer aftershocks and there will be more time to recover before winter sets in. The prefecture, in particular, has also heeded the lessons learned responding and recovering from the 2004 earthquake, as well as the Noto-Hanto peninsula earthquake earlier this year. Many of the funding programs and other response and recovery approaches are based upon the previous earthquake programs and approaches. The prefecture has also developed strong relationships with the several top, disaster management programs at Japanese universities, and these institutions are supporting government in some key disaster management functions. The universities assistance is provided pro-bono.

For the most part, this is the type of moderate earthquake disaster that Japan's disaster management system is well-designed to handle. The compartmentalization of tasks and responsibilities, within a national ministry and local agencies, works when departments are not overwhelmed and able to carry out their specific responsibilities and use mutual aid agreements to get resources from similar departments in other agencies. Personnel from other water, assessor's and building departments across Japan were observed working alongside their local counterparts in Kashiwazaki city.

